THE BIOLOGY AND INTERPLAY OF IMMUNOTHERAPY BY LEUKEMIA-ONCOLYTIC VIRUS (iLOV) IMMUNE RESPONSES

by

Jovian Tsang

A thesis submitted in partial fulfillment of the requirements for the degree Master of Science in Biochemistry with a specialization in Human and Molecular Genetics

Department of Biochemistry, Microbiology and Immunology
Faculty of Medicine
University of Ottawa

Supervisor
Dr. John Bell

ABSTRACT

Oncolytic viruses (OVs) are novel biological agents that selectively infect and kill malignant cells. OVs can also generate anti-cancer immunity. Our lab exploited this phenomenon and developed an *in vitro* vaccine with infected leukemia cells with oncolytic virus vaccine – and named immunotherapy by leukemia-oncolytic virus (iLOV) – that provided *in vivo* protection in a murine model for acute lymphoblastic leukemia. This work further characterizes iLOV biology and the interaction of its immune responses. An *in vitro* immune response assay was optimized to detect and quantify the *in vivo* anti-leukemia immunity generated by iLOV. Anti-viral immunity is an obstacle for OV therapy. Although iLOV created anti-viral antibodies towards itself, these neutralizing antibodies did not hinder the vaccine's ability to initiate complement or dendritic cell activation. We envision personalized versions of iLOV for leukemia patients in remission to prevent the possibility of relapse. This work highlights new advantages for infected cell vaccines and supports the progress of iLOV toward clinical testing.

Tell me and I'll forget;
Show me and I may remember;
Involve me and I'll understand.

-Chinese proverb

ACKNOWLEDGEMENT

I want to thank Dr. John Bell for taking me on as a co-op student in your lab in 2011. He gave me an opportunity of a lifetime to actively participate in some of the most exciting cancer therapeutics research out there! My life probably would've been very different had it not been for his short and concise e-mail reply in late 2010.

Thanks to Madison Gray and Carlyn Figueiredo for taking the time to review this thesis despite its scope of immunology being beyond their field of research.

Theresa and Christiano have helped me become proficient at animal work, have assisted me with too many experiments to count, and have taught me the importance of being punctual.

I want to thank past and present lab members who have taught me along the way, given their advice freely and supportively, and who have put up with my shenanigans. Naomi, Madison Foster, Laura, Casey, Jiqing, Almo, Anu, Carolina, Catia, Chris, Jiahu, Marie-Claude, Dominic, Ramya, Colin, Vanessa, Nicole, and Rozanne… thank you, thank you, thank you!

I want to also thank Victoria "Vicki" Jennings for her help with all things flow cytometry, for providing helpful comments and guidance during the writing process of this thesis, for being a wonderful friend, and for enlightening me on British culture, humour and lifestyle.

Mina Rizk and Girjia "Geeta" Waghray have been the most supportive honours student and lab technician, respectively, and I am so grateful for their help, their good humour and their caring hearts.

I want to thank David Conrad for training me when I was but a wee co-op student. I will miss our enthralling and often late-night discussions about medicine, science, research, politics, music, your (new) dog and life.

I would not have survived graduate school if it were not for my good friend and confidante, Monique Marguerie, who has been such a joy to work with inside and out of the lab. We met as co-op/summer students and you told me to "kick you out" of the lab if upon my return, you were still here. Thank you for the laughs, for listening, for the encouraging words, and for more laughs! I am so happy and thankful to have completed my Masters with you.

I want to thank Dr. Harold Atkins for going above and beyond as a research supervisor. He taught me how to think critically, solve problems, ask questions and then ask better questions. He also gave me the freedom to pursue extracurricular activities that truly filled my graduate school career with memorable and life-changing experiences. Thank you for your constant encouragement, patience, mentorship and belief in me.

Finally, thank you to my mother for the unwavering support throughout my academic endeavours, life choices and for the constant concern of whether I will ever find a job. One day!

TABLE OF CONTENTS

LIST OF ABBREVIATIONS

ADCC	antibody-dependent cellular cytotoxicity
ALL	acute lymphoblastic leukemia
APC	antigen presenting cells
BFA	brefeldin A
BMDC	bone marrow-derived dendritic cells
CAR	chimeric antigen receptor
CMC	complement-mediated cytotoxicity
CTLA-4	cytotoxic T-lymphocyte-associated protein 4
cRPMI media	complete Roswell Park Memorial Institute media
DAMP	danger-associated molecular pattern
DC	dendritic cells
DMEM	Dulbecco's Modified Eagle's Medium
ELISA	enzyme-linked immunosorbent assay
ELISpot assay	enzyme-linked immunospot assay
FACS	flow cytometry analysis
FBS	fetal bovine serum
fiLOV	1% paraformaldehyde-fixed iLOV
fL1210	1% paraformaldehyde-fixed L1210 cells
GvHD	graft-versus-host disease
GzmB	gramzyme B
hC1q	human C1q complement protein
HI-HS	heat-inactivated human serum
HSC	hematopoietic stem cells

HSCT	hematopoietic stem cell transplantation
HSV1	herpes simplex virus type 1
ICS FACS	intracellular cytokine staining by flow cytometry
IgG	immunoglobulin G
iLOV	immunotherapy by leukemia-oncolytic virus (L1210 cells infected with MG1 virus)
IFN-g	interferon-gamma
γL1210	Gamma-irradiated L1210 cells
MG1	Maraba MG1 virus
MG1-GFP	Maraba MG1 virus expressing a transgene for green fluorescent protein
MG1-hDCT	Maraba MG1 virus expressing human dopachrome tautomerase
MHC (I/II)	major histocompatibility complex, class I or class II
MOI	multiplicity of infection
MRD	minimal residual disease
ND	not determined
NDV	New Castle Disease
NK cells	natural killer cells
OV	oncolytic virus(es)
PBS	phosphate buffer saline
PCR	polymerase chain reaction
PI	propidium iodine
RT	room temperature
SFC	spot forming colonies

TCR	T-cell receptor
TK	thymidine kinase
TNF-α	tumour necrosis factor alpha
UV-MG1	UV-inactivated MG1 virus
VSV	vesicular stomatitis virus
VSV-Δ51	VSV containing a deletion in methionine 51 in the viral genome
VSV-Δ51-GFP	VSV-Δ51 expressing a transgene for green fluorescent protein

LIST OF FIGURES AND ILLUSTRATIONS

LIST OF TABLES

1 INTRODUCTION

1.1 Acute lymphoblastic leukemia

Acute lymphoblastic leukemia (ALL) is a hematopoietic malignancy that begins in the bone marrow or blood. It originates from lymphoid cell types such as B-cells, T-cells and even natural killer (NK)-cells (**Figure 1**), although the latter two types are rare (Bennett et al., 1976; Nava and Jaffe, 2005; Vardiman et al., 2009). B-cell ALL incidence rates predominate (Ratei et al., 2013) with some defining characteristics including chromosome translocations, such as t(9;22)(q34;q11) which produces the identifiable BCR-ABL protein (Kurzrock et al., 2003), and hyperdiploidy (Moorman et al., 2003).

ALL is the most diagnosed cancer in children and adolescents (Schrappe et al., 2012). Thankfully, five year survival rates for this cohort are near 90% due to continually optimized risk-stratification and rigorous treatment schedules (Hunger et al., 2012). The same cannot be said for adult ALL with survival rates hovering between 30-40% (Narayanan and Shami, 2012).

Treatment options for ALL involve multi-drug chemoradiotherapy regimens with the addition of hematopoietic stem cell transplantation (HSCT) for high-risk patients. Leukemic resistance to drugs, leukocyte counts, age and drug tolerance are some factors involved in identifying high-risk patients (Pui and Evans, 2006; Schrappe et al., 2012). HSCT is used to rescue or reconstitute normal hematopoiesis following induction chemotherapy as normal hematopoietic elements are damaged during this process.

Figure 1. Origins of acute lymphoblastic leukemia. Lymphoblastic leukemias are derived from lymphoid progenitors and can occur at any stage in development. These cells can differentiate into B-cells, T-cells, NK-cells or plasma cells. Reproduced with permission from Elert (2013).

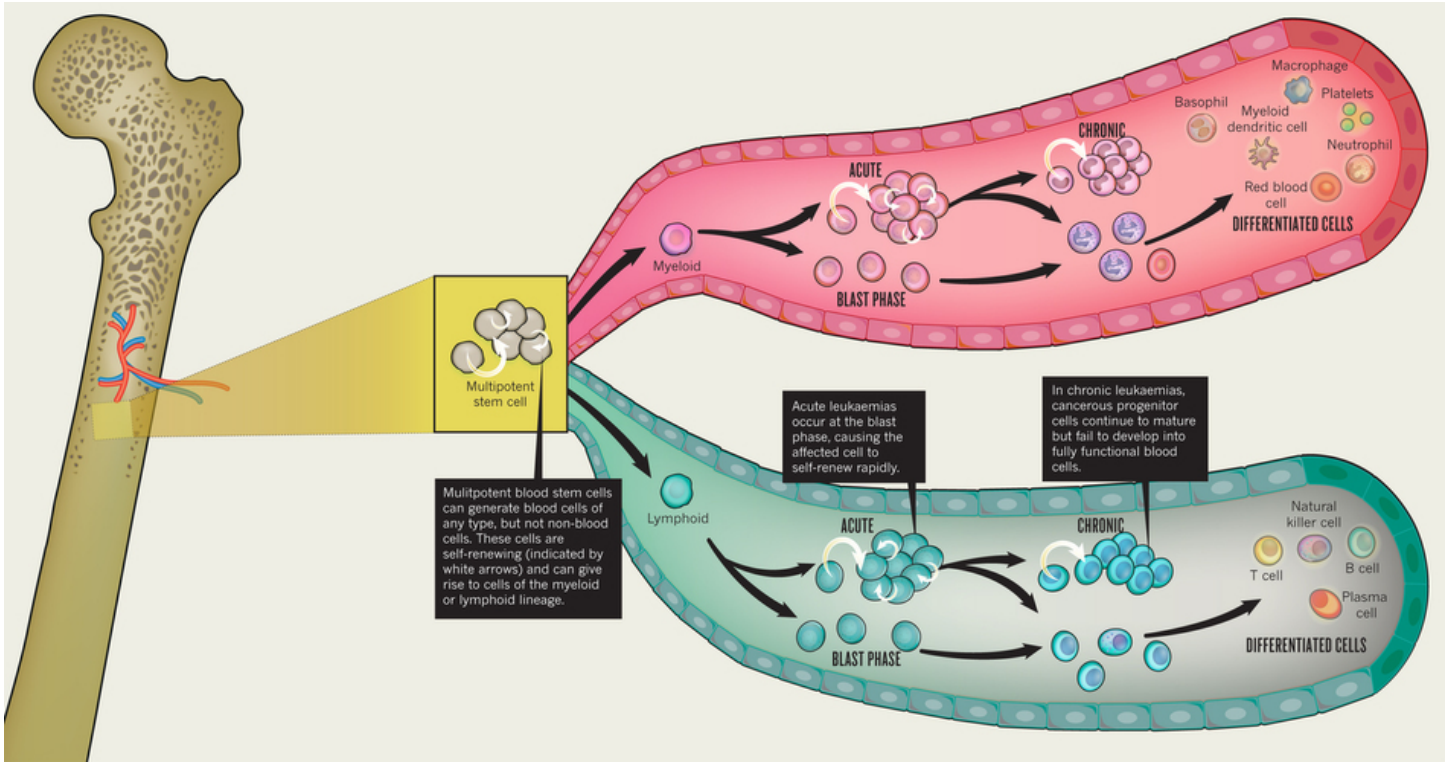
Multipotent stem cell
Mulitpotent blood stem cells can generate blood cells of any type, but not non-blood cells. These cells are self-renewing (indicated by white arrows) and can give rise to cells of the myeloid or lymphoid lineage.
Myeloid
ACUTE
BLAST PHASE
CHRONIC
Macrophage
Platelets
Basophil
Myeloid dendritic cell
Neutrophil
Red blood cell
DIFFERENTIATED CELLS
Lymphoid
Acute leukaemias occur at the blast phase, causing the affected cell to self-renew rapidly.
In chronic leukaemias, cancerous progenitor cells continue to mature but fail to develop into fully functional blood cells.
ACUTE
BLAST PHASE
CHRONIC
Natural killer cell
T cell
B cell
Plasma cell
DIFFERENTIATED CELLS

One therapy outcome is minimal residual disease (MRD), wherein lingering amounts of leukemia are only detectable by sensitive phenotypic and genetic techniques, such as flow cytometry and polymerase chain reaction (PCR), respectively (Campana, 2009). Efforts have been made to refine immunophenotyping by flow cytometry and molecular monitoring by PCR to detect true MRD as it is predictive of relapse risk (Bassan et al., 2009; Cavé et al., 1998). A result of failing to detect MRD in patients in remission may explain why a significant proportion of them succumb to the disease again. MRD is an opportunity for scientists and clinicians to apply additional therapies that truly eliminate ALL entirely and offer long-term cures.

1.2 ALL challenges

Induction chemotherapy in older cohorts often succeeds in getting patients into remission, but is short-lived (Bassan et al., 2004). Similarly, limited progress has been made with successfully treating relapsed childhood ALL (Nguyen et al., 2008).

For these high-risk patients, HSCT is employed so higher doses of chemotherapy can be used in an attempt to eradicate these aggressive malignancies. Hematopoietic stem cells (HSC) are obtained from patients themselves (autologous) or from sibling or unrelated donors (allogeneic). Autologous and allogeneic HSC both have unique issues. Higher rates of relapse are associated with autologous HSCT due to contaminating cancer cells (Pasquini and Wang, 2013). Allogeneic HSCT is associated with graft immune reactions directed against the recipient's tissue, called graft-versus-host disease (GvHD), and when severe can lead to mortality (Ho and Soiffer, 2001).

HSCT is considered an extreme medical procedure as intense doses of chemotherapy are used and an immune system is theoretically reset. These measures are taken for a chance

to live a cancer-free live once more. However, these medical practices continue to fail a portion of patients as evidenced by 30-40% survival rates in the adult population.

The challenging task of preventing relapse in ALL patients presents an opportunity for novel therapies to be developed. Immunotherapies are emerging candidates that could resolve this problem.

1.3 Cancer immunotherapy

Immunotherapy directs or engineers the host's immune responses to induce therapeutic effects. Cancer and immunotherapy are no strangers to each other. In the early 1900s, crude immunotherapy methods were explored that utilized "autolysates" treated with chemicals to induce "oncolytic" cancer killing effects *in vivo* (reviewed by Fichera, 1918). Advances in cancer immunotherapy have brought about the dawn of engineered antibodies and cellular therapies. Rituximab is an anti-CD20 antibody that has become a standard of care against certain B-cell malignancies, while CD19-targeted chimeric antigen receptor (CAR) T-cells have been accumulating impressive results in clinical trials with ALL (Davila et al., 2014). In the next two sections, the therapeutic mechanisms of these immunotherapies will be explained.

1.3.1 Antibody-mediated immunity

Antibodies bind short defined sequences called epitopes. There are various isotypes that have distinct or overlapping functions such as initiating complement or activating immune cells. The prototypical antibody isotype is known as IgG or immunoglobulin G and has two distinct parts: two identical F_{ab} portions and one F_c portion, held together in the shape of a Y (**Figure 2**). The F_{ab} portions serve to recognize the epitope, while the F_c potion

can facilitate an array of innate effector mechanisms through its binding. These mechanisms include complement-mediated cytotoxicity (CMC) which is initiated through C1q binding, antibody-dependent cellular cytotoxicity (ADCC) which recruits NK cells by binding CD16, or facilitating opsonization with antigen-presenting cells (APC) by binding Fcγ receptors (Zinkernagel et al., 2001). Furthermore, these innate effector functions serve to stimulate adaptive immune responses (Weiner et al., 2010). Some immunotherapeutic monoclonal antibodies stimulate these mechanisms. The efficacy of rituximab is facilitated by CMC, ADCC and direct signaling that induces apoptosis (Weiner, 2010). Other therapeutic antibodies augment immune responses. Ipilimumab is a monoclonal antibody that blocks cytotoxic T-lymphocyte-associated protein 4 (CTLA-4) signaling. CTLA-4 is a cell surface receptor expressed on T helper cells that binds to cytotoxic T-cells and down-regulates their killing activity (Krummel and Allison, 1995). Ipilimumab has been used to augment HSC graft immune responses in allogeneic HSCT to stimulate graft-versus-malignancy reactions (Bashey et al., 2009).

Figure 2. Structure and effector functions of Immunoglobulin G (IgG). IgG antibodies are made up of two sections: F_{ab} and F_c portions. Parts of the F_{ab} portion recognize and bind specific antigens, while F_c portions mediate effector functions. These effector mechanisms include neutralization, complement-mediated cytotoxicity, antibody-dependent cellular cytotoxicity, and opsonization.

IgG

Immunoglobulin G

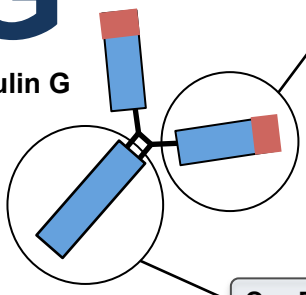

Two F_{ab} portions: recognize an epitope on an antigen

One F_c portion: when bound activates effector mechanisms

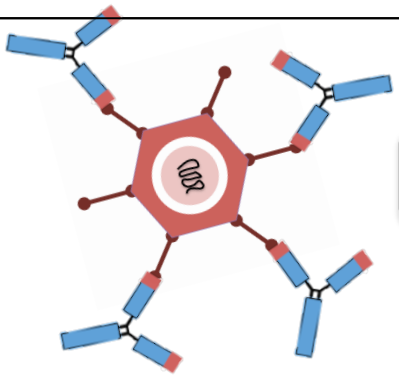

IgG antibodies can specifically bind to and *neutralize viruses*, they can also bind to cell surface antigens

Antibody-bound pathogens are quickly *opsonized by phagocytes* through F_c and F_c-receptor interactions, this leads to their degradation and activation of the phagocyte

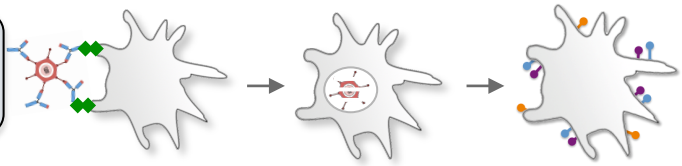

C1q, a complement protein binds to the F_c portion of antibodies and *initiates the complement cascade* which destroys the pathogen

Destroyed pathogens or cells by the latter two processes are phagocytosed by professional antigen-presenting cells and *leads to adaptive immunity*

Fc is bound by CD16 on NK cells, a F_c receptor, and initiates *antibody-dependent cellular cytotoxicity*, which involves degranulation of NK cells and destruction of pathogens

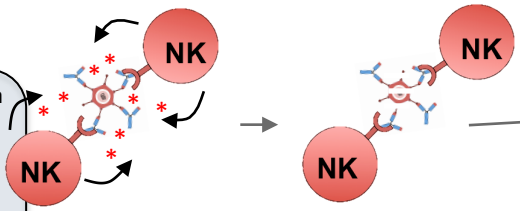

1.3.2 T-cell immunity

Adaptive immunity also has a cellular-mediated component that involves T-cells. $CD8^+$ T-cells are also known as cytotoxic T-cells. When the T-cell receptor (TCR) correctly recognizes its corresponding peptide loaded onto its target cell's major histocompatibility complex class I (MHCI) molecules, the cytotoxic T-cell will release perforin, granzyme B (GzmB) and pro-inflammatory cytokines (Harty et al., 2000). Perforin punctures the cell surface that allows GzmB to enter (Thiery and Lieberman, 2014). GzmB is a caspase-like serine protease that initiates apoptosis in the target cell (Trapani and Sutton, 2003). Pro-inflammatory cytokines include tumour necrosis factor-alpha (TNF-a) and interferon-gamma (IFN-g) which synergize to activate macrophages (Muñoz-Fernández et al., 1992). IFN-g also stimulates anti-viral and anti-proliferative pathways in surrounding tissues (Goodbourn et al., 2000; Huang et al., 1993).

As a secreted cytokine, IFN-g is a particularly popular bio-marker used to measure T-cell activation and can be detected using simple methods such as enzyme-linked immunosorbent assay (ELISA) or enzyme-linked immunospot (ELISpot) assays. There are surface cell markers for T-cell activation and degranulation such as CD69 and CD107, respectively, but these require fluorescently-conjugated antibody binding and an apparatus to measure that binding, such as flow cytometry. There are also functional measurements such as killing or proliferation, but these require the use of radioisotopes or fluorescent cell dyes (Shafer-weaver et al., 2003; Quah, Warren, & Parish, 2007)

Priming of naïve $CD8^+$ T-cells requires professional APC such as dendritic cells that have processed and presented peptides onto their MHCI molecules. When these peptides are obtained exogenously and loaded onto MHCI by a subset of dendritic cells, this process is called cross-presentation (Joffre et al., 2012). Cross-presentation is used to present viral or

tumour peptides. Priming T-cells also requires co-stimulatory and cytokine signals, which include the binding of T-cell CD28 to APC B7 molecules and the secretion of interferon-alpha and interleukin-12 from APC (Hochrein et al., 2001). This three-step prerequisite stimulates naïve $CD8^+$ T-cells to become effector $CD8^+$ T-cells that proceed to proliferate, find and kill their targets. Although foreign pathogens prompt the initiation of this pathway proficiently, tumours often have immunosuppressive microenvironments that do not promote all three needs subsequently evading cellular immunity.

Immunotherapy by chimeric antigen receptor (CAR) T-cell bypasses traditional immunology through *ex vivo* manipulation and incorporation of CARs to directly bind tumour cell surface antigens and enforce selectivity and killing in a MHCI-independent manner (Vonderheide and June, 2014). CAR T-cells are not restricted to peptides loaded onto MHCI molecules, which means they can even bind carbohydrates and glycolipids (Rambaldi et al., 2014). **Figure 3** illustrates the differences between TCR-mediated T-cell immunity and CAR-mediated T-cell immunity.

Exciting additions to the cancer immunotherapy field are viruses that can selectively infect and kill malignant cells. These biological agents are particularly promising because they can stimulate anti-tumor immunity by providing the pro-inflammatory package required for cross-presentation of tumour antigens by APC.

Figure 3. CAR T-cells bypass TCR-mediated immunity. CAR T-cells can bind and be activated by surface cell antigens on tumour cells in a MHCI-independent manner. This bypasses traditional TCR-mediated signaling which is restricted to peptide-loaded MHCI molecule recognition. IC = intracellular; EC = extracellular

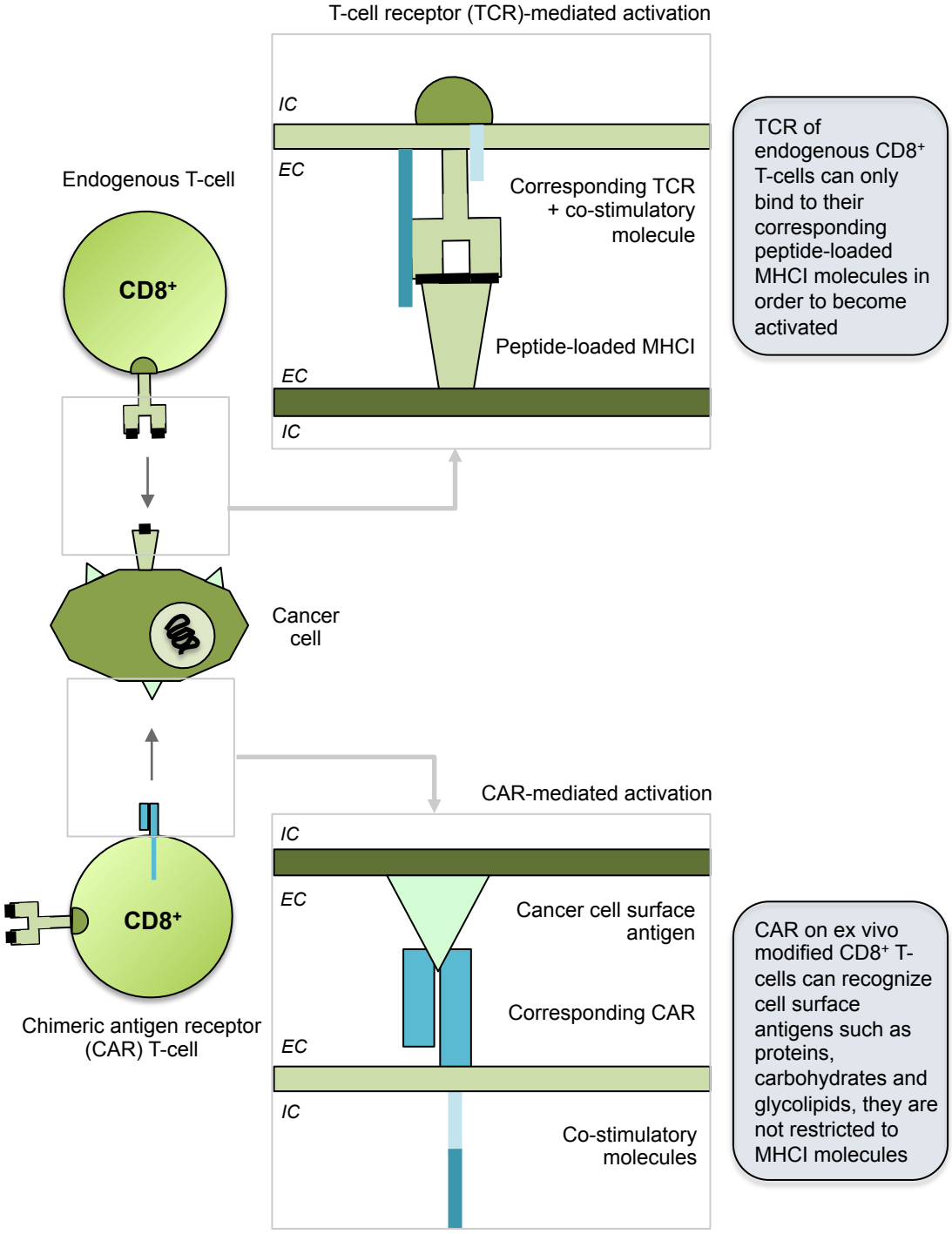
T-cell receptor (TCR)-mediated activation
IC
EC
Corresponding TCR
+ co-stimulatory
molecule
Peptide-loaded MHCI
EC
IC
TCR of endogenous CD8+ T-cells can only bind to their corresponding peptide-loaded MHCI molecules in order to become activated
Endogenous T-cell
CD8+
Cancer cell
CAR-mediated activation
IC
EC
Cancer cell surface antigen
Corresponding CAR
EC
IC
Co-stimulatory molecules
CD8+
Chimeric antigen receptor (CAR) T-cell
CAR on ex vivo modified CD8+ T-cells can recognize cell surface antigens such as proteins, carbohydrates and glycolipids, they are not restricted to MHCI molecules

1.4 Viruses for cancer therapy

Viruses have had a tumultuous relationship with cancer. The first reported incidence of influenza-induced leukemic remission was in the late 19th century (Dock, 1904). However, it was only later, in 1933, that influenza was discovered to be caused by a virus (Smith et al., 1933). In the 1950s, the first oncogenic murine viruses were discovered which led the scientific community to seriously consider viruses as the cause of human cancers (Javier and Butel, 2008). In the same decade though, a small faction of scientists and clinicians studied viruses for the treatment of human cancers (Georgiades et al., 1959; Southam and Moore, 1952). Unfortunately, the results from these clinical trials were not as impressive as the animal models preceding them (Moore, 1949a, 1949b). By the 1960s, chemotherapies became widely adopted (DeVita and Chu, 2008) which coincided with a temporary lull in cancer virotherapy research. It took until the 1990s for the oncolytic virus field to re-emerge with the advent of genetic engineering that allowed scientists to manipulate viral genomes (Kelly and Russell, 2007).

Oncolytic viruses (OV) are naturally occurring or genetically engineered viruses that specifically infect, replicate and kill cancer cells (**Figure 4**). Mutations that create deregulated pathways in malignant cells drive OV specificity. For instance, oncolytic vaccinia virus is thymidine kinase (TK)-inactivated and must utilize host cellular TK to successfully replicate. Certain types of cancer cells such as hepatocellular carcinomas overexpress TK and act as ideal hosts to harbour vaccinia virus replication (Heo et al., 2013). Defects in interferon signaling genes render certain cancers interferon-nonresponsive (Dunn et al., 2005; Wong et al., 1997). Interferon signaling is intimately connected to antiviral pathways. Interferon-sensitive viruses, such as vesicular stomatitis virus (VSV) and other

Figure 4. Oncolytic viruses: mechanism of action. Oncolytic viruses selectively infect and replicate in malignant cells that harbour defective anti-viral pathways due to their accumulated mutations. Normal cells have intact anti-viral signaling pathways and can prevent viral replication from occurring. Thus, cancer cells are killed by the growth of these viruses. Oncolytic viruses also alert and recruit innate immunity to the site of the tumour, which results in stimulating adaptive anti-tumour immunity.

Oncolytic virus

Mechanism of Action

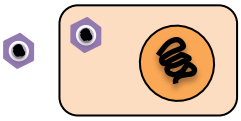

Normal cells resist OV infection with anti-viral signaling pathways

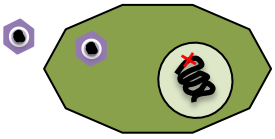

Cancer cells have defective anti-viral signaling pathways

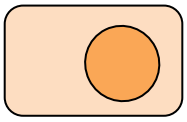

Virus is cleared by innate immunity

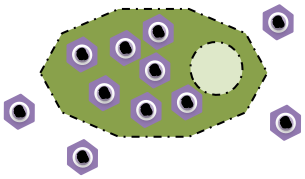

With no way to defend themselves, cancer cells are ideal hosts for OV replication, subsequently killing the cancer cell

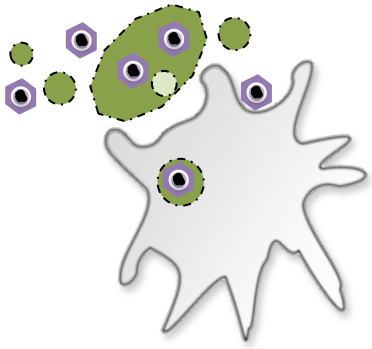

Innate immune cells such as professional antigen-presenting cells are attracted to the site of inflammation and engulf dead cancer cells and virus to initiate adaptive anti-tumour immunity

rhabdoviruses, exploit interferon-nonresponsive cancer cells to selectively replicate within and subsequently kill them (Stojdl et al., 2000).

1.5 Rhabdoviruses: VSV and Maraba

VSV and Maraba virus are closely related small negative-sense RNA rhabdoviruses with only five genes (Brun et al., 2010). Known hosts for VSV are insects and farm animals, while infections in humans are rare and asymptomatic (Lichty et al., 2004a). Immunity to VSV and Maraba in human populations remains low or contained within farming locales due to these reasons (Travassos da Rosa et al., 1984; Tesh et al., 1987). These rhabdoviruses have broad host tropism *in vitro* due to their use of ubiquitous low density lipoprotein receptors to gain cell entry (Finkelshtein et al., 2013). Oncolytic VSV has a deletion of methionine-51 (VSV-Δ51) in the matrix "M" protein, which typically blocks cellular interferon-β production; inhibiting this function increases virus interferon-sensitivity and consequently cancer selectivity (Lun et al., 2006). Similar results were achieved in Maraba virus, with two mutations introduced into its genome affecting the M and G proteins (designated as MG1 virus; Brun et al., 2010).

Hematopoietic malignancies have demonstrated sensitivity to oncolytic VSV therapy. In particular, Lichty *et al.* (2004) showed that several leukemia, lymphoma and myeloma cell lines and multiple myeloma-contaminated patient peripheral blood samples were killed and purged by VSV (Lichty et al., 2004b). Recently, Naik et al. (2012) have demonstrated impressive results with VSV expressing murine IFN-β and human sodium iodide symporter (VSV-mIFNβ-hNIS) in the 5TGM1 myeloma animal model. hNIS allowed I^{131} radiotherapy effects to synergize with oncolytic activity (Naik et al., 2012). The group found that systemic

virus treatment was able to de-bulk 5TGM1 tumours and cure mice. These studies demonstrate the application and advancement of rhabdoviruses to treat hematopoietic cancers.

1.6 Anti-viral immunity versus OV

As promising as OV therapy is, the field is not without its challenges. In particular, the immune system in a healthy individual has no problem neutralizing and clearing oncolytic viruses. OVs encounter anti-viral immunity that is pre-established by exposure or vaccination, or induced following OV therapy, which hinders subsequent use (Ikeda et al., 1999; Tsai et al., 2004). Anti-viral antibodies are particularly troublesome as they can neutralize, recruit complement and promote opsonization of viral particles (Forthal and Moog, 2009). Unique methods have been developed to circumvent anti-viral immunity. Counter-measures range from modifying the exterior components of the virus (Kaufmann and Nettelbeck, 2012; Muik et al., 2014) to using cell carriers to transport OV through the bloodstream (Iankov et al., 2007; Munguia et al., 2008; Power et al., 2007). There is a fine line between eliminating the body's ability to fight off attenuated virus, which is often the case in immune-deficient individuals, and neutralizing the OV before it can imbue its therapeutic effects on the tumour. Promising clinical OV candidates need to find a balance between the two.

1.7 Oncolytic viruses and immunotherapy

Preclinical and clinical studies have highlighted the ability of OV therapy to induce adaptive anti-tumour immunity (reviewed in Melcher, Parato, Rooney, & Bell, 2011). Research on reovirus, which is currently in a number of phase I, II and III clinical trials for

different solid malignancies, has shown that its therapeutic efficacy relies heavily on its ability to stimulate anti-tumour immunity rather than its replication capacity (Prestwich et al., 2009). This phenomenon has also been observed in several other OV platforms such as herpes simplex virus type 1 (HSV-1), vaccinia virus, VSV and Maraba (Mastrangelo et al., 1999; Pol et al., 2014; Willmon et al., 2009; Workenhe et al., 2014).

OV infection in the tumour microenvironment causes inflammation which recruits immune cells such as DCs (Errington et al., 2008). Viruses provide the pathogen-associated molecular patterns (PAMPs) and dying tumour cells provide the danger-associated molecular patters (DAMPs) that ultimately lead DCs to cross-present tumour antigens and stimulate anti-tumour cellular immunity (Workenhe and Mossman, 2014).

OV therapy has attempted to potentiate this immunological phenomenon by incorporating immune-stimulating cytokines (Andtbacka et al., 2013; Heo et al., 2013) and synergizing with monoclonal antibodies (Engeland et al., 2014; Zamarin et al., 2014)**.** The trend in the field points to the continued convergence of powerful immunotherapeutic agents with OV technologies. The concerted efforts of these two fields will usher in some very exciting cancer therapeutic studies.

1.8 Infect-cell vaccines

Infected-cell vaccines have emerged as immunotherapies that exploit the ability of OV to induce anti-tumour immunity. These oncolysates were pioneered by Cassel, Garrett and Lindenmann in the late 1960s to 1970s. Cassel and Garrett demonstrated that Ehrlich ascites tumours were rejected by A2G mice following vaccination with New Castle Disease (NDV) virus-infected Ehrlich ascites cells (Cassel and Garrett, 1966). Later, Lindenmann

demonstrated the same phenomenon with influenza strain WSA-infected (Lindenmann, 1967) and VSV-infected Ehrlich ascites cells (Lindenmann, 1970). Cassel went on to treat post-surgical patients with allogeneic melanoma-NDV oncolysates in the clinic. They showed that oncolysate-treated patients had >60% survival at 10-years, while historical patient populations had only 5-15% (Cassel and Murray, 1992). A follow-up study at 15 years, with 55% survival in the same patient group, showed that $CD8^+$ T-cells played crucial roles in continued therapeutic efficacy in these patients (Batliwalla et al., 1998). More recently, Lemay *et al.* (2012) demonstrated prophylactic and therapeutic protection with B16-F10 murine melanoma cells infected with VSV-Δ51 expressing granulocyte-macrophage colony stimulating factor (VSVgm) in a syngeneic, immune-competent animal model (Lemay et al., 2012). Similar to the NDV oncolysate clinical study, Lemay found that activated T cells, as well as NK cells, mediated the therapeutic response.

1.9 A pre-clinical leukemia vaccine

Our group has applied infected cell vaccines to a preclinical model of ALL. We developed Immunotherapy by Leukemia-Oncolytic Virus (iLOV), which consists of L1210 cells, a murine B-cell leukemia line, infected with Maraba MG1 virus (**Figure 5**). Impressively, when syngeneic and immune-competent DBA/2 mice were vaccinated with iLOV, we observed a >95% survival rate (Conrad et al., 2013). The resultant anti-cancer immunity was long term and L1210-specific. Additionally, this immunity could be adoptively transferred and was determined to be T-cell mediated. iLOV, made with infected EL4 cells (a T-cell murine leukemia cell line) also generated protective immunity in C57BL6 mice. iLOV did not require functional cellular secretion, live virus or replication-competent virus, at the time of administration, to stimulate an anti-L1210 immune response and confer

Figure 5. Immunotherapy by Leukemia-Oncolytic Virus (iLOV). L1210 cells are infected with oncolytic MG1 virus to generate an infected-cell vaccine we call iLOV. iLOV generated a protective anti-L1210 immune response in mice and these mice survived deadly leukemic challenges.

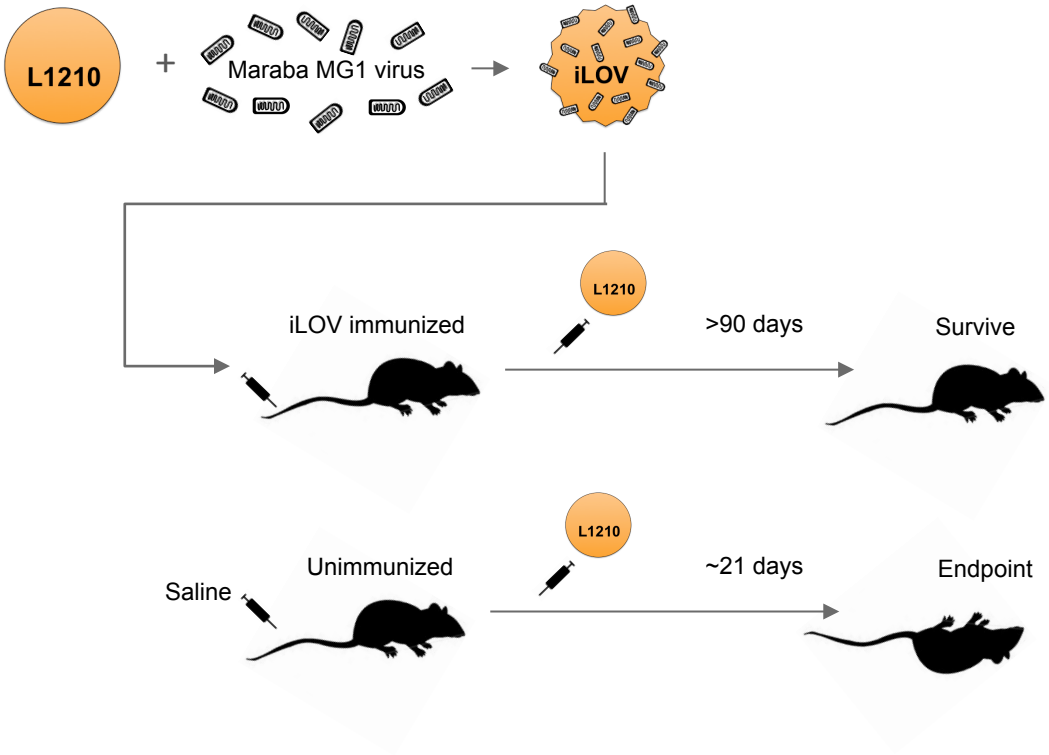
L1210
+
Maraba MG1 virus
iLOV
iLOV immunized
L1210
>90 days
Survive
Saline
Unimmunized
L1210
~21 days
Endpoint

survival benefit. Finally, in a small animal study, we showed that established anti-MG1 virus immunity in mice prior to iLOV vaccination did not hinder subsequent anti-L1210 immunity.

1.10 iLOV: unanswered questions

iLOV is a promising OV-mediated immunotherapeutic with the potential to stimulate protective, anti-cancer immunity *in vivo*. It warrants further investigation. An urgent question that must be answered is: Can iLOV's anti-leukemic immune responses be quantified by *in vitro* methods? Our studies have used survival as the main read-out for vaccine efficacy. In a clinical setting solely monitoring survival benefit would be impractical. Therefore, we need a foundation of knowledge evaluating *in vitro* methods to measure immune responses generated by iLOV. Pro-inflammatory cytokine secretion, such as IFN-g, may be optimal bio-markers to quantify using ELISA and ELISpot assays, while cell surface marker staining, functional proliferation and killing assays may not be as accessible. In this way, we can verify whether immunization with iLOV succeeded or failed.

Another interesting question that begs further investigation is: Is iLOV affected by innate effector mechanisms initiated by anti-viral immunity, specifically anti-viral antibodies? How? iLOV's anti-L12120 immunity does not appear to be impaired by pre-existing anti-viral immunity. This attribute distinguishes iLOV from conventional OV therapies, whose efficacy is greatly affected by anti-viral antibodies. The mechanisms unaffected by, and associated with, this phenomenon should be further explored. The knowledge gained may inform us on anticipated behaviour of iLOV in patients with established anti-viral immunity (which would be present upon additional iLOV doses).

Other aspects to explore include immunization schedules, prognostic markers prior to immunization that could predict vaccine success or failure, vaccine behaviour in different

immune environments such as immune tolerance toward leukemia antigens or immune-deficient hosts, or identifying T-cell subsets responsible for anti-L1210 immunity. Evidently, there are many unanswered questions regarding iLOV. The work in this thesis hopes to answer some of these questions and add to the breadth of knowledge on iLOV.

1.11 Hypotheses and objectives

iLOV has shown preclinical promise as an immunotherapeutic platform to generate protective anti-leukemia immunity. We envision personalized versions of iLOV for ALL patients to stimulate anti-leukemia immune responses and eradicate residual leukemic reservoirs. We want a future without relapse. More knowledge must be gained regarding iLOV biology and immunology following its administration.

Based on the questions posed in Section 1.10, we hypothesized that:

1) iLOV's anti-L1210 immune responses can be quantified *in vitro* using a bio-marker for immune cell activation, such as IFN-g, and
2) iLOV is bound by anti-viral antibodies, but the iLOV immune complexes that form do not affect innate effector mechanisms

Therefore, the aims of this work focused on the following two objectives:

1) develop an *in vitro* immune response assay to detect and quantify anti-L1210 cellular immunity, and
2) evaluate the role of and interactions between anti-viral humoral immunity and iLOV.

2 MATERIALS AND METHODS

2.1 Cell culture

Cell lines were maintained in 1X Dulbecco's Modified Eagle's Medium (DMEM; Corning® Cellgro, VA, USA) supplemented with 10% fetal bovine serum (FBS; Sigma Aldrich, ON, CA) at 37 °C and 5% CO_2. Suspension cell lines were maintained between 0.5-2 × 10^6 cells/mL in 75 cm^2 or 225 cm^2 rectangular flasks (Corning®, NY, USA). Cells were passaged by taking a 1 mL aliquot to determine cell viability and density by a Vi-Cell XR Cell Viability Analyzer (Beckman Coulter, ON, CA). The appropriate volume of cell suspension was transferred to a 50 mL tube (BD Falcon; MA, USA) and centrifuged (Sorvall™ ST 40 Centrifuge; Thermo Scientific, UT, USA) at 1,500 rpm for 5 minutes at room temperature (RT). Supernatant was aspirated, pellet was re-suspended in 10 mL phosphate buffer saline (PBS) "wash," and centrifuged again. The final pellet was resuspended in the appropriate volume of 1X DMEM + 10% FBS for the desired cell density and transferred into a new flask. Adherent cell lines were maintained in 150 cm^2 plates (Corning®) until 95% confluent. For passaging, media was aspirated and plates were washed with 10 mL PBS. 5 mL 0.05% trypsin (Corning®) was added to plates and incubated for 5 minutes at 37 °C. Cell suspension was treated the same as described above, but seeded into plates at the end.

For procedures involving cell harvesting, passaging and staining with tubes or plates, centrifugation was done at 1,500 rpm for 5 minutes at RT, unless otherwise stated.

Murine whole splenocytes were maintained in either complete Roswell Park Memorial Institute (cRPMI) media, which consisted of HyClone™ RPMI 1640 media (Thermo Scientific) supplemented with 10% FBS and 1% Gibco® penicillin-streptomycin

(Life Technologies, ON, CA), or AIM V® media (Life Technologies) supplemented with 2% heat-inactivated human serum (HI-HS; Biosera, MO, USA). Serum was heat-inactivated in a 56 °C water bath for 30 minutes.

2.2 Mice and cell lines

DBA/2 mice were purchased from Charles River Laboratories (ON, CA). They arrived at 6-8 weeks old and were housed, treated and euthanized according to the rules and regulations of the University of Ottawa Animal Care and Veterinary Services.

Vero cells are a kidney epithelial cell line isolated from African green monkeys (ATCC®, VA, USA; CCL-81™). These adherent cells were used to grow and titer virus. L1210 cells are a murine lymphocytic leukemia suspension cell line (ATCC®; CCL-219™). Cell stocks were tested for mycoplasma contamination prior to use.

2.3 Viruses

Oncolytic maraba MG1 virus and VSV-Δ51, with and without green fluorescent protein transgene expression (MG1-GFP and VSV-Δ51-GFP, respectively), were graciously given to our lab by Dr. David Stojdl at the Children's Hospital of Eastern Ontario (Ottawa, ON), wild-type sindbis virus was generously donated to our lab by Dr. Benjamin tenOever from the Mount Sinai Hospital (New York, NY), and E1/E3-gene deleted adenovirus was generously gifted to us by Dr. Robin Parks from the Ottawa Hospital Research Institute (Ottawa, ON).

MG1, MG1-GFP, VSV-Δ51 and VSV-Δ51-GFP viruses were grown and harvested from roller bottles containing Vero cells in 1X DMEM + 10% FBS + 3% HEPES buffer. Briefly, bottles containing confluent cell monolayers were infected at a multiplicity of

infection (MOI) of 0.01 of each virus and were incubated at 37°C for 24 hours. The media was collected and centrifuged to remove whole cells. Supernatant was filtered through a sterile 0.2 μm bottle top filter apparatus (Millipore, ON, CA; SCGPU05RE) to remove whole cell debris. Filtered supernatant was centrifuged at 14,000 rpm for 90 minutes at 4°C. Supernatant was aspirated and the remaining pellet was re-suspended in 200-500 μL PBS, divided into 10-20 μL aliquots and frozen at -80 °C until use.

2.4 Serum samples

Murine serum was obtained from DBA/2 mice. Blood was obtained by cardiac puncture, placed immediately into sterile 1.5 mL eppendorf tubes and left at 4 °C overnight. Saphenous bleeding from the hind leg was also utilized to obtain small volumes of blood; blood capillary tubes were used for collection in these instances. Serum was isolated from coagulated blood through centrifugation (Centrifuge 5415C; Eppendorf, NY, USA) at 14,000 rpm for 10 minutes at RT and stored at -20 °C until use. Naïve serum was obtained from untreated, naïve mice. Anti-MG1 virus (αMG1), anti-adenovirus (αAdeno) and anti-sindbis virus (αSindbis) sera were obtained from mice treated with 1e8 PFU MG1 virus, 1e9 PFU adenovirus and 1e6 PFU Sindbis virus at Days -21 and -7, while blood was harvested on Day 0. Anti-MG1 virus rabbit serum (with a MG1 virus neutralizing antibody titer of 1:3200) was a kind gift from Dr. David Stojdl and naïve rabbit serum was a generous gift from Dr. Rozanne Arulanandam (OHRI; Ottawa, ON). Rabbit serum was heat-inactivated in a 56 °C water bath for 30 minutes.

2.5 Generation of bone marrow derived dendritic cells

Bone marrow-derived dendritic cells (BMDC) were harvested from femurs and tibia of DBA/2 mice. Briefly, the bones were separated from muscle and ligaments, soaked in 70% ethanol for 10 seconds and then placed in cold PBS. The ends of the bones were removed and bone marrow was flushed out using a sterile syringe filled with MACS buffer, which consisted of PBS + 0.5% FBS + 2 mM EDTA, and connected to a 30-gauge needle. The cell suspension was filtered through a 100 μm cell strainer (Fisherbrand™, ON, CA; 352360) and centrifuged. The pellet was re-suspended in 250 μL MACS buffer per mouse. Biotinylated antibodies against non-monocytic lineage murine markers anti-B220, anti-MHCII, anti-GR1, anti-CD3ε and anti-CD4 (list of antibody information can be found in Table 1), were added at a dilution of 1:100 per mouse and incubated for 15 minutes at 4 °C. The cell suspension was washed with a large volume of MACS buffer and centrifuged for 10 minutes. The cell pellet was re-suspended in 90 μL MACS buffer containing 10 μL Streptavidin MicroBeads (Miltenyi Biotec, CA, USA; 130-048-101) per 10^7 cells and incubated for 15 minutes at 4ºC. The cell-bead suspension was washed once more with a large volume of MACS buffer and re-suspended in 500 μL MACS buffer per 10^8 cells. MS separation columns (Miltenyi Biotec; 130-042-201) were prepared and used to negatively select BMDC according to manufacturer's protocols. The unlabeled BMDC eluted fraction was centrifuged and re-suspended in 30 mL DMEM + 10% FBS + 10 ng/mL murine GM-CSF (R&D Systems, MN, USA; 415-ML) per mouse. On Day 7, 10 mL of this supplemented media was added to each flask. On Day 10, flasks were lightly shaken and suspension cells were harvested for experimentation.

2.6 Isolation of murine T and B-lymphocytes

T-cells and B-cells were isolated from mouse spleens. Briefly, spleens were harvested from mice and placed into cold sterile PBS. Each spleen was pressed through a 100 μm cell strainer to create single cell suspensions of whole splenocytes. Cell suspensions were centrifuged and pellets were re-suspended in 5 mL ACK lysis buffer and left at RT for 5 minutes to remove the red blood cells. 30 mL PBS was added before the cell suspensions were once again centrifuged. These pellets containing whole splenocytes were re-suspended in 5 mL of media, cell densities were determined at this point and samples were kept on ice until use. T-cells and B-cells were negatively selected from these whole splenocyte preparations using mouse pan T Cell Isolation Kit II (Miltenyi Biotec; 130-095-130) and mouse pan B Cell Isolation Kit II (Miltenyi Biotec; 130-104-443), respectively. Manufacturer's protocols were followed.

2.7 Vaccine preparation

iLOV vaccine preparation has been previously outlined by our group (Conrad et al., 2013). Briefly, L1210 cells were seeded at a cell density of 1×10^6 cells/mL in 1X DMEM + 10% FBS. The appropriate amount of MG1 maraba virus was re-suspended in 1 mL PBS at a MOI of 10.0 and added to the flask. The flask was lightly shaken to mix its contents. The flask was incubated for 18-20 hours at 37 °C and 5% CO_2.

The following day, the cell suspension was gently re-suspended against the bottom of the flask to dislodge sticky MG1-infected L1210 cells and transferred to a 50 mL falcon tube. A 500 μL aliquot was used to determine cell viability and density. To another 500 μL aliquot, 5 μL propidium iodine (PI; 1 mg/mL) was added, mixed and evaluated by flow cytometry analysis using a Beckman Coulter Quanta SC flow cytometer to quantify GFP and

PI expression in infected cells. The rest of the cells were centrifuged at 1500 rpm for 5 minutes, the supernatant was aspirated, 10 mL of sterile PBS was added and the cells were gently re-suspended. The cells were washed once more, brought up to a final cell density of 1×10^7 cells/mL in PBS and transferred into sterile 1.5 mL eppendorf tubes. Aliquots were irradiated at 30 Gy using a gamma irradiator (HF-320; Pantak). After irradiation, this preparation was designated as iLOV vaccine and aliquots were put on ice until use. For diluted vaccine preparations, iLOV was diluted to 1×10^4 or 1×10^5 cells in PBS after irradiation. This procedure was the same for preparations of irradiated L1210 cells (γL1210) but without virus infection.

2.8 Immunization and survival studies

Mice were intravenously administered with PBS, virus or cells by tail vein injection. iLOV and L1210 challenge cells were given at a dose of 1×10^6 cells in 100 µL PBS, unless otherwise specified. iLOV immunizations were administered at 7 day intervals for a maximum of three doses.

2.9 iLOV and L1210 coated with serum

iLOV and L1210 cells were prepared as described in Section 2.7. Instead of irradiating the cells as the last step, they were fixed with 10-20 mL 1% paraformaldehyde (PFA) solution for 30 minutes at RT. 30 mL PBS was added and the cell suspension was centrifuged for 10 minutes. The pellet was washed once more and re-suspended back to 1×10^7cells/mL in PBS. In a 96-well V-bottom plate (Corning®; 3894), 1 µL of heat-inactivated αMG1, αAdeno, αSindbis or naïve mouse serum was added to 2×10^6 cells for 15 minutes at 4 °C. For the C1q deposition assay, αMG1 or naïve rabbit serum was used instead. The cells

were centrifuged and washed with 200 μL PBS. To image the amount of binding by serum antibodies, cells were then incubated with 1:100 goat anti-mouse IgG-PE antibody in PBS or 1:100 goat anti-rabbit IgG-Pacific Blue antibody in PBS for 15 minutes at 4 °C. The labeled cells were washed with PBS twice and stored in the dark until imaging with a fluorescent microscope or binding quantified by flow cytometric analysis.

2.10 Microscopy and flow cytometry

All microscopy photos were taken with the EVOS™ fl Digital Inverted Fluorescence Microscope (Thermo Fisher Scientific Inc., MA, USA). Flow cytometry analysis was evaluated by a Beckman Coulter Quanta™ SC flow cytometer or a Beckman Coulter CyAn™ ADP 9 Color Analyzer. FACS buffer, which consisted of PBS + 0.5% FBS, was used as the final solution for flow cytometry samples. A complete list of the unconjugated, fluorescently labeled or biotinylated antibodies used can be found in Table 1.

Table 1. List of antibodies
A complete list of the unconjugated, fluorescently labeled or biotinylated antibodies used.

Species	Reactivity	Target	Format	Brand	Cat. #
Mouse	Human	C1q	--	Abcam	ab71940
Arm. ham.	Mouse	CD11c	PE-Cyanine 7	eBioscience	25-0114
Rat	Mouse	MHCI	APC	eBioscience	17-5957
Rat	Mouse	MHCII	PE	eBioscience	12-5321
Rat	Mouse	CD86	PE	eBioscience	12-0862
Rat	Mouse	CD19	APC-eFluor® 780	eBioscience	47-0193
Rat	Mouse	CD3	PE-Cyanine 5	BD Pharmigen™	555276
Arm. ham.	Mouse	CD69	FITC	BD Biosciences	553236
Rat	Mouse	B220	Biotin	BD Pharmigen™	553086
Mouse	Mouse	MHCII	Biotin	BD Pharmigen™	550554
Rat	Mouse	GR1	Biotin	BD Pharmigen™	553125
Arm. ham.	Mouse	CD3ε	Biotin	BD Pharmigen™	553060
Rat	Mouse	CD4	Biotin	BD Pharmigen™	553045
Rat	Mouse	CD252	Biotin	BD Pharmigen™	559798
Rat	Mouse	CD28	--	BD Pharmigen™	553294
Rat	Mouse	CD16/CD32 (Fc Block™)	--	BD Pharmigen™	553142
Goat	Mouse	IgG	PE	Jackson ImmunoResearch Laboratories, Inc.	115-116-146
Goat	Rabbit	IgG	Pacific Blue	Life Technologies	P10994

Arm. ham. = Armenian hamster

2.11 Virus plaque assay and antibody neutralization assay

For titering virus, virus aliquots were thawed and diluted to Log and half Log dilutions of 10^{-6}, 10^{-7}, 3.16×10^{-7}, 10^{-8}, 3.16×10^{-8}, 10^{-9} in serum-free 1X DMEM. Confluent Vero 6-well plates (Corning®) were aspirated of media and 200 µL of the viral dilutions were added to wells. Plates were incubated for 45 minutes at 37 °C and 5% CO_2. Media was removed and 2 mL of 1:1 mixture of 2X DMEM + 20% FBS and 1% sterile agarose was added to each well. Plates were incubated for an additional 24 hours, and then fixed with 3:1 methanol-acetic acid solution and stained with 0.5% coomassie blue stain. Tap water was used to de-stain wells. Viral titers (PFU/mL) were calculated as follows:

$$Viral\ titer\ \left(\frac{PFU}{mL}\right) = \frac{Number\ of\ plaques\ in\ well}{(Dilution\ of\ input\ virus)\times(Volume\ of\ input\ virus)}$$

To quantify the antibody neutralizing titer in serum, serum samples were diluted by two from 1:50 to 1:12,800 in a final volume of 50 µL serum-free 1X DMEM. Virus was added to these serum dilutions at 1.2×10^4 PFU/well and left to incubate for 1 hour at 37 °C. These virus-serum dilutions were added to confluent Vero 96-well plates and were incubated for up to 96 hours. The neutralizing antibody titer was noted as the highest dilution without any cytopathic effects.

2.12 C1q deposition on the surface of iLOV

iLOV and L1210 cells were prepared as described in Section 2.7. Instead of irradiating the cells as the last step, they were fixed with 1% PFA solution for 30 minutes at RT. A large volume of PBS was added and the cell suspension was centrifuged for 10

minutes. The pellet was re-suspended back to 1×10^7cells/mL in PBS. In a 96-well V-bottom plate, 1 μL of heat-inactivated anti-MG1 or naïve rabbit serum was added to 2×10^6cells for 15 minutes at 4 °C. The cells were centrifuged and washed with 200 μL PBS. The pellet was re-suspended in 5 μg/mL human C1q purified protein and allowed to incubate for 0, 15 or 60 minutes at 37°C, 5% CO_2. After the designated incubation periods, the cells were centrifuged, washed with PBS once and stored at 4 °C. Cells were re-suspended with 50 μL of 1:50 mouse anti-human C1q antibody in PBS and incubated for 15 minutes at 4°C. The cells were washed once and finally re-suspended in 1:100 goat anti-mouse IgG-PE antibody for 15 minutes at 4 °C. The labeled cells were then washed twice with PBS, re-suspended in 200 μL FACS buffer and stored in the dark at 4 °C until flow cytometric analysis.

2.13 Dendritic cell activation assay

Isolated BMDC were co-cultured with irradiated L1210 and iLOV cells in cRPMI. L1210 and iLOV cells were also coated in naïve serum or αMG1 serum at a 1:200 dilution in PBS, as described above. Co-cultures were set up in 96-well round-bottom plates (Corning®; 3799) and consisted of 5×10^5 BMDC/well as well as 5×10^4 iLOV or γL1210 cells/well (10:1 ratio) and MG1 virus at MOI 0.1. After plates were incubated for 24 hours at 37 °C and 5% CO_2, the co-cultures were washed with PBS once, fixed with 1% PFA and stained with 1:100 dilutions of CD11c, CD86, MHCI and MHCII fluorescently-labeled antibodies (antibody information in Table 1) for 15 minutes at 4 °C. Stained cells were washed with PBS twice and stored in the dark at 4 °C until flow cytometry analysis.

2.14 IFN-g ELISA

Effector cells were prepared as 2.5×10^6 whole splenocytes/mL in cRPMI media. Effector cells were re-stimulated with media, UV-inactivated MG1 virus (UV-MG1), VSV_N peptide (N protein, polypeptide between 52–59: RGYVYQGL; Bio-Synthesis, Inc., TX, USA; 13657-01), iLOV cells or L1210 cells. UV-inactivation of MG1 virus was performed in a similar manner as described by Conrad *et al*. (2013) using the Spectrolinker UV Crosslinker XL-1000 (Spectronics, NY, USA). Re-stimulants were prepared in cRPMI media as 5×10^5 iLOV or L1210 cells/mL, 5×10^5 PFU/mL UV-MG1 or 10 μg/mL VSV_N peptide. Additionally, 4 μg/mL anti-mouse CD28 antibody was added to all re-stimulant preparations as a co-stimulation factor.

Co-cultures were set up by adding 125 μL of effector cell and re-stimulant preparations to each well. The effector to target ratio was 5 to 1. Co-cultures were incubated for 48 hours at 37 °C and 5% CO_2. Plates were centrifuged, 150-200 μL aliquots of supernatant was taken and stored at -80 °C until evaluated by ELISA (R&D Systems® Quantikine; SMIF00). Manufacturer's protocols were followed. Briefly, sample supernatants and recombinant murine IFN-g were added in duplicate to the IFN-g pre-coated plates for 2 hours at RT. The plates were washed four times with PBS. An IFN-g secondary (horseradish peroxidase-conjugated) antibody was then added to the plate and incubated for 2 hours at RT. The amount of bound conjugate antibody was quantified by a solution colour change resulting from catalysis of 1:1 hydrogen peroxide and tetramethylbenzidine solution by HRP. This colour change was quantified at 450 nm and corrected at 540 nm by spectrophotometry (Multiskan Ascent™ 96/384 Plate Reader; MTX Lab Systems, Inc., VA, USA).

2.15 IFN-g ELISpot assay

Effector cells were prepared as 5×10^6 whole splenocytes/mL or a 4:1 mixture of 4×10^6 isolated T-cells/mL and 1×10^6 naïve whole splenocytes/mL in AIM® V + 2% HI-HS. Re-stimulants consisted of media, UV-MG1 or VSV_N peptide, 1% PFA-fixed iLOV or 1% PFA-fixed L1210 cells. GolgiPlug™ (BD Biosciences, ON, CA; 555029) was also tested on re-stimulant cells. All re-stimulants were prepared in AIM® V + 2% HI-HS and were prepared as 1×10^6 fixed iLOV or L1210 cells/mL, 1×10^6 PFU/mL UV-MG1 or 10 μg/mL VSV_N peptide. Additionally, 4 μg/mL anti-mouse CD28 antibody was added to all re-stimulant preparations as a co-stimulation factor.

AIM® V + 2% HI-HS was added to the murine IFN-g ELISpot assay plate (MabTech AB, OH, USA; 3321-2A) and left for 30 minutes at RT, as instructed by the manufacturer's protocols. This media was removed and co-cultures were set up by adding 100 μL of effector cell and re-stimulant preparations to each well with re-stimulants added first. Thus, each well would contain 5×10^5 effector cells and 1×10^5 re-stimulant cells (5:1 ratio) or 1×10^5 PFU UV-MG1 or 1 μg VSV_N peptide. Co-cultures were incubated for 16-20 hours at 37 °C and 5% CO_2.

Spots on the IFN-g ELISpot assay plates were developed according to manufacturer's protocols. Briefly, secreted IFN-g from reactive cells was captured by anti-mouse IFN-g antibodies coating the well's surface. Cells and supernatants were removed after overnight co-culture and a biotinylated anti-mouse IFN-g antibody was incubated with the wells. Streptavidin-alkaline phosphatase (ALP) was added followed by a substrate that precipitated when it reacted with ALP. This coloured precipitate was absorbed onto the opaque well's surface and was visualized as a spot.

The number of spots in each well was quantified by an ImmunoSpot® ELISpot plate reader (Cellular Technology Limited, OH, USA). Data is represented as spot forming colonies (SFC) per number of effector cells added to the well.

2.16 Statistical analysis

Statistics analyses were conducted using Prism, version 5.0a (GraphPad Software, Inc., CA, USA). Statistical tests included: product limit estimator (Kaplan-Meier), Welch's corrected t-test, Grubbs' test or Mantel-Cox tests. Mean and standard error of the mean (SEM) are shown. P-values, unless otherwise specified, are indicated as * < 0.05 and ** 0.005.

3 RESULTS

3.1 Developing an *in vitro* assay to detect iLOV immune responses

One requirement before iLOV can be tested in the clinic is the need for an *in vitro* immune response assay. This assay should be able to measure specific anti-leukemia immune responses from the vaccinated host's immune cells. We opted to quantify IFN-g as an *in vitro* measure for the generation of anti-leukemia cellular immunity.

3.1.1 IFN-g ELISA

We sought to evaluate whether IFN-g secretion was quantifiable and specific to iLOV-immunized ("iLOV" hereafter) splenocytes when co-cultured with L1210 cells. Whole splenocytes were harvested from iLOV mice following three intravenous doses of iLOV (injection schedule outlined in **Figure 6A**).

These splenocytes were co-cultured with re-stimulants and supernatant IFN-g was quantified by ELISA (**Figure 6B**). iLOV splenocytes re-stimulated by UV-MG1, iLOV or γL1210 cells secreted large amounts of IFN-g compared to unimmunized splenocytes.

Although IFN-g amounts in re-stimulated co-cultures versus splenocytes alone (media control) were significantly different ($p < 0.05$), more than half of the IFN-g secreted from iLOV splenocytes could be attributed to non-specific IFN-g secretion.

We sought to determine whether the large, non-specific secretion of IFN-g was an artifact of the co-culture set up. Specifically, these co-cultures (**Figure 6B**) were completed in round-bottom wells where cells form loose pellets. Perhaps this promoted excessive contact between activated immune cells causing non-specific responses to occur.

Figure 6. IFN-g ELISA quantified higher IFN-g secretion from iLOV immunized splenocytes. IFN-g from iLOV immunized or unimmunized mice was quantified by ELISA. iLOV splenocytes secreted more IFN-g than unimmunized splenocytes.
***A*,** Immunization schedule for iLOV-immunized mice. Each vaccine dose contained 1×10^6 iLOV cells and was administered by intravenous tail vein injection. Splenocytes and isolated T-cells were harvested from spleens on Day 0 and used in the following IFN-g ELISAs and ELISpot. ***B*,** IFN-g concentrations in supernatant from co-cultures of iLOV (n = 3) and unimmunized (n = 2) splenocytes with the designated re-stimulants. Cellular re-stimulants were irradiated to prevent proliferation. Co-cultures were set up in round-bottom 96-well plates and incubated for 48-hours. ***C*,** Identical experimental set up as B, with co-cultures set up in flat-bottom 96-well plates. ***D*,** IFN-g concentrations in supernatant from co-cultures of iLOV or unimmunized splenocytes/isolated T-cells with the designated re-stimulants. The T-cell to unimmunized splenocytes ratio was 1:4. Number of bio-replicates was n = 1 unimmunized mouse and n = 2 iLOV mice. Technical duplicates were performed.
* p-value < 0.05 and ** p-value < 0.005

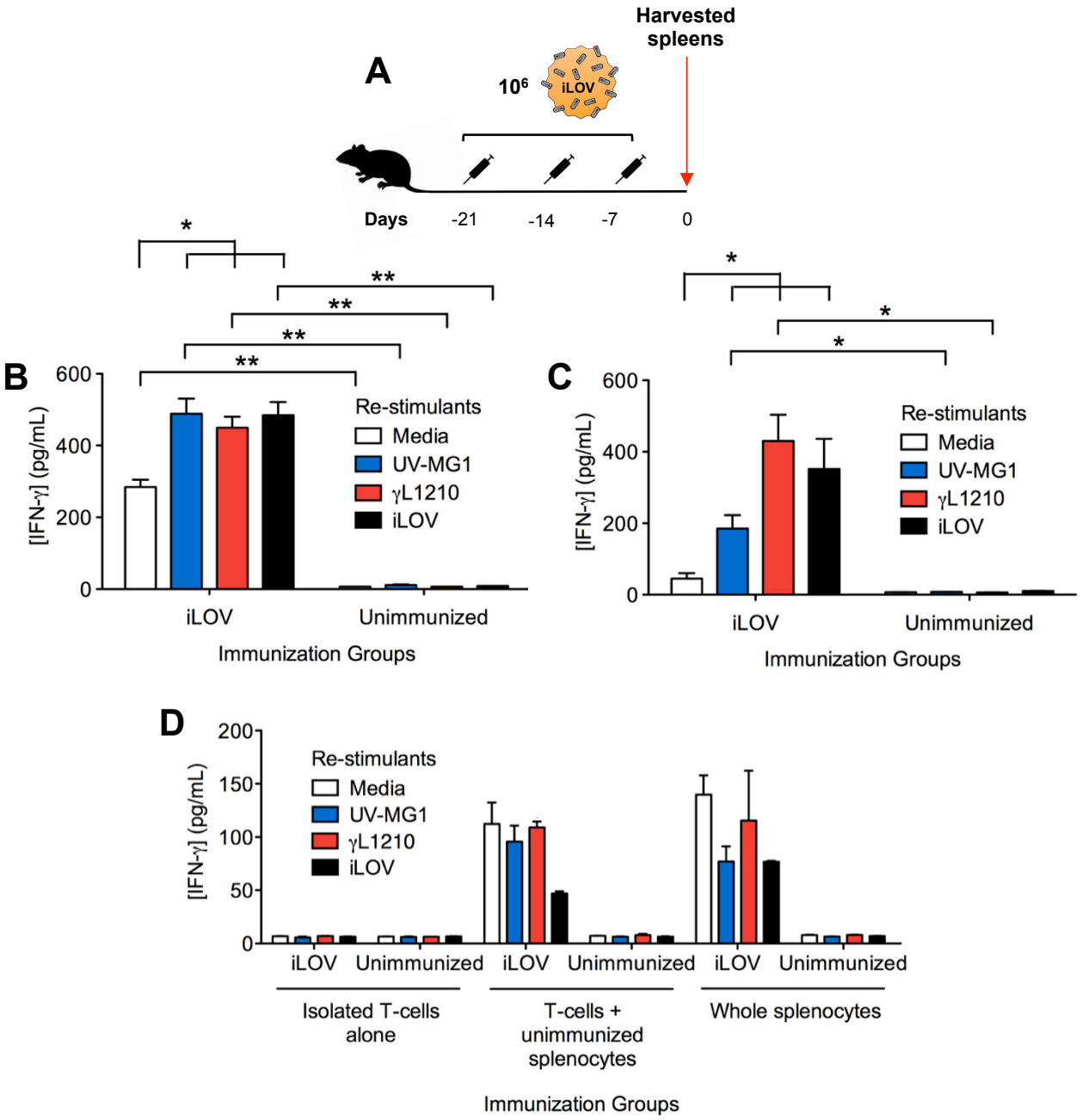
A
Harvested spleens
10⁶
iLOV
Days
-21
-14
-7
0
B
[IFN-γ] (pg/mL)
600
400
200
0
Re-stimulants
Media
UV-MG1
γL1210
iLOV
iLOV
Unimmunized
Immunization Groups
C
[IFN-γ] (pg/mL)
600
400
200
0
Re-stimulants
Media
UV-MG1
γL1210
iLOV
iLOV
Unimmunized
Immunization Groups
D
[IFN-γ] (pg/mL)
200
150
100
50
0
Re-stimulants
Media
UV-MG1
γL1210
iLOV
iLOV
Unimmunized
iLOV
Unimmunized
iLOV
Unimmunized
Isolated T-cells alone
T-cells + unimmunized splenocytes
Whole splenocytes
Immunization Groups

This experiment was therefore repeated in flat-bottom (FB) wells (**Figure 6C**). The amount of non-specific IFN-g from iLOV splenocytes dropped significantly. In contrast, large amounts of IFN-g were still detected from co-cultures between iLOV splenocytes and L1210 cells.

We also tested whether isolating T-cells, thereby removing innate immune cells, would eliminate non-specific IFN-g secretion. T-cells were negatively selected from whole splenocytes and co-cultured in round-bottom wells (**Figure 6D**). Antigen-presenting cells (from unimmunized splenocytes) were required to initiate T-cell immune responses, as T-cells alone were insufficient (**6D**, left panel). It is interesting to note that despite selecting out innate immune populations, non-specific secretion of IFN-g was still quantified from iLOV T-cells (**6D**, middle panel).

In this trial, the amount of IFN-g secreted from immunized splenocytes was much less compared to previous tests. This suggested variability in the immunity generated between iLOV mice. Furthermore, this variability could be detected and quantified using IFN-g ELISA.

Taken together, Figure 6 demonstrated the use of IFN-g ELISA to detect anti-L1210 immune responses from iLOV splenocytes. iLOV T-cells also appeared to secrete IFN-g non-specifically, but this process may be due to over contact. The biological mechanism behind this remains unknown.

Before further troubleshooting IFN-g ELISAs, we pursued IFN-g ELISpots as a means to quantify the number of reactive immune cells in iLOV immunized mice.

3.1.2 IFN-g ELISpot assay

ELISpots assays are more sensitive than ELISAs because cytokine is directly bound onto the plate whereas cytokine in the supernatant can be degraded and diluted. Furthermore, no information can be obtained about individual IFN-g secreting cells from ELISAs. In contrast, ELISpots can quantify the number of cytokine-secreting cells. Secretion by these cell colonies appear as spots on the developed plates. We tested the applicability of ELISpot assays in detecting and quantifying anti-L1210 immune cells from iLOV mice.

It should be noted that we began using VSV_N peptide instead of UV-MG1 as a positive control because we detected similar amounts of IFN-g secretion from iLOV mice during initial ELISA experiments (data not shown).

The results of this spot-forming reaction can be observed in Figure 7, which displays representative wells from preliminary tests with the IFN-g ELISpot assay. Wells containing iLOV whole splenocytes had qualitatively more spot-forming colonies than unimmunized whole splenocytes (**Figure 7A**). A similar trend was observed by using isolated T-cells as the main effector population (**Figure 7B**).

The minimal amount of spot-forming colonies from isolated T-cells indicated that the T-cell to unimmunized whole splenocyte ratio (1:4) was too low. This was particularly clear when comparing VSV_N peptide controls between wells in **Figure 7A** and **7B**. Future ELISpot assays using isolated T-cells will need a higher ratio.

In both plates, the unimmunized groups co-cultured with iLOV appeared to have many spot-forming colonies. This suggested that innate immune cells, such as NK cells, were secreting IFN-g non-specifically most likely due to live virus (from iLOV) in the wells.

A major concern with these preliminary ELISpot assays was the high background IFN-g "haze" observed in wells containing iLOV or γL1210 as re-stimulants.

Figure 7. High background "haze" observed in IFN-g ELISpot assays with splenocytes or isolated T-cells. In preliminary ELISpot assays, more spots were detected from iLOV immune cells. However, high background haze made it impossible to accurately count the number of spots in co-cultures containing iLOV or γL1210 as re-stimulants. *A*, Whole splenocytes were co-cultured with irradiated cellular re-stimulants at a 5:1 ratio for 16-20 hours. *B*, Isolated T-cells were mixed with unimmunized splenocytes at a ratio of 1:4. This constituted the effector cell population, which was co-cultured with irradiated cellular re-stimulants at a 5:1 ratio for 16-20 hours.
Representative wells shown from technical duplicates. cRPMI media was used for co-cultures. Number of bio-replicates were n = 2 iLOV and n = 1 unimmunized mice.

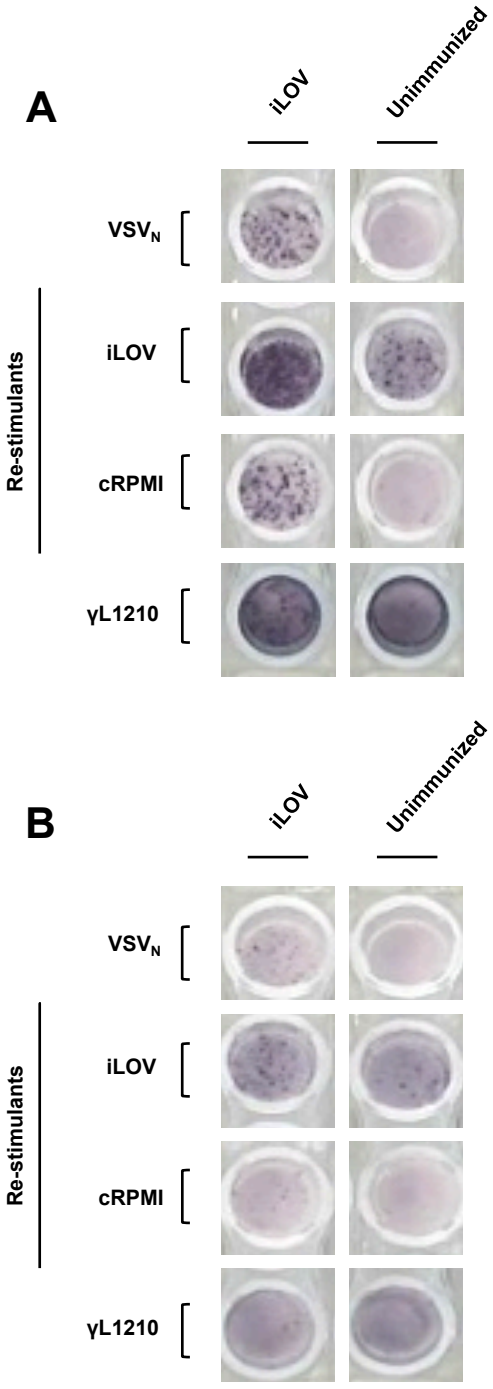
A
iLOV
Unimmunized
VSV$_N$
Re-stimulants
iLOV
cRPMI
γL1210
B
iLOV
Unimmunized
VSV$_N$
Re-stimulants
iLOV
cRPMI
γL1210

This monolayer of IFN-g appeared to interfere with accurate spot counting in the wells. Therefore, this concern warranted further investigation and troubleshooting.

The background haze occurred despite co-culturing iLOV and γL1210 with immunized or unimmunized effector cells. This suggested that the re-stimulants, themselves, were the source of the discrepancy. As both γL1210 and iLOV displayed this monolayer of IFN-g haze, the primary source of this secretion was most likely the L1210 cells (because it occurred regardless of MG1 infection in iLOV). As the goal of the assay was to quantify IFN-g secretion from the effector cell population, the re-stimulant cells were fixed with 1% PFA or treated with GolgiPlug™ to eliminate cytokine secretion (**Figure 8A**). GolgiPlug™ solution contains brefeldin A (BFA), which is a protein transport inhibitor. Specifically, BFA inhibits the machinery to initiate the assembly of transport vesicles in the Golgi apparatus (Nebenführ et al., 2002). Wells containing untreated iLOV and γL1210 cells alone, without effector cells present, continued to have a faint background haze. In contrast, the treated cell preparations did not have any haze. Thus, fixing with 1% PFA or treatment with GolgiPlug™ halted basal IFN-g secretion from iLOV and L1210 cells. A disadvantage of GolgiPlug™ for long assays is that prolonged exposure negatively affects viability. The co-culturing step of the immune assay required a 16-20 hour overnight incubation. Consequently, we proceeded with 1% PFA fixed iLOV (fiLOV) and L1210 (fL1210) preparations for further ELISpot assay troubleshooting

Next, we evaluated whether 1% PFA fixed cells could re-stimulate immunized effector cells. iLOV immunized or unimmunized whole splenocytes were co-cultured with the fixed re-stimulants (**Figure 8B**). Wells containing γL1210 cells were unreadable by the spot reader because of high IFN-g background secretion issues. Non-fixed iLOV co-cultures

Figure 8. Fixed cellular re-stimulants eliminated background haze issues. By fixing re-stimulants or treating them with a protein transport inhibitor, background haze issues were resolved. iLOV splenocytes reacted to these fixed re-stimulants and produced spots. ***A*****,** L1210 and iLOV cells were fixed with 1% PFA solution or treated with 1:1000 GolgiPlug™ in media for the duration of the assay and cultured in ELISpot assay wells for 16-20 hours. Representative wells are shown from technical duplicates. ***B*****,** Irradiated or 1% PFA-fixed iLOV and L1210 were co-cultured with iLOV or unimmunized splenocytes for 16-20 hours. Wells were developed and spots were counted.
Number of bio-replicates were n = 1 unimmunized and n = 2 iLOV-immunized mice, all samples had technical duplicates. cRPMI media was used for cultures unless otherwise specified. Mean and SEM are shown. ND = not detectable due to intense background haze.

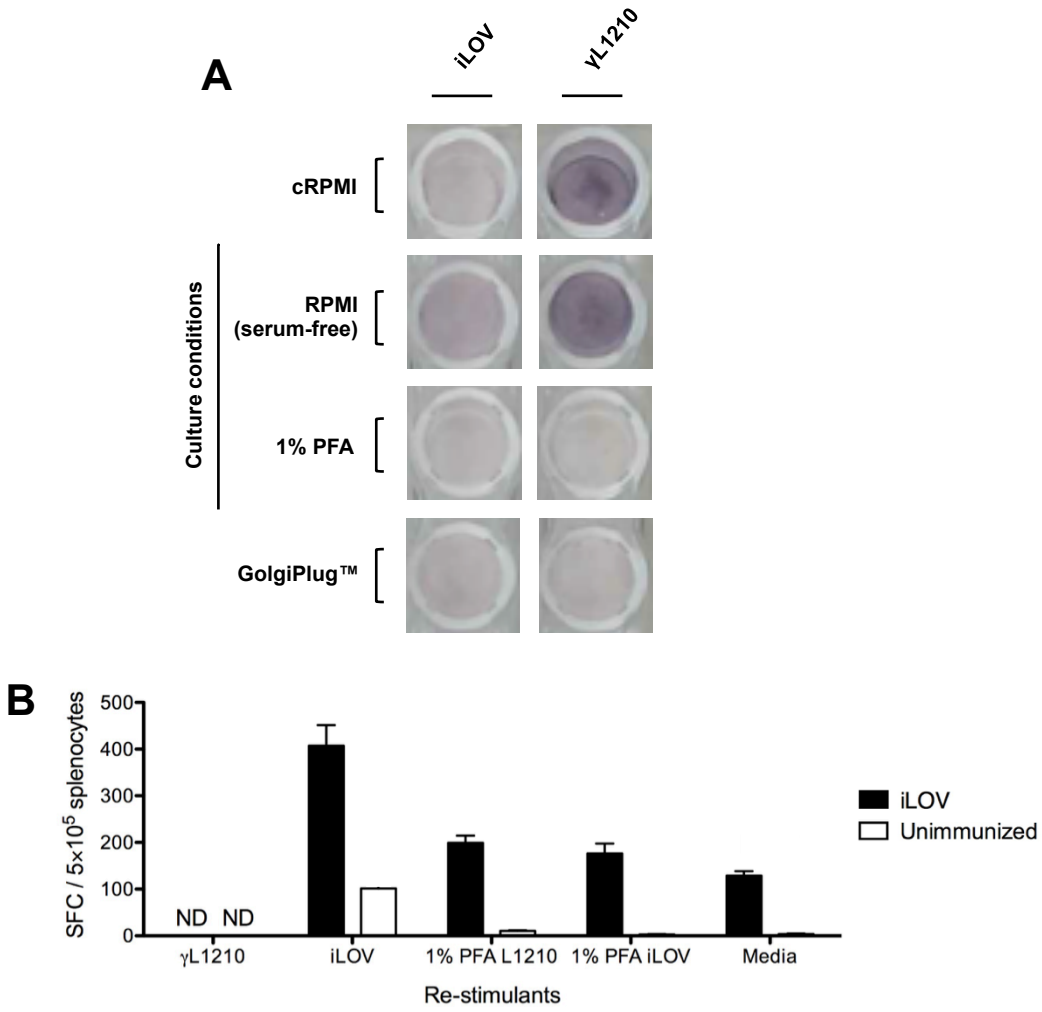
A
iLOV
γL1210
cRPMI
RPMI
(serum-free)
1% PFA
GolgiPlug™
Culture conditions
B
SFC / 5x10^5 splenocytes
500
400
300
200
100
0
ND ND
γL1210
iLOV
1% PFA L1210
1% PFA iLOV
Media
Re-stimulants
iLOV
Unimmunized

had a faint haze in the wells (photo not shown), but were countable. Conversely, wells containing co-cultures with 1% PFA-fixed re-stimulants had no haze (photos not shown).

Wells containing iLOV whole splenocytes co-cultured with fiLOV had half as many spots as co-cultures with non-fixed iLOV. This could be due to fiLOV being less immunogenic, thus less non-specific innate immune cell activation. This would also explain why unimmunized splenocytes no longer secreted non-specific IFN-g in wells containing fiLOV. It is important to note that the number of spots from iLOV splenocytes co-cultured with fL1210 cells was significantly different ($p < 0.05$) from iLOV splenocytes cultured in media alone. Therefore, this response was not entirely due to non-specific IFN-g secretion. Undoubtedly, the issues we faced in our IFN-g ELISA tests with non-specific IFN-g secretion by iLOV immune cells followed us to these ELISpot assays. Finally, a significant difference in the number of spots between immunized and unimmunized whole splenocytes could be observed by using fL1210 cells ($p < 0.05$).

Long-term splenocyte viability experiments compared different media and supplements, such as AIM V® media, 1X DMEM and cRPMI media. We determined that AIM V® media supplemented with 2% HI-HS best sustained murine splenocyte viability. Therefore, this media was used in future ELISpot assays.

IFN-g ELISpot assays incorporating these optimized conditions (i.e., fixed re-stimulants, AIM V® media, and a 4:1 T-cell to unimmunized splenocytes ratio) were performed with iLOV immunized and unimmunized T-cells (**Figure 9**). iLOV T-cells re-stimulated with fiLOV, fL1210 cells, and VSV_N peptide had 2.31, 4.55 and 7.48 times, respectively, more spot forming colonies than their unimmunized T-cell counterparts (all $p < 0.005$). There were 8 times more non-specific IFN-g secreting iLOV T-cells than

Figure 9. IFN-g ELISpot assay detects specific anti-L1210 immune response from iLOV T-cells. T-cells were negatively selected and mixed with unimmunized splenocytes at a 4:1 ratio. These effector cells were co-cultured with fixed cellular re-stimulants at a 5:1 ratio for 16-20 hours.
AIM V® media supplemented with 2% HI-HS was used for all co-cultures. N = 3 mice for all groups, all samples had technical duplicates. Mean and SEM are shown. * $p < 0.05$ ** p-value < 0.005

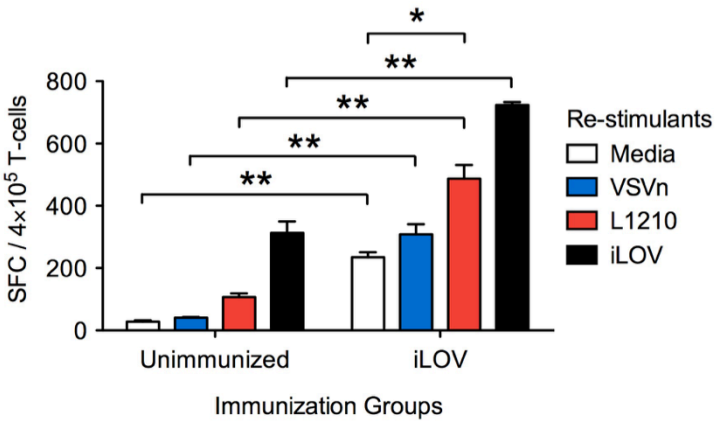
*
**
**
**
**
800
600
400
200
0
SFC / 4x10^5 T-cells
Unimmunized
iLOV
Immunization Groups
Re-stimulants
Media
VSVn
L1210
iLOV

unimmunized T-cells. This latter finding suggested that immunized T-cells had a basal level of activation following iLOV vaccination that was much higher than naïve T-cells.

Thus far, immune cells from iLOV immunized and unimmunized treatment groups were evaluated by the IFN-g ELISpot. Next, we wanted to assess the specificity of the ELISpot assay. To do this, we vaccinated mice with γL1210 cells, MG1 virus, iLOV or PBS and compared IFN-g secretion from their T-cells (**Figure 10A**). iLOV T-cells co-cultured with fixed L1210 cells secreted 1.73 times more spots than γL1210 T-cells, 3.06 times more than MG1 T-cells and 11.84 times more spots than unimmunized T-cells (for all, $p < 0.05$). Unfortunately, the IFN-g response from iLOV T-cells co-cultured with L1210 cells was not significantly different from T-cells cultured in media alone. Therefore, the IFN-g secretion from iLOV mice in this experiment cannot be fully attributed to anti-L1210 immune responses.

L1210 cells are malignant B-cells and by vaccinating against them, perhaps cellular immunity could also be generated to naïve B-cells. To evaluate whether iLOV T-cells were reacting against B-cells, we co-cultured pooled iLOV or unimmunized T-cells with isolated B-cells (**Figure 10B**). B-cells were isolated from unimmunized or iLOV mice. Pooled iLOV T-cells did not secrete significantly more IFN-g when cultured with naïve B-cells or iLOV B-cells than pooled T-cells in media alone. This suggested that the non-specific IFN-g from iLOV T-cells was not due to reactions with naïve B-cells from unimmunized splenocytes, thus autoimmune reactions may be absent in iLOV mice.

Figure 10 demonstrates the ability of the IFN-g ELISpot assay to differentiate the immune responses from iLOV immunized, MG1 immunized, γL1210 immunized and unimmunized T-cells toward fixed L1210 cells. However, due to the high level of nonspecific activation in iLOV T-cells, we recommend further optimization of these assays.

Figure 10. More anti-L1210 T-cells in iLOV mice, but also more non-specific IFN-g secretion. Mice were immunized with PBS, γL1210, MG1 or iLOV. T-cells were isolated and ELISpot assay was performed. iLOV T-cells secreted the most IFN-g when re-stimulated with 1% PFA-fixed L1210 compared to the other groups. Also, iLOV T-cells did not secrete significantly more IFN-g when co-cultured with isolated B-cells. However, in this experiment there was a confounding amount of non-specific IFN-g secretion from iLOV T-cells. ***A*****,** Unimmunized, γL1210, MG1 or iLOV immunized T-cells were mixed with unimmunized whole splenocytes at a 4:1 ratio. These effector cells were co-cultured with fixed cellular re-stimulants at a 5:1 ratio for 16-20 hours. UV-MG1 input was at a MOI 0.2. AIM V® media supplemented with 2% HI-HS was used for all co-cultures. N = 3 mice for all groups, all samples had technical duplicates. Mean and SEM are shown. * p-value < 0.05 ***B,*** Pooled unimmunized or iLOV T-cells were mixed with unimmunized whole splenocytes at a 4:1 ratio. These effector cells were co-cultured with isolated B-cells at a 5:1 ratio for 16-20 hours. B-cells were isolated from unimmunized or iLOV whole splenocytes. AIM V® media supplemented with 2% HI-HS was used for all co-cultures. Technical duplicates were performed for each sample. Mean and SEM are shown.

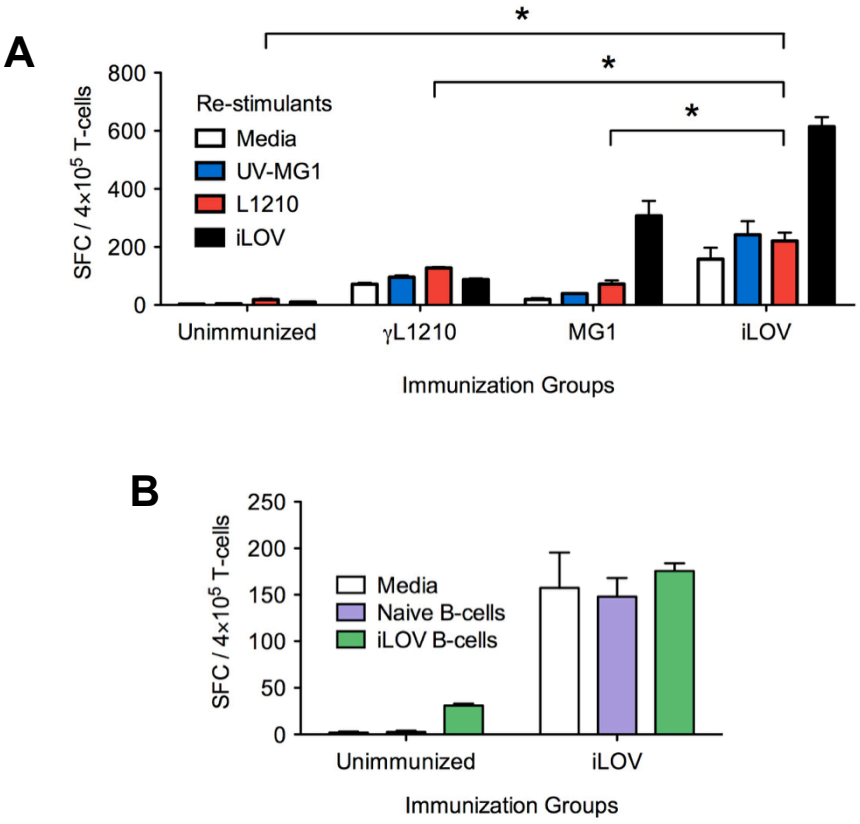
A
*
*
*
800
600
400
200
0
SFC / 4×10^5 T-cells
Re-stimulants
Media
UV-MG1
L1210
iLOV
Unimmunized
γL1210
MG1
iLOV
Immunization Groups
B
250
200
150
100
50
0
SFC / 4×10^5 T-cells
Media
Naive B-cells
iLOV B-cells
Unimmunized
iLOV
Immunization Groups

3.2 iLOV and anti-viral immunity

Anti-viral immunity presents a major challenge for conventional OV therapies. Our next aim was to evaluate how anti-viral immunity interacted with iLOV processing and outcomes.

3.2.1 Anti-viral immunity does not augment iLOV's anti-L1210 immunity

Our group has previously shown that pre-existing anti-viral immunity did not hinder iLOV immunizations from generating a protective anti-L1210 immune response (Conrad et al., 2013). In that experiment, we observed 100% survival in mice immunized with virus prior to iLOV vaccination, and 40% survival in mice immunized with iLOV only. We repeated this experiment (experimental outline in **Figure 11A**) with a larger sample size of nine mice per group compared to the original study using five mice per group. The presence of anti-viral immunity was confirmed prior to iLOV administration in the MG1/iLOV group by performing neutralizing antibody assays (data not shown). After 90-days post-leukemic challenge, the MG1/iLOV and --/iLOV groups each had 89% survival, while all unimmunized control mice perished by Day 17 (**Figure 11B**).

This result confirmed that anti-MG1 viral immunity did not obstruct the ability of iLOV to generate robust and protective anti-L1210 immunity. This experiment could not effectively evaluate an enhancement of anti-L1210 immunity by pre-immunization with virus. In the original experiment, the MG1/iLOV group had a much higher percent survival compared to the --/iLOV group. This lead us to consider that anti-viral immunity could improve iLOV vaccine processing *in vivo* by antigen-presenting cells and result in better anti-L1210 protection. A limitation of this experiment was the inability to observe a possible survival advantage within the MG1/iLOV group. As both MG1/iLOV and --/iLOV treatment

Figure 11. Anti-viral immunity does not hinder iLOV therapy. Reduced survival was not observed in iLOV mice pre-immunized with MG1 virus prior to iLOV administration. ***A*,** Immunization schedule of survival study evaluating mice immunized with 1×10^7 PFU MG1 virus and then 1×10^6 iLOV and challenged with 1×10^7 healthy L1210 cells (designated MG1/iLOV group). Other groups injected were iLOV with challenge (--/iLOV) and the unimmunized control (--/--). All doses were administered by intravenous tail vein injections. ***B*,** Kaplan-Meier survival curve. N = 9 mice per group. Survival was monitored until end point or for 90 days post-challenge.

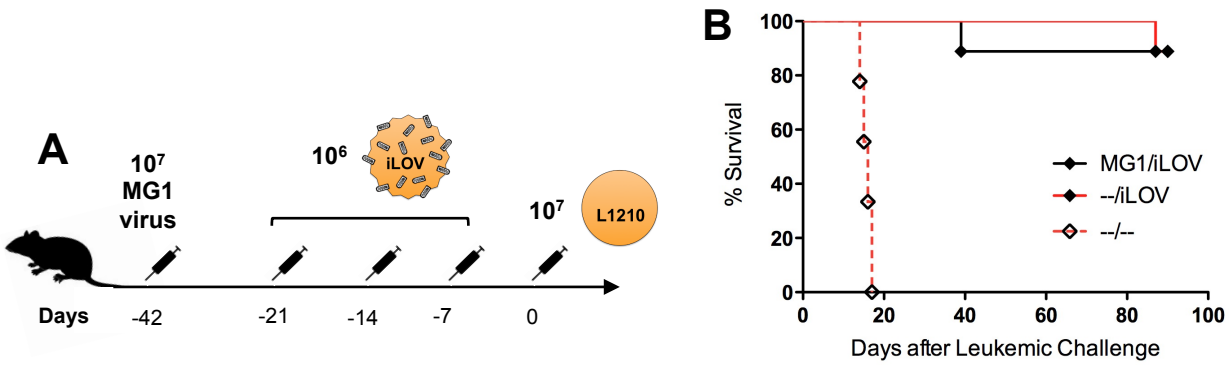
A
10^7
MG1
virus
10^6
iLOV
10^7
L1210
Days
-42
-21
-14
-7
0
B
% Survival
100
80
60
40
20
0
0
20
40
60
80
100
Days after Leukemic Challenge
MG1/iLOV
--/iLOV
--/--

groups had 89% survival, any increase in survival benefit would not be significantly different. Therefore, to evaluate whether anti-viral immunity prior to iLOV could enhance the generation of anti-L1210 immunity, we developed a different immunization schedule.

Dr. Harold Atkins and Girjia Waghray have demonstrated that protection by iLOV is dose-dependent with lower doses conferring lower percent survival. Specifically, three doses of 1×10^4 iLOV conferred 40% survival when challenged with 1×10^6 L1210 cells, while 1×10^5 iLOV cells conferred 80% and 1×10^6 iLOV cells conferred 100% survival (all groups n = 5; unpublished data).

We hypothesized that by using an immunization schedule with 1×10^4 iLOV vaccine doses, any positive augmentation in survival in the MG1/iLOV group could be evaluated. The experimental outline of this survival study (**Figure 12A**) utilized a virus dose of 1×10^8 PFU MG1 virus, 1×10^4 iLOV and a leukemic challenge dose of 1×10^6 L1210 cells. We confirmed anti-viral immunity prior to iLOV in the MG1/iLOV group with neutralizing antibody assays (data not shown). After 90-days post-leukemic challenge, no difference in percent survival was observed between the MG1/iLOV and --/iLOV groups (all mice perished by Day 38; **Figure 12B**). This experiment suggests that no survival benefit was conferred when mice were pre-immunized with MG1 virus prior to iLOV vaccination.

These survival studies provide additional evidence to suggest that anti-viral immunity does not affect iLOV from generating protective anti-L1210 immunity. Although the end result is not affected, we wanted to evaluate whether the presence of anti-viral immunity affected iLOV processing upon administration. Specifically, we wanted to evaluate anti-viral humoral immunity as neutralizing antibodies pose the biggest problem to OV therapies in the clinic. Scenarios wherein iLOV would encounter anti-viral immunity in a clinical setting would be repeated dosing.

Figure 12. Anti-viral immunity does not improve iLOV therapy. Survival was not enhanced in iLOV mice pre-immunized with MG1 virus prior to iLOV administration. ***A*,** Modified immunization schedule of survival study evaluating mice immunized with 1×10^7 PFU MG1 virus and then 1×10^4 iLOV and challenged with 1×10^6 healthy L1210 cells (designated MG1/iLOV group). Other groups included iLOV only with challenge (--/iLOV) and the unimmunized control (--/--). All doses were administered by intravenous tail vein injections. ***B*,** Kaplan-Meier survival curve. N = 9 mice per group. Survival was monitored until end point or for 90 days post-challenge.

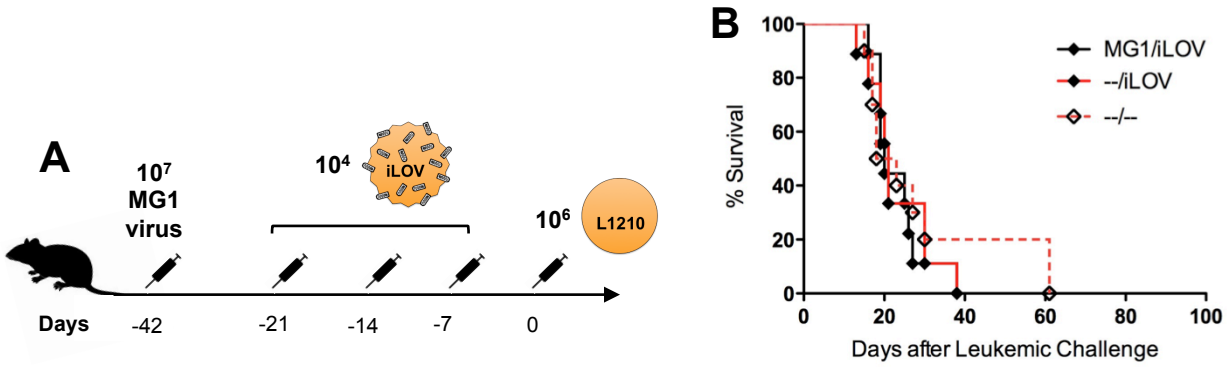
A
10^7
MG1
virus
10^4
iLOV
10^6
L1210
Days
-42
-21
-14
-7
0
B
% Survival
100
80
60
40
20
0
0
20
40
60
80
100
Days after Leukemic Challenge
MG1/iLOV
--/iLOV
--/--

3.2.2 iLOV generates anti-MG1 antibodies

First, we wanted to detect anti-viral humoral and cellular immunity generated by iLOV. The IFN-g ELISpot assays demonstrated the presence of anti-MG1 T-cell immunity following iLOV immunization. To detect anti-viral humoral immunity, blood from mice immunized with iLOV was harvested one day before leukemic challenge (**Figure 13A**). We quantified the neutralizing antibody titer from the serum of these mice and determined the αMG1 antibody titer to be 1:2400 (**Figure 13B**).

Antibodies initiate many innate effector functions once bound to antigens. To begin testing our hypothesis regarding the effects of anti-viral antibodies on iLOV, we needed anti-MG1 antibodies. Mice were given MG1 virus and boosted at a later date to generate anti-MG1 virus (αMG1) antibodies in serum. This was done with adenovirus (αAdenovirus) and sindbis virus (αSindbis virus) as well. We used these specific and control antibodies to determine how readily iLOV bound anti-viral antibodies.

Antibodies in αMG1 serum readily bound the surface of 96.5% iLOV cells as determined by fluorescence microscopy (**Figure 14A**) and flow cytometry analysis (**Figure 14C**). No binding occurred using naïve, αAdenovirus or αSindbis virus serum. This demonstrated that the external cellular membrane of iLOV was sufficiently covered in MG1 epitopes and αMG1 antibodies bound these epitopes to form immune complexes (herein referred to as iLOV immune complexes). In contrast, L1210 cells did not bind any serum antibodies as detected and quantified by fluorescence microscopy and flow cytometry (**Figure 15A** and **15C**).

This experiment demonstrates the ability of iLOV immune complexes to form readily when exposed to αMG1 antibodies. This lead us to evaluate whether innate effector functions

Figure 13. iLOV generates anti-viral humoral immunity. Anti-MG1 antibodies were detected in mice immunized with iLOV. ***A*,** Immunization schedule for iLOV-immunized mice. Mice were immunized with 1×10^6 iLOV and blood was harvested by hind leg saphenous bleeding one day before challenge with 1×10^6 healthy L1210 cells. ***B*,** Titer of anti-MG1 virus antibodies in unimmunized or iLOV mouse serum determined by neutralizing antibody assay.
Serum obtained from n = 5 mice for both groups evaluated. Mean and SEM are shown.

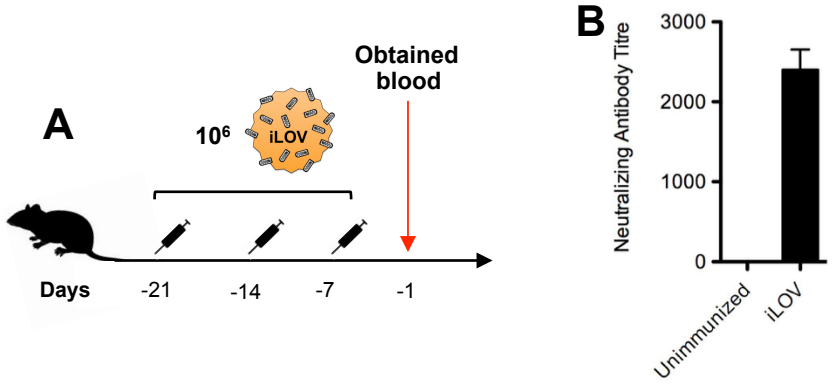
A
Obtained blood
10^6
iLOV
Days
-21
-14
-7
-1
B
Neutralizing Antibody Titre
3000
2000
1000
0
Unimmunized
iLOV

Figure 14. iLOV was specifically bound by anti-MG1 virus antibodies. Only serum from mice immunized with MG1 virus had detectable antibodies binding to iLOV. ***A*****,** Fluorescent photomicrographs of iLOV cells labeled with serum from mice immunized with the indicated viruses. PBS and unimmunized serum serve as negative controls. GFP expression correlated with MG1-GFP virus infection. PE staining correlated with goat anti-mouse IgG-PE binding to cells. Representative photos from five independent experiments are shown. Scale bar represents 200 μm. ***B*****,** Flow cytometry gating strategy used to quantify αMG1 serum binding to iLOV cells. Gate was based on healthy L1210 cell populations. GFP expression from MG1-GFP infection depicted but not quantified. Example dot plot and histograms are from iLOV cells coated in αMG1 virus serum. ***C*****,** Percent gated PE-positive cells were quantified by flow cytometry. Grey reference histogram belongs to iLOV cells incubated with unimmunized mouse serum. Representative histograms from one of five independent experiments are depicted. Mean and SEM are shown.

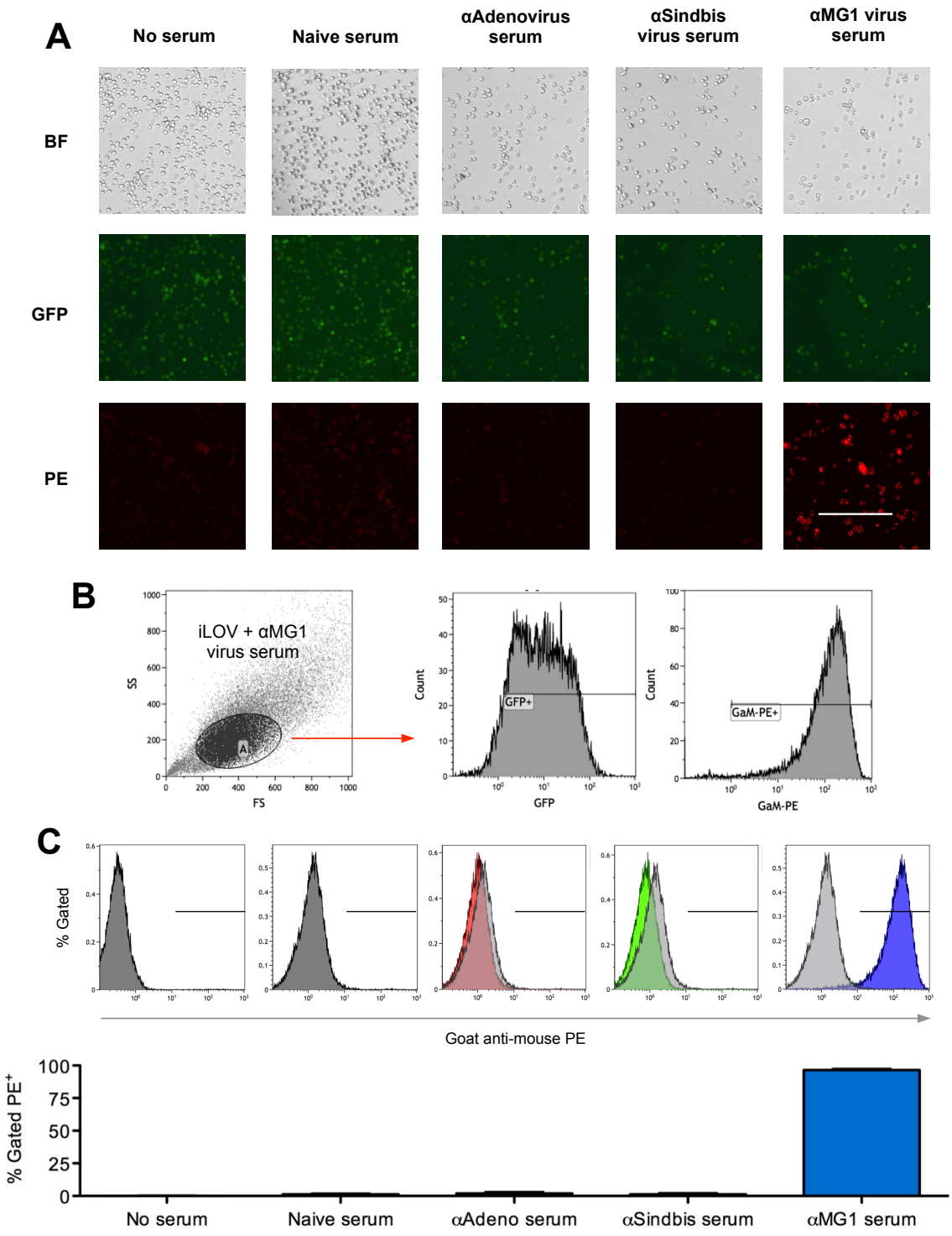
A
No serum
Naive serum
αAdenovirus serum
αSindbis virus serum
αMG1 virus serum
BF
GFP
PE
B
iLOV + αMG1 virus serum
SS
FS
A
Count
GFP+
GFP
GaM-PE+
GaM-PE
C
% Gated
Goat anti-mouse PE
% Gated PE+
No serum
Naive serum
αAdeno serum
αSindbis serum
αMG1 serum

Figure 15. L1210 was not bound by anti-MG1 virus antibodies. No serum antibodies from mice immunized with the designated viruses bound to L1210 cells.
***A*,** Fluorescent photomicrographs of L1210 cells labeled with serum from mice immunized with the indicated viruses. PBS and unimmunized serum serve as negative controls. GFP expression correlated with MG1-GFP virus infection. PE staining correlated with goat anti-mouse IgG-PE binding to cells. Representative photos from five independent experiments are shown. Scale bar represents 200 μm. ***B*,** Flow cytometry gating strategy used to quantify αMG1 serum binding to L1210 cells. Gate was based on healthy L1210 cell populations. GFP expression depicted, but not quantified. Example dot plot and histograms are from L1210 cells coated in αMG1 virus serum. ***C*,** Percent gated PE-positive cells were quantified by flow cytometry. Grey reference histogram belongs to iLOV cells incubated with unimmunized mouse serum (hidden behind coloured histograms). Representative histograms from one of five independent experiments are depicted. Mean and SEM are shown.

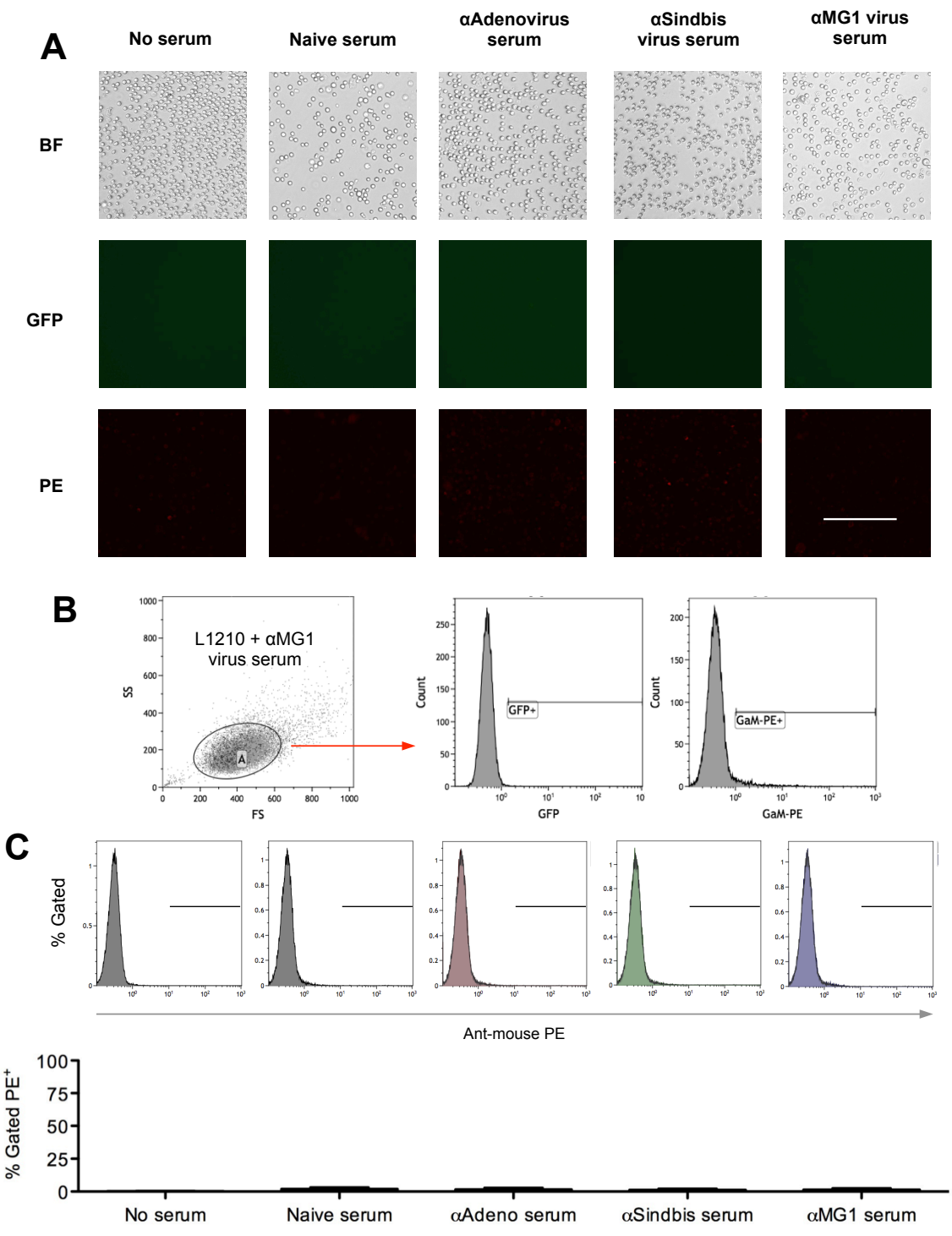
A
No serum
Naive serum
αAdenovirus serum
αSindbis virus serum
αMG1 virus serum
BF
GFP
PE
B
L1210 + αMG1 virus serum
SS
FS
A
Count
GFP+
GFP
GaM-PE+
GaM-PE
C
% Gated
Ant-mouse PE
% Gated PE+
100
75
50
25
0
No serum
Naive serum
αAdeno serum
αSindbis serum
αMG1 serum

such as complement and APC activation were affected by iLOV immune complexes.

3.2.3 C1q deposition on iLOV is Fc-independent

Complement can be activated through Fc-mediated processes involving C1q protein. We tested whether complement deposition was enhanced on iLOV immune complexes. To evaluate this, purified human C1q protein was incubated with iLOV immune complexes and deposition was quantified by flow cytometry. Heat inactivated αMG1 rabbit serum was also used, instead of αMG1 mouse serum, to accommodate the use of the mouse anti-human C1q antibody (schematic outline of reagents in **Figure 16**). These rabbit serum antibodies were confirmed to bind iLOV cells by fluorescence microscopy and flow cytometry (**Figure 17A** and **17C**).

Over the course of an hour, we observed human C1q complement protein efficiently binding iLOV, which was quantified by flow cytometry analysis (**Figure 18B** and **18C**). This effect was not enhanced significantly when iLOV was exposed to αMG1 rabbit serum antibodies. Longer incubation times with iLOV had higher C1q binding. This effect was not observed with L1210 cells with or without exposure to serum. These findings indicate that complement binds iLOV in an antibody Fc-independent manner. Furthermore, these results show that iLOV administered *in vivo* would quickly bind C1q and could be a proficient activator of the complement cascade.

Figure 16. Schematic for C1q complement protein deposition experiment. iLOV or L1210 were fixed with 1% PFA and incubated with heat-inactivated αMG1 or naïve rabbit serum or PBS (no serum). Cell immune complexes were then incubated with human C1q complement protein for 0, 15 or 60 minutes at 37 °C. Mouse anti-human C1q antibody was added to detect the amount of hC1q bound to cells. Goat anti-mouse IgG PE-conjugated antibody was used as the secondary antibody to visualize and quantify C1q binding.

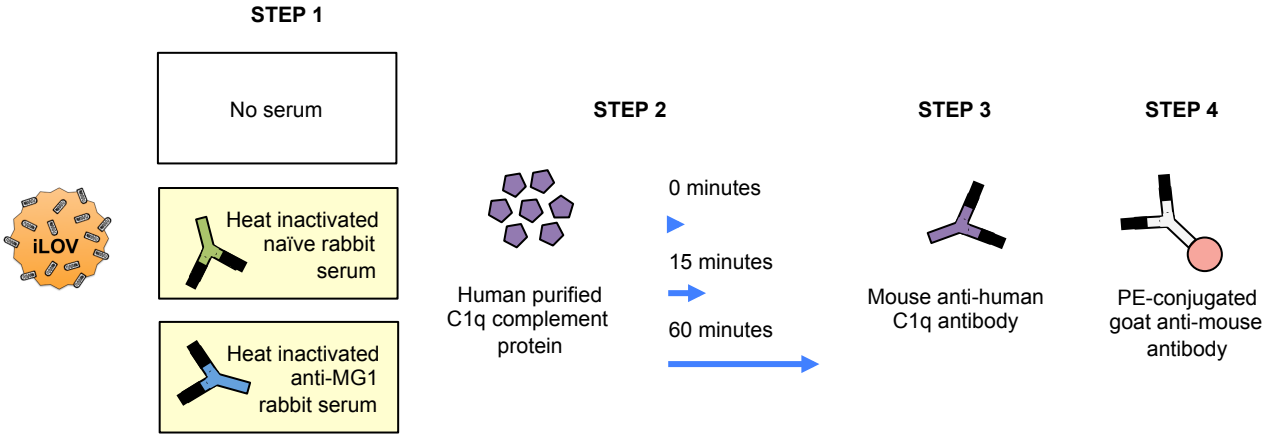
STEP 1
No serum
Heat inactivated naïve rabbit serum
Heat inactivated anti-MG1 rabbit serum
iLOV
STEP 2
Human purified C1q complement protein
0 minutes
15 minutes
60 minutes
STEP 3
Mouse anti-human C1q antibody
STEP 4
PE-conjugated goat anti-mouse antibody

Figure 17. Anti-MG1 virus rabbit serum readily bound iLOV cells. Rabbits were immunized with MG1 virus and their serum was isolated. A neutralizing antibody assay was performed and determined the anti-MG1 antibody titer to be 1:3200. Antibodies in this serum bound to iLOV proficiently. ***A*****,** Representative fluorescent photomicrographs of αMG1 rabbit serum labeling (blue) of iLOV and L1210 cells. GFP expression correlated with MG1-GFP infection. PBS and unimmunized rabbit serum serve as negative controls. Scale bar represents 100 μm. ***B*****,** Gating strategy to quantify Pacific Blue positive cells. Gates based on healthy L1210 cells with unimmunized serum. Example dot plots and histograms depicted belong to iLOV and L1210 cells coated in αMG1 rabbit serum. ***C*****,** Flow cytometry was used to quantify the percent positive Pacific Blue cells in each sample. This quality control experiment was performed twice. Mean and SEM are shown.

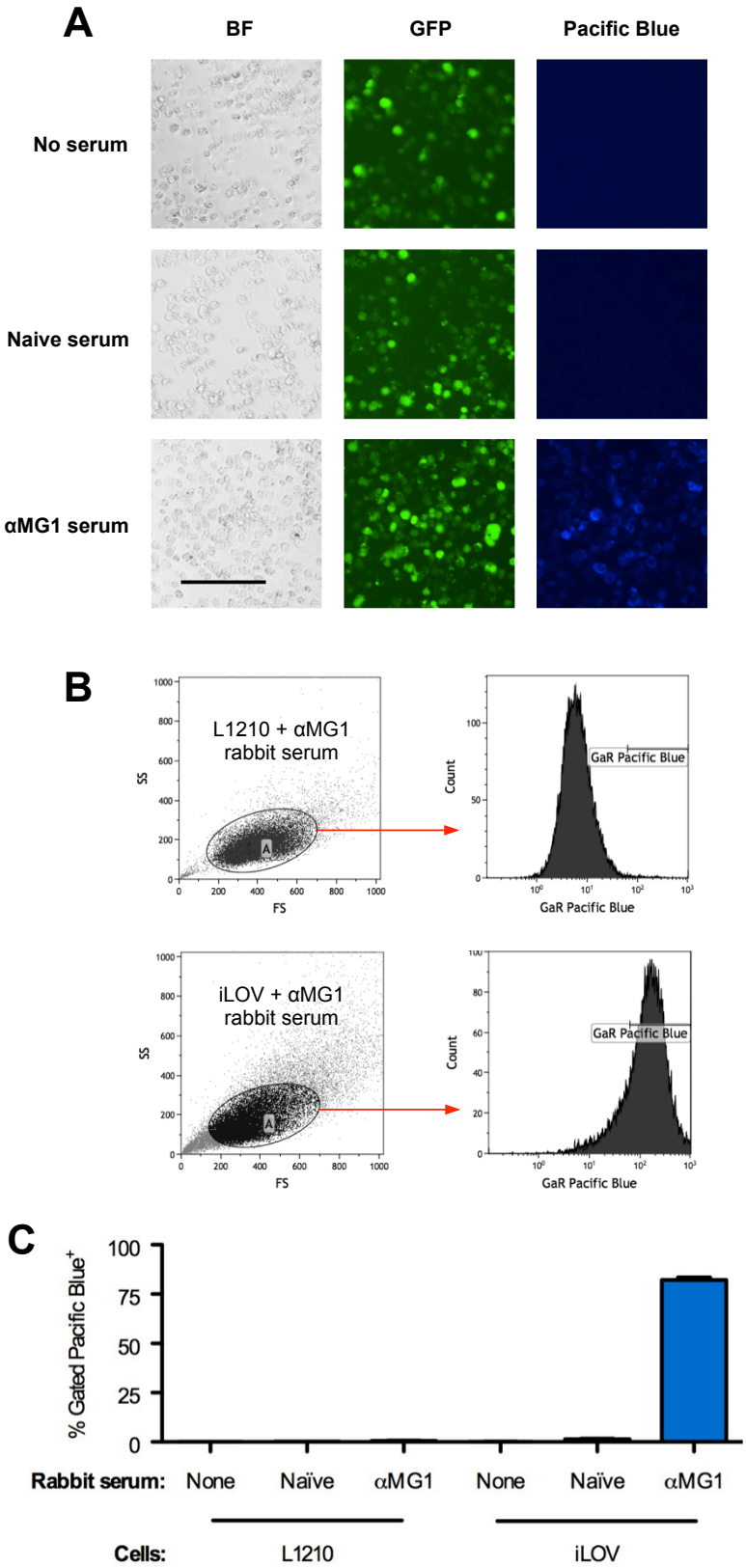
A
BF
GFP
Pacific Blue
No serum
Naive serum
αMG1 serum
B
L1210 + αMG1
rabbit serum
SS
FS
A
Count
GaR Pacific Blue
iLOV + αMG1
rabbit serum
C
% Gated Pacific Blue+
100
75
50
25
0
Rabbit serum:
None
Naïve
αMG1
None
Naïve
αMG1
Cells:
L1210
iLOV

Figure 18. C1q complement protein binds iLOV independently of antibody binding. C1q was imcubated with iLOV and L1210 cells for the designated durations. Over time, only iLOV and iLOV coated in the two different serums had C1q deposition. Deposition between the three samples was not significantly different. ***A*****,** Gating strategy for quantifying C1q binding on iLOV and L1210 cells. Gates based on healthy L1210 cells alone. Example dot plots and histograms belong to iLOV or L1210 cells coated in anti-MG1 rabbit serum. ***B*****,** Representative histograms at each of the timepoints from three replicates are shown. ***C*****,** Percent gated PE positive cells were quantified by flow cytometry. Mean and SEM are shown from three independent experiments.

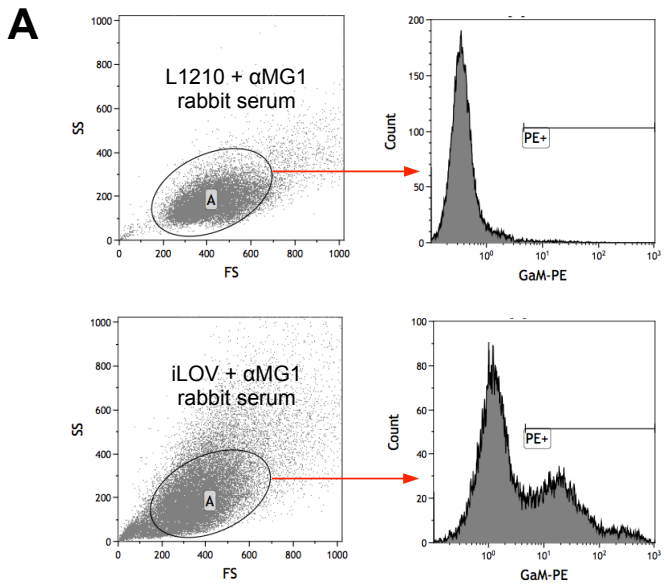
A
L1210 + αMG1
rabbit serum
SS
FS
A
Count
PE+
GaM-PE
iLOV + αMG1
rabbit serum
SS
FS
A
Count
PE+
GaM-PE

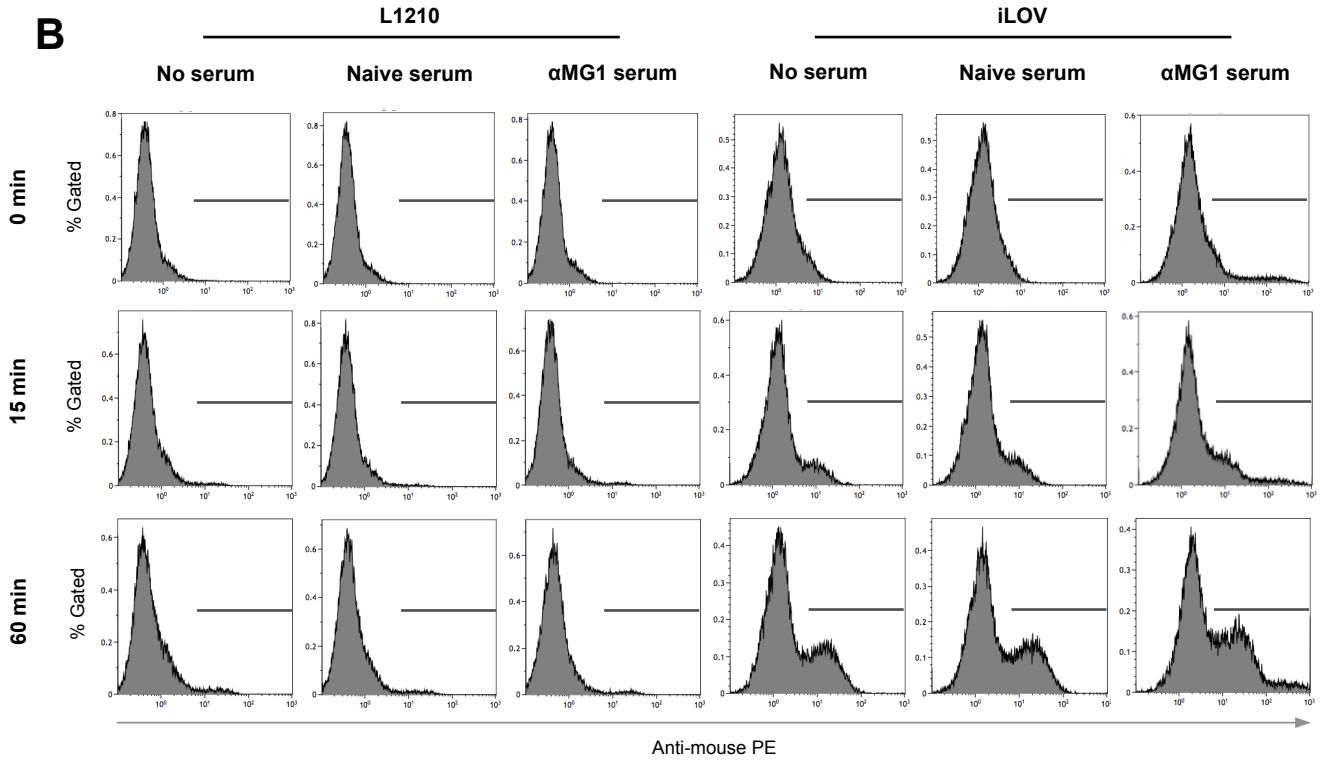
B
L1210
iLOV
No serum
Naive serum
αMG1 serum
No serum
Naive serum
αMG1 serum
0 min
15 min
60 min
% Gated
% Gated
% Gated
Anti-mouse PE

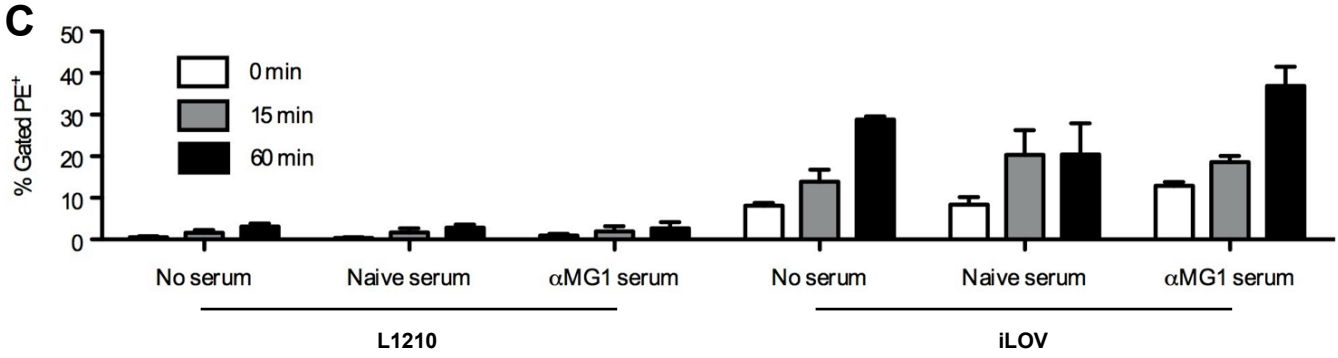
C
% Gated PE+
0 min
15 min
60 min
No serum
Naive serum
αMG1 serum
No serum
Naive serum
αMG1 serum
L1210
iLOV

Figure 19. iLOV activates CD11c$^+$ BMDC despite immune complexes. iLOV and iLOV immune complexes (iLOV + αMG1 serum) were co-cultured with BMDC for 24 hours. Expression of activation markers was not significantly different between these two groups. ***A*,** Flow cytometry gating strategy for quantifying CD86, MHCI and MHCII surface markers on CD19$^-$CD11c$^+$ BMDC. Example dot plots and histograms are from BMDC co-cultured with L1210 cells and no serum. Gates based on isotype controls. ***B*,** Compiled histograms comparing CD86, MHCI and MHCII surface marker expression on CD19$^-$CD11c$^+$ BMDC. Representative histograms from three bio-replicates (BMDC generated from three different mice). Gates based on isotype controls. ***C*,** Mean fluorescence intensity (MFI) quantified by flow cytometry. Mean and SEM are shown from three bio-replicates.

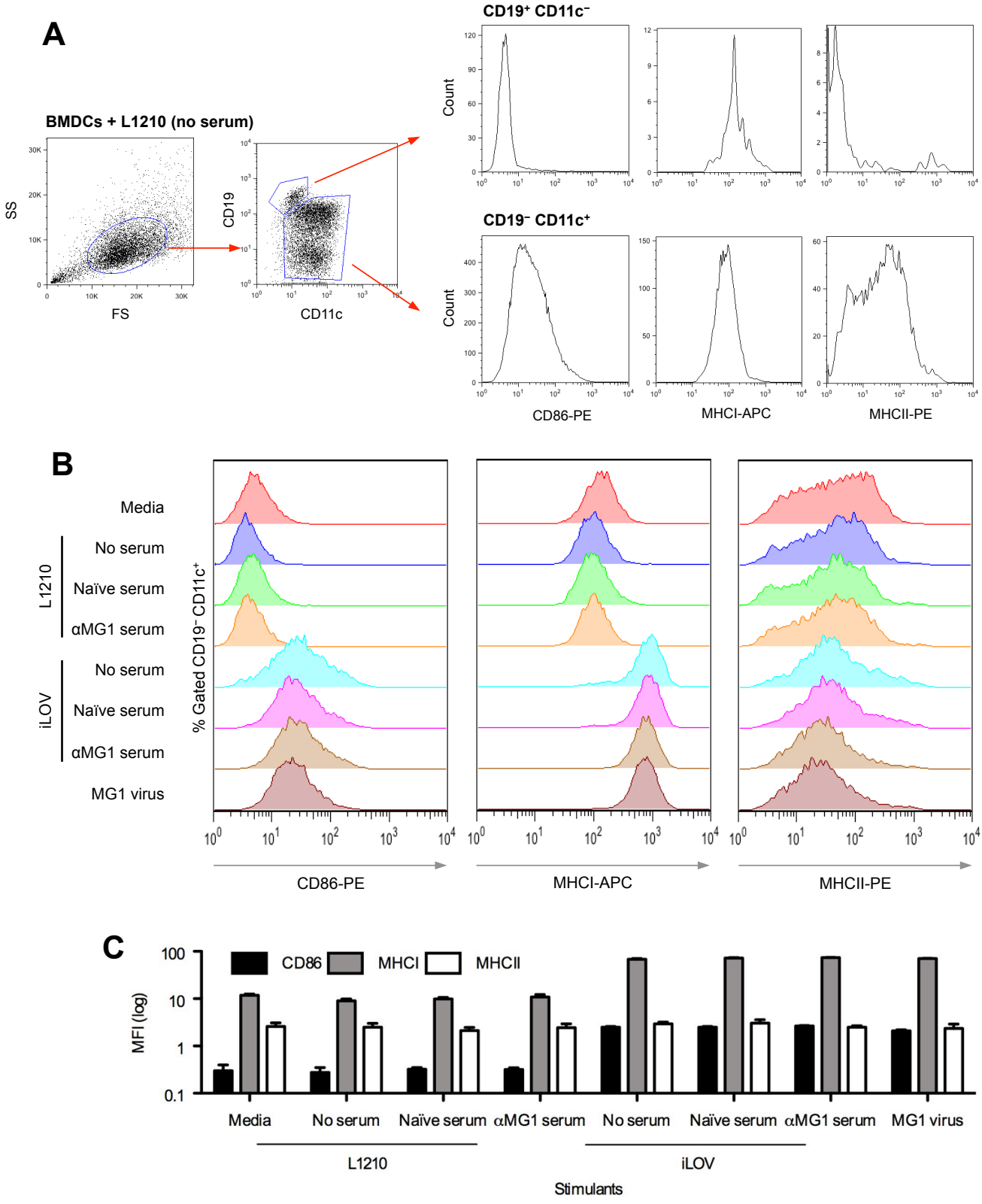
A
BMDCs + L1210 (no serum)
SS
FS
CD19
CD11c
CD19⁺ CD11c⁻
CD19⁻ CD11c⁺
Count
CD86-PE
MHCI-APC
MHCII-PE
B
Media
L1210
No serum
Naïve serum
αMG1 serum
iLOV
No serum
Naïve serum
αMG1 serum
MG1 virus
% Gated CD19⁻ CD11c⁺
CD86-PE
MHCI-APC
MHCII-PE
C
CD86
MHCI
MHCII
MFI (log)
Media
No serum
Naïve serum
αMG1 serum
No serum
Naïve serum
αMG1 serum
MG1 virus
L1210
iLOV
Stimulants

3.2.4 Dendritic cell activation is unaffected by iLOV immune complexes

Immune complexes are recognized by Fc receptors on APC and lead to MHC, class I and II, antigen presentation (Nimmerjahn and Ravetch, 2008). We tested whether iLOV immune complexes enhanced this process with BMDC and quantified the mean fluorescence intensity (MFI) of activation markers by flow cytometry (**Figure 19B** and **19C**). iLOV was capable of activating $CD11c^+$ BMDC as measured by increased expression of the classic activation marker, CD86. Expression of MHC class I molecules also increased, but no significant changes were observed in MHC class II expression. Compared to iLOV alone, iLOV immune complexes did not increase the expression of any of these activation markers on $CD11c^+$ BMDC. Live MG1 virus appeared to be the major contributor of BMDC activation as the virus alone also increased expression of these markers. These results demonstrate that iLOV immune complexes do not hinder efficient BMDC activation and antigen presentation.

4 DISCUSSION

Oncolytic viruses have demonstrated an ability to generate anti-tumour immunity *in vivo*. Our group has exploited this ability by generating an *ex vivo* infected-cell vaccine that can induce *in vivo* anti-leukemia immunity and protecting mice from leukemic challenge. The aim of this work was to advance progress with iLOV in two main areas: 1) develop an *in vitro* immune response assay to detect iLOV anti-leukemia cellular immunity, and 2) elucidate the role and interaction of anti-viral humoral immunity with iLOV.

4.1 Using *in vitro* assays to quantify *in vivo* immune responses

Our preclinical experiments characterizing iLOV used survival curves to evaluate the generation of anti-L1210 immunity (Conrad et al., 2013). For clinical studies, an *in vitro* method to verify the generation of anti-leukemia immunity in patients is needed, as waiting for survival would not be ideal. Therefore, an *in vitro* immune response assay to detect and quantify anti-leukemia immunity must be developed. This *in vitro* assay would ideally differentiate between specific and non-specific as well as protective and non-protective immune responses. We hypothesized that iLOV immune responses could be detected by quantifying the pro-inflammatory cytokine IFN-g. IFN-g is secreted alongside T-cell degranulation on recognized target cells, therefore it serves as an indicator of activation. With this in mind, we developed and tested two *in vitro* immune response assays that quantified IFN-g in iLOV immunized mice.

We first quantified IFN-g using ELISA (**Figure 6**). We found that iLOV splenocytes and specifically iLOV T-cells, compared to unimmunized immune cells, secreted more IFN-g when co-cultured with L1210 cells. IFN-g ELISpots had to be optimized as we ran into

several issues regarding background secretion of IFN-g by target cells (**Figure 7**). We finally found that 1% PFA fixed whole cells resolved these issues (**Figure 8A**) and also re-stimulated immunized splenocytes (**Figure 8B**). Our optimized ELISpot assays showed more IFN-g secreting iLOV T-cell that were re-stimulated by L1210 (**Figure 9**). Unimmunized T-cells did not react to L1210 cells. Additionally, iLOV T-cells did not secrete significantly more IFN-g when re-stimulated with normal B-cells (**Figure 10B**), which may indicate that autoimmune reactions were absent in iLOV mice. When co-cultured with fixed L1210 cells, there were more IFN-g secreting T cells in iLOV mice compared to unimmunized, γL1210 or MG1 virus immunized mice (**Figure 10A**). However, in this particular experiment there was no significant difference between non-specific and anti-L1210 secretion from iLOV T-cells. Non-specific IFN-g secretion from iLOV splenocytes continued to confound certain experiments in ELISpot assay development as it did in our ELISA tests.

4.1.1 Non-specific immune responses

Heightened non-specific immunity can be expected from hosts infected with virus. Zhang et al. (2014) observed splenomegaly and increased innate immune cell numbers, specifically NK cells and DCs, following MG1 virus administration into naïve mice. The amount of IFN-g secreting NK cells spiked one day after MG1 virus infection, but fell rapidly back to baseline at day 5 (Zhang et al., 2014). For the immune response assays, iLOV splenocytes were harvested 7 days following the last iLOV immunization. At this time, the number of activated NK cells would likely be back to baseline levels. However, activated DCs are known to stimulate resting NK cells to secrete IFN-g in a contact-dependent and exogenous cytokine-independent manner (Fernandez et al., 1999). This mechanism could explain the non-specific IFN-g secretion observed from iLOV splenocytes (**Figure 9B** and

10A), especially during ELISA co-cultures in round-bottom 96-well plates where cell pellets naturally form. However, this explanation seems doubtful as non-specific IFN-g was also detected from isolated iLOV T-cells in flat-bottom ELISpot wells. This suggested that T-cells were the main secreting cell type for this non-specific IFN-g response.

Vitiligo autoimmune reactions have been observed in mice treated with Maraba MG1 virus expressing human dopachrome tautomerase (MG1-hDCT) in a prime-boost vaccination setting (Pol et al., 2014). As our isolated T-cells were mixed with unimmunized splenocytes to constitute the effector cell population in ELISA and ELISpot assays, we briefly considered the possibility that autoimmune reactions toward B-cells, the progenitor cell type for L1210 cells, were the source of non-specific IFN-g. Upon culturing isolated T-cells with isolated B-cells, we found that this was not the case and no enhanced IFN-g secretion could be detected (**Figure 10B**). The culprits of non-specific IFN-g secretion are a subset of reactive T cells from iLOV mice and autoimmune reactions are unlikely the cause for this phenomenon.

Oncolytic VSV infection has been documented to generate antigen non-specific T-cell responses, which occurred despite using replication defective or formalin fixed VSV (Galivo et al., 2010). Using depletion experiments, these VSV-induced antigen non-specific T-cells were found to play essential roles in anti-tumour immunity (Willmon et al., 2009). However, their mechanism of action remains unknown. These non-specific IFN-g secreting T-cells may boost weak immune responses of antigen-specific T-cells by secreting various cytokines that could help to initiate the appropriate immune responses. In the L1210 murine model, this would be challenging to test as no L1210-specific peptide has been identified by our group or otherwise reported. Hypothetically, intracellular cytokine staining by flow cytometry (ICS FACS) could identify and compare cytokine profiles and the number of peptide specific T-cells to antigen non-specific T-cells. Based on the literature and our

observations, it would appear these non-specific T-cells are not an artifact of the *in vitro* IFN-g assays and may play an undefined role in iLOV therapy.

Our objective in this section was to develop an *in vitro* immune response assay to detect specific IFN-g secretion from iLOV immunized mice. We partially succeeded in developing an assay that could differentiate between immunized and unimmunized hosts. However, results were complicated by non-specific IFN-g secretion from iLOV splenocytes, particularly from iLOV T-cells.

Although, several insights into the biology of iLOV immune responses have been elucidated from these *in vitro* immune response assays, ELISA and ELISpot assays have their limitations. Information regarding reactive immune cell subpopulations could not be identified using these methods. In order to do this, further purification methods would need to be employed. ICS FACS can identify and quantify expression of surface cell markers and production of cytokines in immune cells en masse. It is a powerful tool that should be optimized to further evaluate iLOV immune responses.

IFN-g production can only be used as a correlate to the protective effects of iLOV therapy. In no way does the detection of anti-L1210 IFN-g secreting T-cells translate to survival upon L1210 leukemia challenge. A more implicative measurement would be to quantify the amount of cytotoxicity in target cells using Chromium-51 or CFSE fluorescent dye. However, a combination of several tools, to profile and characterize the immune responses following iLOV immunization, would be the most robust. The more information gained, the better we can translate these methods for clinical testing.

4.2 Anti-viral humoral immunity

In a clinical setting, iLOV would encounter anti-viral immunity upon subsequent dosing of the patient's personalized iLOV. We showed that anti-viral immunity does not hinder the generation of anti-leukemia immunity. Furthermore, we explored the role of two antibody-mediated mechanisms likely to be encountered when iLOV is administered systemically. Antibodies can initiate several innate effector functions including complement, antibody-dependent cellular cytotoxicity and other Fc receptor-mediated pathways. The first step was to determine whether anti-MG1 antibodies bound iLOV. We found that iLOV was readily bound by anti-MG1 antibodies and that these iLOV immune complexes were sufficiently coated. Our work following this illustrates how anti-MG1 antibodies on iLOV immune complexes do not augment complement deposition or dendritic cell activation.

4.2.1 iLOV immune complexes and complement

Regarding complement, C1q deposition on iLOV was not antibody Fc-mediated. Antibody Fc binding by C1q is a major initiator for the classical complement pathway. Therefore, it was very interesting to observe that when no serum was added, C1q still bound iLOV (**Figure 18B and 18C**). VSV is known to activate complement through natural IgM, which was observed with non-immune human serum (Mills et al., 1979). Although, MG1 maraba virus is a close relative to VSV, it is relatively resistant to natural antibody neutralization (Tesfay et al., 2014). It remains unknown whether serum components in rabbits can facilitate C1q binding to MG1 virus. Despite this, C1q bound readily to iLOV when no rabbit serum was added. Therefore, serum components can be ignored, at least for the purposes of explaining this experiment. C1q protein binds to apoptotic cells, specifically cells undergoing late apoptosis, and this process mediates clearance of dying cells (Nauta et

al., 2002). iLOV is sufficiently apoptotic and we have shown that the majority of iLOV cells undergo late apoptosis by 18-20 hours after MG1 virus infection (Conrad et al., 2013). Cells undergoing apoptosis is a consequence of MG1 virus infection and mediates C1q binding to iLOV.

Complement, itself, interacts with other innate effector systems, such as enhancing opsonization by phagocytes (van Lookeren Campagne et al., 2007) and synergizing with Toll-like receptor signaling (Zhang et al., 2007), both have implications on shaping adaptive immune responses. The relationship between iLOV and complement was previously unknown. Here, we highlight complement's efficient binding to iLOV and its possible influence on vaccine processing by APC and anti-L1210 immunity.

4.2.2 iLOV immune complexes and activating antigen-presenting cells

We next explored whether iLOV immune complexes affected APC activation. Antigen-immune complexes activate dendritic cells in a Fc receptor-mediated manner which leads to enhanced MHC, class I and class II, antigen presentation (Regnault et al., 1999). iLOV or iLOV immune complex co-cultures had higher percentages of BMDC expressing CD86 and MHCI compared to co-cultures with L1210 cells (**Figure 19B and 19C**). However, no difference was observed between iLOV immune complexes and iLOV without serum. This indicated that iLOV, in itself, was a potent BMDC activator after 24 hours of incubation. Live MG1 virus also had enhanced CD86 and MHCI expression. This data suggests that MG1 virus infection was responsible for BMDC activation by iLOV.

Opsonization is another Fc receptor mediated process used by APC. Although there was no difference observed in activation, perhaps iLOV immune complexes are bound and phagocytized more readily through Fc mediated opsonization. To test this, co-cultures

between fluorescently labeled iLOV immune complexes and BMDC could be set up and the amount of co-staining could be observed by fluorescent microscopy and quantified by flow cytometry.

ADCC is also an important Fc-mediated process facilitated by Fc receptor CD16 on NK cells (Lanier, 1998). iLOV immune complexes interacting with ADCC could be evaluated by co-cultures with splenocytes and conducting FACS ICS or measuring Cr-51 release from iLOV. It would be particularly interesting to compare the levels of ADCC between iLOV and iLOV immune complexes.

4.3 iLOV to prevent relapse in ALL

Relapse is a major challenge in ALL. iLOV is a promising immunotherapeutic OV technology that could be applied to resolve issues with relapse. iLOV has the potential to prompt strong anti-leukemia immune responses in patients. In a clinical setting, iLOV could be applied during MRD which is presently not used as a period of time to mount protective immune responses against the malignancy. Current immunotherapies must be genetically engineered, which is time consuming. Furthermore, monoclonal antibodies and CAR T-cells target broadly expressed surface markers on tumours. Compared to conventional immunotherapies, iLOV is advantageous in three aspects: 1) less manipulation is needed, therefore it would be cheaper, 2) vaccines can be created quickly, and 3) every vaccine is personalized. A patient's leukemia cells could be stored at the time of diagnosis, and created into a vaccine following the individual's chemotherapy regimen and if needed HSCT (**Figure 20**). Once their immune system has recovered, the personalized iLOV would be

Figure 20. Clinical context of iLOV. Leukemia cells could be harvested, frozen and stored at the time of diagnostic testing or before therapy. Patients would undergo their recommended chemoradiotherapy regimens and high-risk patients would also undergo hematopoietic stem cell transplantation. When patients have minimal residual disease following therapy recovery, their leukemia cells would be thawed, infected with oncolytic virus and a personalized iLOV vaccine would be administered to them. Patients may require more than one dose to initiated robust anti-leukemia immune responses, which would be evaluated by *in vitro* methods. All this with the opportunity to prevent relapse and provide long term cures.

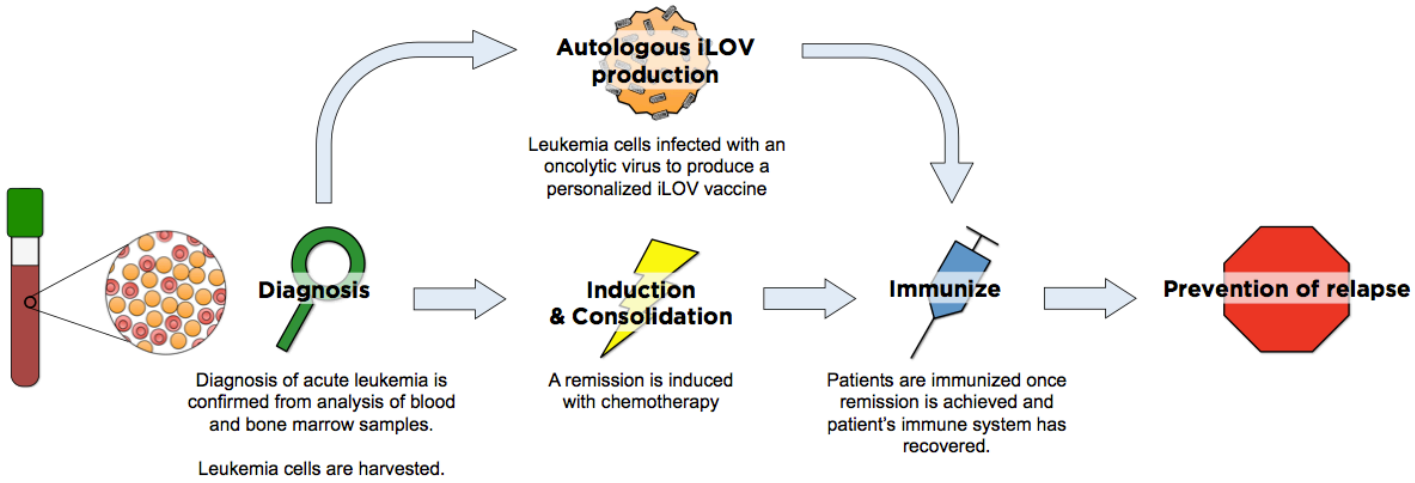
Autologous iLOV production
Leukemia cells infected with an oncolytic virus to produce a personalized iLOV vaccine
Diagnosis
Induction & Consolidation
Immunize
Prevention of relapse
Diagnosis of acute leukemia is confirmed from analysis of blood and bone marrow samples.
Leukemia cells are harvested.
A remission is induced with chemotherapy
Patients are immunized once remission is achieved and patient's immune system has recovered.

administered and anti-leukemia immunity would be tracked with several *in vitro* immune response assays.

The work presented in this thesis outlines the feasibility of using *in vitro* immune response assays to monitor *in vivo* iLOV immune responses directed against L1210 cells. By using IFN-g ELISpot assays, we detected anti-L1210 T-cells upon L1210 re-stimulation. We also discovered a subset of activated T-cells that appeared to be antigen non-specific. More work must be done to fine tune the IFN-g ELISpot assay. We envision its use alongside other *in vitro* immune response assays in order to gain the most accurate picture of iLOV immune responses. This thesis also confirmed that anti-viral immunity did not augment iLOV therapy. We highlighted the ability of iLOV to proficiently bind C1q and activate BMDC. These innate effector processes occurred despite αMG1 antibodies bound to iLOV. Interactions with other innate effector functions could be explored to better understand how repeated doses of iLOV may be affected *in vivo*. In short, we have taken the first steps to demonstrate a systemically delivered OV platform that is not thwarted by neutralizing anti-viral antibodies.

iLOV is a promising immunotherapeutic that aims to provide leukemia relapse prevention on an individualized basis. There is still a long road ahead until iLOV can have its own clinical trial, but meaningful progress will be made with incremental steps.

REFERENCES

Andtbacka, R.H.I., Collichio, F.A., Amatruda, T., Senzer, N.N., Chesney, J., Delman, K.A., Spitler, L.E., Puzanov, I., Doleman, S., Ye, Y., et al. (2013). OPTiM: A randomized phase III trial of talimogene laherparepvec (T-VEC) versus subcutaneous (SC) granulocyte-macrophage colony-stimulating factor (GM-CSF) for the treatment (tx) of unresected stage IIIB/C and IV melanoma. J. Clin. Oncol. *31*, LBA9008.

Bashey, A., Medina, B., Corringham, S., Pasek, M., Carrier, E., Vrooman, L., Lowy, I., Solomon, S.R., Morris, L.E., Holland, H.K., et al. (2009). CTLA4 blockade with ipilimumab to treat relapse of malignancy after allogeneic hematopoietic cell transplantation. Blood *113*, 1581–1588.

Bassan, R., Gatta, G., Tondini, C., and Willemze, R. (2004). Adult acute lymphoblastic leukaemia. Crit. Rev. Oncol. Hematol. *50*, 223–261.

Bassan, R., Spinelli, O., Oldani, E., Intermesoli, T., Tosi, M., Peruta, B., Rossi, G., Borlenghi, E., Pogliani, E.M., Terruzzi, E., et al. (2009). Improved risk classification for risk-specific therapy based on the molecular study of minimal residual disease (MRD) in adult acute lymphoblastic leukemia (ALL). Blood *113*, 4153–4162.

Batliwalla, F.M., Bateman, B. a, Serrano, D., Murray, D., Macphail, S., Maino, V.C., Ansel, J.C., Gregersen, P.K., and Armstrong, C. a (1998). A 15-year follow-up of AJCC stage III malignant melanoma patients treated postsurgically with Newcastle disease virus (NDV) oncolysate and determination of alterations in the CD8 T cell repertoire. Mol. Med. *4*, 783–794.

Bennett, J.M., Catovsky, D., Daniel, M.T., Flandrin, G., Galton, D.A., Gralnick, H.R., and Sultan, C. (1976). Proposals for the classification of the acute leukaemias. French-American-British (FAB) co-operative group. Br. J. Haematol. *33*, 451–458.

Brun, J., McManus, D., Lefebvre, C., Hu, K., Falls, T., Atkins, H., Bell, J.C., McCart, J.A., Mahoney, D., and Stojdl, D.F. (2010). Identification of genetically modified Maraba virus as an oncolytic rhabdovirus. Mol. Ther. *18*, 1440–1449.

Campana, D. (2009). Role of minimal residual disease monitoring in adult and pediatric acute lymphoblastic leukemia. Hematol. Oncol. Clin. North Am. *23*, 1083–1098, vii.

Cassel, W.A., and Garrett, R.E. (1966). Tumor immunity after viral oncolysis. J. Bacteriol. *92*, 792.

Cassel, W.A., and Murray, D.R. (1992). A ten-year follow-up on stage II malignant melanoma patients treated postsurgically with Newcastle disease virus oncolysate. Med. Oncol. Tumor Pharmacother. *9*, 169–171.

Cavé, H., van der Werff ten Bosch, J., Suciu, S., Guidal, C., Waterkeyn, C., Otten, J., Bakkus, M., Thielemans, K., Grandchamp, B., and Vilmer, E. (1998). Clinical significance of minimal residual disease in childhood acute lymphoblastic leukemia. European Organization for Research and Treatment of Cancer--Childhood Leukemia Cooperative Group. N. Engl. J. Med. *339*, 591–598.

Conrad, D.P., Tsang, J., Maclean, M., Diallo, J.-S., Le Boeuf, F., Lemay, C.G., Falls, T.J., Parato, K.A., Bell, J.C., and Atkins, H.L. (2013). Leukemia cell-rhabdovirus vaccine: personalized immunotherapy for acute lymphoblastic leukemia. Clin. Cancer Res. *19*, 3832–3843.

Davila, M.L., Bouhassira, D.C.G., Park, J.H., Curran, K.J., Smith, E.L., Pegram, H.J., and Brentjens, R. (2014). Chimeric antigen receptors for the adoptive T cell therapy of hematologic malignancies. Int. J. Hematol. *99*, 361–371.

DeVita, V.T., and Chu, E. (2008). A history of cancer chemotherapy. Cancer Res. *68*, 8643–8653.

Dock, G. (1904). The influence of complicating diseases upon leukemia. Am J Med Sci *127*, 563–592.

Dunn, G.P., Sheehan, K.C.F., Old, L.J., and Schreiber, R.D. (2005). IFN unresponsiveness in LNCaP cells due to the lack of JAK1 gene expression. Cancer Res. *65*, 3447–3453.

Elert, E. (2013). Living with leukaemia. Nature *498*, S2–S3.

Engeland, C.E., Grossardt, C., Veinalde, R., Bossow, S., Lutz, D., Kaufmann, J.K., Shevchenko, I., Umanksy, V., Nettelbeck, D.M., Weichert, W., et al. (2014). CTLA-4 and PD-L1 Checkpoint Blockade Enhances Oncolytic Measles Virus Therapy. Mol. Ther.

Errington, F., Steele, L., Prestwich, R., Harrington, K.J., Pandha, H.S., Vidal, L., de Bono, J., Selby, P., Coffey, M., Vile, R., et al. (2008). Reovirus activates human dendritic cells to promote innate antitumor immunity. J. Immunol. *180*, 6018–6026.

Fernandez, N.C., Lozier, A., Flament, C., Ricciardi-Castagnoli, P., Bellet, D., Suter, M., Perricaudet, M., Tursz, T., Maraskovsky, E., and Zitvogel, L. (1999). Dendritic cells directly trigger NK cell functions: cross-talk relevant in innate anti-tumor immune responses in vivo. Nat. Med. *5*, 405–411.

Fichera, G. (1918). The Biological Treatment of Cancer. J. Cancer Res. *111*, 303–319.

Finkelshtein, D., Werman, A., Novick, D., Barak, S., and Rubinstein, M. (2013). LDL receptor and its family members serve as the cellular receptors for vesicular stomatitis virus. Proc. Natl. Acad. Sci. U. S. A. *110*, 7306–7311.

Forthal, D.N., and Moog, C. (2009). Fc receptor-mediated antiviral antibodies. Curr. Opin. HIV AIDS *4*, 388–393.

Galivo, F., Diaz, R.M., Wongthida, P., Thompson, J., Kottke, T., Barber, G., Melcher, A., and Vile, R. (2010). Single-cycle viral gene expression, rather than progressive replication and oncolysis, is required for VSV therapy of B16 melanoma. Gene Ther. *17*, 158–170.

Georgiades, J., Zielinski, T., Cicholska, A., and Jordan, E. (1959). Research on the oncolytic effect of APC viruses in cancer of the cervix uteri; preliminary report. Biul. Inst. Med. Morsk. Gdansk. *10*, 49–57.

Goodbourn, S., Didcock, L., and Randall, R.E. (2000). Interferons: cell signalling, immune modulation, antiviral response and virus countermeasures. J. Gen. Virol. *81*, 2341–2364.

Harty, J.T., Tvinnereim, A.R., and White, D.W. (2000). CD8+ T cell effector mechanisms in resistance to infection. Annu. Rev. Immunol. *18*, 275–308.

Heo, J., Reid, T., Ruo, L., Breitbach, C.J., Rose, S., Bloomston, M., Cho, M., Lim, H.Y., Chung, H.C., Kim, C.W., et al. (2013). Randomized dose-finding clinical trial of oncolytic immunotherapeutic vaccinia JX-594 in liver cancer. Nat. Med. *19*, 329–336.

Ho, V.T., and Soiffer, R.J. (2001). The history and future of T-cell depletion as graft-versus-host disease prophylaxis for allogeneic hematopoietic stem cell transplantation. Blood *98*, 3192–3204.

Hochrein, H., Shortman, K., Vremec, D., Scott, B., Hertzog, P., and O'Keeffe, M. (2001). Differential production of IL-12, IFN-alpha, and IFN-gamma by mouse dendritic cell subsets. J. Immunol. *166*, 5448–5455.

Huang, S., Hendriks, W., Althage, A., Hemmi, S., Bluethmann, H., Kamijo, R., Vilcek, J., Zinkernagel, R., and Aguet, M. (1993). Immune response in mice that lack the interferon-gamma receptor. Science (80-.). *259*, 1742–1745.

Hunger, S.P., Lu, X., Devidas, M., Camitta, B.M., Gaynon, P.S., Winick, N.J., Reaman, G.H., and Carroll, W.L. (2012). Improved survival for children and adolescents with acute lymphoblastic leukemia between 1990 and 2005: a report from the children's oncology group. J. Clin. Oncol. *30*, 1663–1669.

Iankov, I.D., Blechacz, B., Liu, C., Schmeckpeper, J.D., Tarara, J.E., Federspiel, M.J., Caplice, N., and Russell, S.J. (2007). Infected cell carriers: a new strategy for systemic delivery of oncolytic measles viruses in cancer virotherapy. Mol. Ther. *15*, 114–122.

Ikeda, K., Ichikawa, T., Wakimoto, H., Silver, J.S., Deisboeck, T.S., Finkelstein, D., Harsh, G.R., Louis, D.N., Bartus, R.T., Hochberg, F.H., et al. (1999). Oncolytic virus therapy of multiple tumors in the brain requires suppression of innate and elicited antiviral responses. Nat. Med. *5*, 881–887.

Javier, R.T., and Butel, J.S. (2008). The history of tumor virology. Cancer Res. *68*, 7693–7706.

Joffre, O.P., Segura, E., Savina, A., and Amigorena, S. (2012). Cross-presentation by dendritic cells. Nat. Rev. Immunol. *12*, 557–569.

Kaufmann, J.K., and Nettelbeck, D.M. (2012). Virus chimeras for gene therapy, vaccination, and oncolysis: adenoviruses and beyond. Trends Mol. Med. *18*, 365–376.

Kelly, E., and Russell, S.J. (2007). History of oncolytic viruses: genesis to genetic engineering. Mol. Ther. *15*, 651–659.

Krummel, M.F., and Allison, J.P. (1995). CD28 and CTLA-4 have opposing effects on the response of T cells to stimulation. J. Exp. Med. *182*, 459–465.

Kurzrock, R., Kantarjian, H.M., Druker, B.J., and Talpaz, M. (2003). Philadelphia chromosome-positive leukemias: from basic mechanisms to molecular therapeutics. Ann. Intern. Med. *138*, 819–830.

Lanier, L.L. (1998). NK cell receptors. Annu. Rev. Immunol. *16*, 359–393.

Lemay, C.G., Rintoul, J.L., Kus, A., Paterson, J.M., Garcia, V., Falls, T.J., Ferreira, L., Bridle, B.W., Conrad, D.P., Tang, V.A., et al. (2012). Harnessing oncolytic virus-mediated antitumor immunity in an infected cell vaccine. Mol. Ther. *20*, 1791–1799.

Lichty, B.D., Power, A.T., Stojdl, D.F., and Bell, J.C. (2004a). Vesicular stomatitis virus: re-inventing the bullet. Trends Mol. Med. *10*, 210–216.

Lichty, B.D., Stojdl, D.F., Taylor, R.A., Miller, L., Frenkel, I., Atkins, H., and Bell, J.C. (2004b). Vesicular stomatitis virus: a potential therapeutic virus for the treatment of hematologic malignancy. Hum. Gene Ther. *15*, 821–831.

Lindenmann, J. (1967). Viral oncolysis: increased immunogenicity of host cell antigen associated with influenza virus. J. Exp. Med. *126*, 93–108.

Lindenmann, J. (1970). Immunogenicity of oncolysates obtained from Ehrlich ascites tumors infected with vesicular stomatitis virus. Arch. Gesamte Virusforsch. *31*, 61–70.

Van Lookeren Campagne, M., Wiesmann, C., and Brown, E.J. (2007). Macrophage complement receptors and pathogen clearance. Cell. Microbiol. *9*, 2095–2102.

Lun, X., Senger, D.L., Alain, T., Oprea, A., Parato, K., Stojdl, D., Lichty, B., Power, A., Johnston, R.N., Hamilton, M., et al. (2006). Effects of intravenously administered recombinant vesicular stomatitis virus (VSV(deltaM51)) on multifocal and invasive gliomas. J. Natl. Cancer Inst. *98*, 1546–1557.

Mastrangelo, M.J., Maguire, H.C., Eisenlohr, L.C., Laughlin, C.E., Monken, C.E., McCue, P.A., Kovatich, A.J., and Lattime, E.C. (1999). Intratumoral recombinant GM-CSF-encoding virus as gene therapy in patients with cutaneous melanoma. Cancer Gene Ther. *6*, 409–422.

Melcher, A., Parato, K., Rooney, C.M., and Bell, J.C. (2011). Thunder and lightning: immunotherapy and oncolytic viruses collide. Mol. Ther. *19*, 1008–1016.

Mills, B.J., Beebe, D.P., and Cooper, N.R. (1979). Antibody-independent neutralization of vesicular stomatitis virus by human complement. II. Formation of VSV-lipoprotein complexes in human serum and complement-dependent viral lysis. J. Immunol. *123*, 2518–2524.

Moore, A. (1949a). The destructive effect of the virus of Russian Far East encephalitis on the transplantable mouse sarcoma 180. Cancer *2*, 525–534.

Moore, A. (1949b). Effect of inoculation of the viruses of influenza A and herpes simplex on the growth of transplantable tumors in mice. Cancer *2*, 516–524.

Moorman, A. V, Richards, S.M., Martineau, M., Cheung, K.L., Robinson, H.M., Jalali, G.R., Broadfield, Z.J., Harris, R.L., Taylor, K.E., Gibson, B.E.S., et al. (2003). Outcome heterogeneity in childhood high-hyperdiploid acute lymphoblastic leukemia. Blood *102*, 2756–2762.

Muik, A., Stubbert, L.J., Jahedi, R.Z., Geiβ, Y., Kimpel, J., Dold, C., Tober, R., Volk, A., Klein, S., Dietrich, U., et al. (2014). Re-engineering vesicular stomatitis virus to abrogate neurotoxicity, circumvent humoral immunity, and enhance oncolytic potency. Cancer Res. *74*, 3567–3578.

Munguia, A., Ota, T., Miest, T., and Russell, S.J. (2008). Cell carriers to deliver oncolytic viruses to sites of myeloma tumor growth. Gene Ther. *15*, 797–806.

Muñoz-Fernández, M.A., Fernández, M.A., and Fresno, M. (1992). Activation of human macrophages for the killing of intracellular Trypanosoma cruzi by TNF-alpha and IFN-gamma through a nitric oxide-dependent mechanism. Immunol. Lett. *33*, 35–40.

Naik, S., Nace, R., Federspiel, M.J., Barber, G.N., Peng, K., and Russell, S.J. (2012). Curative one-shot systemic virotherapy in murine myeloma. Leukemia *26*, 1870–1878.

Narayanan, S., and Shami, P.J. (2012). Treatment of acute lymphoblastic leukemia in adults. Crit. Rev. Oncol. Hematol. *81*, 94–102.

Nauta, A.J., Trouw, L. a, Daha, M.R., Tijsma, O., Nieuwland, R., Schwaeble, W.J., Gingras, A.R., Mantovani, A., Hack, E.C., and Roos, A. (2002). Direct binding of C1q to apoptotic cells and cell blebs induces complement activation. Eur. J. Immunol. *32*, 1726–1736.

Nava, V.E., and Jaffe, E.S. (2005). The pathology of NK-cell lymphomas and leukemias. Adv. Anat. Pathol. *12*, 27–34.

Nebenführ, A., Ritzenthaler, C., and Robinson, D.G. (2002). Brefeldin A: deciphering an enigmatic inhibitor of secretion. Plant Physiol. *130*, 1102–1108.

Nguyen, K., Devidas, M., Cheng, S.-C., La, M., Raetz, E. a, Carroll, W.L., Winick, N.J., Hunger, S.P., Gaynon, P.S., and Loh, M.L. (2008). Factors influencing survival after relapse from acute lymphoblastic leukemia: a Children's Oncology Group study. Leukemia *22*, 2142–2150.

Nimmerjahn, F., and Ravetch, J. V (2008). Fcgamma receptors as regulators of immune responses. Nat. Rev. Immunol. *8*, 34–47.

Pasquini, M., and Wang, Z. (2013). Current use and outcome of hematopoietic stem cell transplantation.

Pol, J.G., Zhang, L., Bridle, B.W., Stephenson, K.B., Rességuier, J., Hanson, S., Chen, L., Kazdhan, N., Bramson, J.L., Stojdl, D.F., et al. (2014). Maraba virus as a potent oncolytic vaccine vector. Mol. Ther. *22*, 420–429.

Power, A.T., Wang, J., Falls, T.J., Paterson, J.M., Parato, K.A., Lichty, B.D., Stojdl, D.F., Forsyth, P.A.J., Atkins, H., and Bell, J.C. (2007). Carrier cell-based delivery of an oncolytic virus circumvents antiviral immunity. Mol. Ther. *15*, 123–130.

Prestwich, R.J., Ilett, E.J., Errington, F., Diaz, R.M., Steele, L.P., Kottke, T., Thompson, J., Galivo, F., Harrington, K.J., Pandha, H.S., et al. (2009). Immune-mediated antitumor activity of reovirus is required for therapy and is independent of direct viral oncolysis and replication. Clin. Cancer Res. *15*, 4374–4381.

Pui, C.-H., and Evans, W.E. (2006). Treatment of acute lymphoblastic leukemia. N. Engl. J. Med. *354*, 166–178.

Quah, B.J.C., Warren, H.S., and Parish, C.R. (2007). Monitoring lymphocyte proliferation in vitro and in vivo with the intracellular fluorescent dye carboxyfluorescein diacetate succinimidyl ester. Nat. Protoc. *2*, 2049–2056.

Rambaldi, A., Biagi, E., Bonini, C., Biondi, A., and Introna, M. (2014). Cell-based strategies to manage leukemia relapse: efficacy and feasibility of immunotherapy approaches. Leukemia 1–10.

Ratei, R., Schabath, R., Karawajew, L., Zimmermann, M., Möricke, A., Schrappe, M., and Ludwig, W.-D. (2013). Lineage classification of childhood acute lymphoblastic leukemia according to the EGIL recommendations: results of the ALL-BFM 2000 trial. Klin. Pädiatrie *225 Suppl*, S34–S39.

Regnault, A., Lankar, D., Lacabanne, V., Rodriguez, A., Théry, C., Rescigno, M., Saito, T., Verbeek, S., Bonnerot, C., Ricciardi-Castagnoli, P., et al. (1999). Fcgamma receptor-mediated induction of dendritic cell maturation and major histocompatibility complex class I-restricted antigen presentation after immune complex internalization. J. Exp. Med. *189*, 371–380.

Schrappe, M., Hunger, S.P., Pui, C.-H., Saha, V., Gaynon, P.S., Baruchel, A., Conter, V., Otten, J., Ohara, A., Versluys, A.B., et al. (2012). Outcomes after induction failure in childhood acute lymphoblastic leukemia. N. Engl. J. Med. *366*, 1371–1381.

Shafer-weaver, K., Sayers, T., Strobl, S., Derby, E., Ulderich, T., Baseler, M., and Malyguine, A. (2003). The Granzyme B ELISPOT assay: an alternative to the 51 Cr-release assay for monitoring cell-mediated cytotoxicity. J. Transl. Med. *1*, 1–9.

Smith, W., Andrewes, C.H., and Laidlaw, P.P. (1933). A virus obtained from influenza patients. Lancet *2*, 66–68.

Southam, C.M., and Moore, A.E. (1952). Clinical studies of viruses as antineoplastic agents with particular reference to Egypt 101 virus. Cancer *5*, 1025–1034.

Stojdl, D.F., Lichty, B., Knowles, S., Marius, R., Atkins, H., Sonenberg, N., and Bell, J.C. (2000). Exploiting tumor-specific defects in the interferon pathway with a previously unknown oncolytic virus. Nat. Med. *6*, 821–825.

Tesfay, M.Z., Ammayappan, A., Federspiel, M.J., Barber, G.N., Stojdl, D., Peng, K.-W., and Russell, S.J. (2014). Vesiculovirus neutralization by natural IgM and complement. J. Virol. *88*, 6148–6157.

Tesh, R.B., Boshell, J., Modi, G.B., Morales, A., Young, D.G., Corredor, A., Ferro de Carrasquilla, C., de Rodriguez, C., Walters, L.L., and Gaitan, M.O. (1987). Natural infection of humans, animals, and phlebotomine sand flies with the Alagoas serotype of vesicular stomatitis virus in Colombia. Am. J. Trop. Med. Hyg. *36*, 653–661.

Thiery, J., and Lieberman, J. (2014). Perforin: a key pore-forming protein for immune control of viruses and cancer. Subcell. Biochem. *80*, 197–220.

Trapani, J.A., and Sutton, V.R. (2003). Granzyme B: pro-apoptotic, antiviral and antitumor functions. Curr. Opin. Immunol. *15*, 533–543.

Travassos da Rosa, A.P., Tesh, R.B., Travassos da Rosa, J.F., Herve, J.P., and Main, A.J. (1984). Carajas and Maraba viruses, two new vesiculoviruses isolated from phlebotomine sand flies in Brazil. Am. J. Trop. Med. Hyg. *33*, 999–1006.

Tsai, V., Johnson, D.E., Rahman, A., Wen, S.F., LaFace, D., Philopena, J., Nery, J., Zepeda, M., Maneval, D.C., Demers, G.W., et al. (2004). Impact of human neutralizing antibodies on

antitumor efficacy of an oncolytic adenovirus in a murine model. Clin. Cancer Res. *10*, 7199–7206.

Vardiman, J.W., Thiele, J., Arber, D.A., Brunning, R.D., Borowitz, M.J., Porwit, A., Harris, N.L., Le Beau, M.M., Hellström-Lindberg, E., Tefferi, A., et al. (2009). The 2008 revision of the World Health Organization (WHO) classification of myeloid neoplasms and acute leukemia: rationale and important changes. Blood *114*, 937–951.

Vonderheide, R.H., and June, C.H. (2014). Engineering T cells for cancer: our synthetic future. Immunol. Rev. *257*, 7–13.

Weiner, G.J. (2010). Rituximab: mechanism of action. Semin. Hematol. *47*, 115–123.

Weiner, L.M., Surana, R., and Wang, S. (2010). Monoclonal antibodies: versatile platforms for cancer immunotherapy. Nat. Rev. Immunol. *10*, 317–327.

Willmon, C.L., Saloura, V., Fridlender, Z.G., Wongthida, P., Diaz, R.M., Thompson, J., Kottke, T., Federspiel, M., Barber, G., Albelda, S.M., et al. (2009). Expression of IFN-beta enhances both efficacy and safety of oncolytic vesicular stomatitis virus for therapy of mesothelioma. Cancer Res. *69*, 7713–7720.

Wong, L.H., Krauer, K.G., Hatzinisiriou, I., Estcourt, M.J., Hersey, P., Tam, N.D., Edmondson, S., Devenish, R.J., and Ralph, S.J. (1997). Interferon-resistant human melanoma cells are deficient in ISGF3 components, STAT1, STAT2, and p48-ISGF3gamma. J. Biol. Chem. *272*, 28779–28785.

Workenhe, S.T., and Mossman, K.L. (2014). Oncolytic virotherapy and immunogenic cancer cell death: sharpening the sword for improved cancer treatment strategies. Mol. Ther. *22*, 251–256.

Workenhe, S.T., Simmons, G., Pol, J.G., Lichty, B.D., Halford, W.P., and Mossman, K.L. (2014). Immunogenic HSV-mediated oncolysis shapes the antitumor immune response and contributes to therapeutic efficacy. Mol. Ther. *22*, 123–131.

Zamarin, D., Holmgaard, R.B., Subudhi, S.K., Park, J.S., Mansour, M., Palese, P., Merghoub, T., Wolchok, J.D., and Allison, J.P. (2014). Localized oncolytic virotherapy overcomes systemic tumor resistance to immune checkpoint blockade immunotherapy. Sci. Transl. Med. *6*, 226ra32.

Zhang, J., Tai, L.-H., Ilkow, C.S., Alkayyal, A.A., Ananth, A.A., de Souza, C.T., Wang, J., Sahi, S., Ly, L., Lefebvre, C., et al. (2014). Maraba MG1 virus enhances natural killer cell function via conventional dendritic cells to reduce postoperative metastatic disease. Mol. Ther. *22*, 1320–1332.

Zhang, X., Kimura, Y., Fang, C., Zhou, L., Sfyroera, G., Lambris, J.D., Wetsel, R. a, Miwa, T., and Song, W.-C. (2007). Regulation of Toll-like receptor-mediated inflammatory response by complement in vivo. Blood *110*, 228–236.

Zinkernagel, R.M., LaMarre, A., Ciurea, A., Hunziker, L., Ochsenbein, a F., McCoy, K.D., Fehr, T., Bachmann, M.F., Kalinke, U., and Hengartner, H. (2001). Neutralizing antiviral antibody responses. Adv. Immunol. *79*, 1–53.

CONTRIBUTIONS OF COLLABORATORS

Mina Rizk conducted splenocyte viability experiments to determine the best media and serum combinations to use for short-term and long-term culturing experiments. Theresa Falls skillfully executed all intravenous tail vein injections for animal work. Girjia “Geeta” Waghray and Dr. Harold Atkins conducted the iLOV dose-dependent animal study.

APPENDIX I

Leukemia Cell-Rhabdovirus Vaccine: Personalized Immunotherapy for Acute Lymphoblastic Leukemia

David P. Conrad, **Jovian Tsang**, Meaghan Maclean, Jean-Simon Diallo, Fabrice Le Boeuf, Chantal G. Lemay, Theresa J. Falls, Kelley A. Parato, John C. Bell, and Harold L. Atkins

Contributions of author: J. Tsang was an ongoing collaborator on this project. He conducted the L1210 cell viability/virus infection time-course, assisted with several animal experiments and with preparing the manuscript for submission.

Published: *Clinical Cancer Research*, June 2013

Published OnlineFirst May 28, 2013; DOI: 10.1158/1078-0432.CCR-12-3199

Clinical Cancer Research

Leukemia Cell-Rhabdovirus Vaccine: Personalized Immunotherapy for Acute Lymphoblastic Leukemia

David P. Conrad, Jovian Tsang, Meaghan Maclean, et al.

Clin Cancer Res 2013;19:3832-3843. Published OnlineFirst May 28, 2013.

Published OnlineFirst May 28, 2013; DOI: 10.1158/1078-0432.CCR-12-3199

Cancer Therapy: Preclinical

Clinical Cancer Research

Leukemia Cell-Rhabdovirus Vaccine: Personalized Immunotherapy for Acute Lymphoblastic Leukemia

David P. Conrad[1,2,3,5], Jovian Tsang[1,4], Meaghan Maclean[1], Jean-Simon Diallo[1,2], Fabrice Le Boeuf[1,2], Chantal G. Lemay[1,4], Theresa J. Falls[1], Kelley A. Parato[1], John C. Bell[1,2,4], and Harold L. Atkins[1,2,5]

Abstract

Purpose: Acute lymphoblastic leukemia (ALL) remains incurable in most adults. It has been difficult to provide effective immunotherapy to improve outcomes for the majority of patients. Rhabdoviruses induce strong antiviral immune responses. We hypothesized that mice administered *ex vivo* rhabdovirus-infected ALL cells [immunotherapy by leukemia-oncotropic virus (iLOV)] would develop robust antileukemic immune responses capable of controlling ALL.

Experimental Design: Viral protein production, replication, and cytopathy were measured in human and murine ALL cells exposed to attenuated rhabdovirus. Survival following injection of graded amounts of ALL cells was compared between cohorts of mice administered γ-irradiated rhabdovirus-infected ALL cells (iLOV) or multiple control vaccines to determine key immunotherapeutic components and characteristics. Host immune requirements were assessed in immunodeficient and bone marrow–transplanted mice or by adoptive splenocyte transfer from immunized donors. Antileukemic immune memory was ascertained by second leukemic challenge in long-term survivors.

Results: Human and murine ALL cells were infected and killed by rhabdovirus; this produced a potent antileukemia vaccine. iLOV protected mice from otherwise lethal ALL by developing durable leukemia-specific immune-mediated responses ($P < 0.0001$), which required an intact CTL compartment. Preexisting antiviral immunity augmented iLOV potency. Splenocytes from iLOV-vaccinated donors protected 60% of naïve recipients from ALL challenge ($P = 0.0001$). Injecting leukemia cells activated by, or concurrent with, multiple Toll-like receptor agonists could not reproduce the protective effect of iLOV. Similarly, injecting uninfected irradiated viable, apoptotic, or necrotic leukemia cells with/without concurrent rhabdovirus administration was ineffective.

Conclusion: Rhabdovirus-infected leukemia cells can be used to produce a vaccine that induces robust specific immunity against aggressive leukemia. *Clin Cancer Res; 19(14); 3832–43. ©2013 AACR.*

Introduction

Acute lymphoblastic leukemia (ALL) is an aggressive hematopoietic malignancy characterized by rapid accumulation of lymphoblasts in the marrow with suppression of hematopoiesis (1). Children are treated with prolonged multiagent radio-chemotherapy, achieving at least 80% long-term survival (2), but this is associated with frequent late adverse effects including secondary malignancies, various chronic medical problems, and psychologic and cognitive impairments (3, 4). Although adults with ALL frequently obtain complete remission, most relapse with only a third surviving 5 years from diagnosis (2, 5). Immunologically mediated graft versus leukemia (GvL) effects are responsible, in part, for improved outcomes in the minority of patients eligible for allogeneic hematopoietic stem cell transplantation (HSCT; refs. 6–12). Unfortunately, the benefits of GvL are difficult to separate from the detrimental effects of GVHD (13). Thus, measures that reduce the intensity or duration of chemotherapy without compromising disease control would improve the quality of life for survivors of childhood ALL, whereas more potent therapies are required for curing adult ALL. ALL is amenable to immunotherapy as shown by the effectiveness of GvL, consequently administering vaccines targeting residual leukemic cells remaining after induction chemotherapy may help achieve these goals.

Leukemia cells often harbor unique antigens with immunogenic potential. For instance, the presence of

Authors' Affiliations: [1]Ottawa Hospital Research Institute, Center for Cancer Therapeutics; Departments of [2]Medicine, [3]Cellular and Molecular Medicine, and [4]Biochemistry, Immunology and Microbiology, University of Ottawa; and [5]Ottawa Hospital Blood and Marrow Transplant Program, Ottawa, Ontario, Canada

Note: Supplementary data for this article are available at Clinical Cancer Research Online (http://clincancerres.aacrjournals.org/).

Corresponding Author: Harold L. Atkins, Ottawa Hospital Research Institute, Center for Cancer Therapeutics, 501 Smyth Road, Ottawa, Ontario K1H-8L6, Canada. Phone: 613-737-7700, ext. 70532; Fax: 613-737-8768; E-mail: hatkins@ohri.ca

doi: 10.1158/1078-0432.CCR-12-3199

Published OnlineFirst May 28, 2013; DOI: 10.1158/1078-0432.CCR-12-3199

Translational Relevance

Treating acute lymphoblastic leukemia (ALL) involves prolonged multiagent radio-chemotherapy. Although children are often cured, they develop significant late adverse treatment-related health effects. The majority of adult patients unfortunately succumb to the disease. Evidence derived from recipients of allogeneic hematopoietic stem cell grafts support the concept that ALL is susceptible to immune attack but treatment-related toxicity limits its broad application. Robust, yet nontoxic leukemia-specific immunotherapy could improve outcomes for all patients. Using several murine models of ALL, we test the immunotherapeutic potential of leukemia cells infected with engineered attenuated rhabdoviruses [immunotherapy by leukemia-oncotropic virus (iLOV)]. These preclinical studies show the potency and durability of the antileukemic immune response induced by iLOV. This is the first time an oncotropic virus has been successfully used in clinically relevant orthotopic models using syngeneic acute leukemia cells. This novel immunotherapeutic has the potential to advance toward early-phase clinical trials for patients with ALL.

autologous $CD8^+$ and $CD4^+$ T-cell immune responses to peptides derived from the leukemia-specific antigen $NPM1^{mut}$ has been shown in patients with acute myelogenous leukemia (AML; ref. 14). The use of adjuvants or mechanisms that upregulate cell-surface immune activation molecules, improve the intrinsic immunogenicity and therapeutic potential of leukemia cell vaccines (15–17). Indeed, allogeneic HSCT recipients with advanced high-risk ALL and AML were shown to generate tumor-specific responses and survive longer following treatment with autologous leukemia cells mixed with syngeneic skin fibroblasts expressing CD40L and interleukin (IL)-2 from adenoviral vectors (18). Phase I/II clinical studies of idiotype and dendritic cell–based vaccines have shown a modest survival benefit for patients with acute and chronic lymphomas (19). Unfortunately, available immunotherapeutic technologies suffer from inefficient recognition and processing of tumor peptide(s), leading to suboptimal antitumor T-cell responses *in vivo* (20). These challenges limit the potential impact of current immune-based anticancer therapies.

Neoplastic transformation is associated with defects of cellular antiviral defenses allowing selective infection of cancer cells by diverse families of attenuated viruses (21–23). Rhabdoviruses, such as the engineered VSVd51 with deletion at methionine-51 of the matrix protein, and MG1, a recombinant Maraba virus with cooperative attenuating mutations in its matrix protein (L123W) and glycoprotein (Q242R), complement the IFN signaling defects in cancer cells. These specific mutations attenuate virulence and increase their tropism toward malignant cells (24, 25). Vesicular stomatitis virus (VSV) can be rendered incapable of spreading between cells by creating mutants with deletion of the viral glycoprotein gene (VSVΔG) required for final virion assembly and egress (26). The biology of these enveloped single-stranded negative-sense RNA viruses has been reviewed (24). Infection of tumor cells by these oncotropic viruses initiates a chain of events causing peri-tumor inflammation, activation of natural killer (NK) cells, macrophage-mediated innate immune attack, as well as induction of adaptive antitumor immune responses (21, 27, 28).

Rhabdoviruses are capable of infecting leukemia cells *in vitro*, however, viral replication is quite limited in these cells (29). This hinders their use as direct cytolytic agents for treatment of ALL. However, using immunocompetent murine models of ALL, we show that a vaccine composed of syngeneic leukemia cells infected *ex vivo* with rhabdovirus [immunotherapy by leukemia-oncotropic virus (iLOV)] generates a potent and durable antileukemia effect that is specifically directed toward the leukemia cell used to produce this vaccine.

Materials and Methods

Reagents

Blasticidin and Zeocin, used for VSVd51ΔG production, were purchased from Invitrogen. The Toll-like receptor (TLR) 3 agonist polyinosinic-polycytidylic acid (poly I:C) and TLR4 agonist lipopolysaccharide (LPS) were purchased from Sigma-Aldrich. Anti-mouse CD40-allophycocyanin (APC), propidium iodide (PI), 7-amino-actinomycin D (7-AAD) viability-staining solutions, and Annexin V apoptosis detection kit APC were obtained from eBioscience. Anti-mouse CD19-FITC, CD3-PE, CD4-PerCP, CD8-PerCPCy5.5, biotin anti-mouse CD252 (Ox40L), and phycoerythrin (PE)–streptavidin were obtained from BD Biosciences.

Tumor cells

L1210 and EL4 murine lymphoblastic cell lines, from American Type Culture Collection (ATCC), were maintained in suspension culture, Dulbecco's modified Eagle medium (DMEM)-high glucose (HyClone), with 10% fetal calf serum (FCS; CanSera) at 37°C and 5% CO_2. Cells were routinely split every 2 to 4 days to maintain concentration between 0.5 to 1.0 × 10^6 cells/mL. The Jurkat human acute T-cell lymphoblastic leukemia cell line (from ATCC), the human acute immunoblastic B-cell line OCI-Ly-18 (kind gift of Dr. Hans Messner, Ontario Cancer Institute, Toronto, ON, Canada), and the human acute T-cell lymphoblastic cell line A301 (kind gift from Dr. Thomas Folks, AIDS Research and Reference Reagent Program, Division of AIDS, National Institute of Allergy and Infectious Disease, NIH, Germantown, MD), were maintained in similar culture conditions. The Vero cell line (from ATCC) was maintained as adherent cell cultures in DMEM and 10% FCS. Vero cells were used for virus propagation, detection, or enumeration of infectious viral particles and for viral-neutralization antibody assays. T-Rex-293 cells (Invitrogen) were used for manufacturing of VSVd51ΔG virus.

Published OnlineFirst May 28, 2013; DOI: 10.1158/1078-0432.CCR-12-3199

Mice

DBA/2, C57BL/6, athymic nude nu/nu, and B6D2F1 hybrid mice (all 6–8 weeks of age) were purchased from Charles River Laboratories and housed in a biosafety unit at the University of Ottawa (Ottawa, ON, Canada), accredited by the Canadian Council on Animal Care (CCAC). Institutional guidelines and review board for animal care (The Animal Care and Veterinary Service of the University of Ottawa) approved all animal studies.

Oncotropic viruses

The rhabdoviruses, MG1 and VSVd51 were propagated in Vero cells and purified as previously described (22). MG1-eGFP and VSVd51-eGFP, genetically engineered to express enhanced GFP (eGFP) gene, were grown and purified in similar manner. VSVd51 with deletion of the glycoprotein gene (VSVd51ΔG) was propagated in T-REx-293 cells stably transfected with pcDNA4/TO plasmid expressing VSV glycoprotein gene. VSVd51ΔG was grown by infecting this cell line with virus stock, 24 hours after glycoprotein induction with 1 μg/mL tetracycline. Supernatants were collected 24 hours after infection and virus purified. For certain experiments, 50 μL aliquots of viral preparation were exposed to UVC radiation (Spectrolinker UV Crosslinker XL-1000; Spectronics); complete inactivation was confirmed by testing for absence of cytopathic effects and infectious particles on Vero cells. Enumeration of virus particles was conducted as previously described (28). Suspension cultures of human and murine leukemic cells were infected by adding virus preparations directly to culture (at 1×10^6 cells/mL), at a multiplicity of infection (MOI) of 0.1.

Vaccine preparations

iLOV was prepared by infecting suspension cultures of L1210 or EL4 cells at 1×10^6/mL with virus at MOI of 10, and maintained at 37°C in humidified (5% CO_2) incubator. Eighteen hours after infection, an aliquot of culture was analyzed by flow cytometry, assessing extent of infection (eGFP expression), concentration, and viability. The remainder was pelleted by centrifugation at 1500 RPM, media aspirated, washed once in PBS, and resuspended for final concentration of 1×10^7 cells/mL in PBS. Vaccine preparations received 30 Gy γ-irradiation (γ-IR; HF-320; Pantak) before administration. Specific experiments used uninfected leukemia cell vaccine prepared analogously and injected alone, coinjected with MG1 (MOI 10) in a separate syringe or mixed with MG1 at MOI of 10, at room temperature 60 minutes before administration. In other experiments, virus infected L1210 cells were fixed in 1% (final) paraformaldehyde (PFA) before γ-IR. In specific experiments, TLR agonists replaced virus infection in the vaccine. Standard murine doses of either 150 μg/100 μL poly I:C or 17 μg/100 μL LPS were added to L1210 cells before γ-IR and injection. In other experiments, 150 μg/10^6 cells poly I:C and/or 17 μg/10^6 cells LPS were added to cultures of L1210 cells for 18 hours before washing and γ-IR. Apoptotic leukemia cell vaccine was prepared from uninfected L1210 cell cultures. Cells were pelleted by centrifugation, washed once, and resuspended in PBS at 2×10^6/mL. Ten milliliter of cell suspension was placed in a 150 mm × 25 mm plate and exposed to 500 mJ/cm^2 UVC. Cells were then pelleted, resuspended in fresh media, and incubated at 37°C for 4 hours before preparation for use in a manner analogous to iLOV. Necrotic leukemia cell vaccine was prepared by pressure disruption (1,500 PSI) of washed uninfected L1210 cells at 1×10^7 cells/mL in a French hydraulic press (AMINCO J5-598A; Newport Scientific).

Virus treatment of leukemia

DBA/2 mice received tail vein injections of 1×10^6 L1210 leukemia cells. Leukemic mice were treated with 100 μL PBS or PBS containing 1×10^8 plaque-forming units (pfu) MG1 by tail vein injection 7, 10, and 14 days later (Supplementary Fig. S1A). Mice were euthanized upon development of typical signs of advanced leukemia such as hind-leg paralysis, focal tumor development, significant weight loss, and/or respiratory distress.

Immunization and leukemic challenge

Immunization was conducted by tail vein injection of 100 μL per mouse per dose of freshly prepared iLOV, an alternative vaccine or PBS. Vaccines were administered once weekly for 3 doses, followed 1 week later by intravenous tail vein injection of viable leukemia cells from suspension cultures. Cells were pelleted by centrifugation, media aspirated, washed once in PBS, and resuspended at 1×10^7 cells/mL in PBS. Mice received a dose of 1×10^6 cells unless otherwise specified. Mice were euthanized upon development of predetermined signs of advanced leukemia endpoints, (Supplementary Fig. S1B).

Adoptive cell transfer

Under sterile conditions, single-cell suspensions of splenocytes were prepared from donor spleens removed from iLOV immunized or naïve DBA/2 mice using gentleMACS Dissociator (Miltenyi Biotec) according to the manufacturer's recommendations with red blood cells lysed by ammonium-chloride-potassium lysis buffer. Donor splenocytes were pooled and 15×10^7 cells were injected intravenously via tail vein into syngeneic recipients. Splenocyte recipients received a leukemia challenge of 1×10^6 L1210 cells, administered intravenously via tail vein, 1 week after adoptive transfer.

Bone marrow transplantation and vaccination

Eight-week-old DBA/2 mice received total body irradiation (TBI) using two fractions of 450 cGy given 2 hours apart. Under aseptic conditions, 10^6 bone marrow cells, collected from flushed femurs of 8-week-old B6D2F1 donors, were intravenously infused into each TBI-treated recipient. On day 43, cohorts (n = 5–6/group) of bone marrow transplantation (BMT) recipient DBA/2 mice and healthy B6D2F1 mice, received the first of 3 weekly iLOV vaccinations. On day 63, a leukemia challenge of 1×10^7 L1210 cells was administered to all mice, including parallel-unimmunized cohorts (n = 5/group). Additional cohorts of unimmunized TBI-treated DBA/2 and naïve B6D2F1 were

Published OnlineFirst May 28, 2013; DOI: 10.1158/1078-0432.CCR-12-3199

euthanized at day 43 for enumeration of the major lymphocyte compartments by flow cytometry.

Flow cytometry

Leukemia cell infections were evaluated by flow-cytometric analysis of 10,000 cells using Quanta SC (Beckman Coulter). A 500 μL aliquot of infected cells was stained with 5 μL PI (1 mg/mL) approximately 30 minutes before data acquisition. All vaccine preparations were analyzed by flow cytometry in similar fashion to allow dose standardization and quality control of virus expression. For analysis of apoptosis and necrosis, acquisition was conducted on CyAn ADP (Beckman Coulter) using Annexin V apoptosis detection kit APC and cell viability dye 7-AAD, with minimum of 50,000 cells counted. Cell-surface expression of activation/costimulation molecules CD40 and Ox40 ligand (CD252) on L1210 cells incubated for 18 hours with either MG1 (MOI 10), LPS (17 μg/10^6 cells), or Poly I:C (150 μg/10^6 cells) was analyzed on CyAn ADP (minimum of 60,000 cells acquired) and conducted in triplicate with background mean fluorescence intensity (MFI) of unstained cells under each condition subtracted from the MFI of stained cells. Single-cell suspensions of splenocytes were collected from unimmunized TBI-treated DBA/2 and naïve age-matched B6D2F1 mice and total cells/spleen were measured by Trypan blue exclusion. Enumeration of B cell ($CD19^+$), T cell ($CD3^+/CD4^+$ and $CD3^+/CD8^+$), and NK cell ($NK1.1^+$) subpopulations was conducted on CyAn ADP, counting a minimum of 60,000 cells, conducted in technical duplicates for each biologic replicate. Data analysis was conducted with Kaluza software version 1.1 (Beckman Coulter) and Cell Lab Quanta Analysis (Beckman Coulter).

Statistical analysis

Survival curves were generated using product limit (Kaplan–Meier) method and comparisons were conducted using log-rank (Mantel–Cox) test, all P values are two-tailed. Elsewhere, data presented as mean + SEM with significance determined by Welch corrected t test. Statistical significance was determined at level of $P < 0.05$. Analyses were conducted using Prism 5 software (GraphPad Software).

Results

MG1 infects leukemia lines *in vitro* but is ineffective in halting leukemia progression *in vivo*

We first wished to explore whether mice with disseminated ALL could be successfully treated by systemic delivery of live oncotropic rhabdovirus. We first established that MG1 was able to infect and kill various murine and human leukemia cell lines *in vitro* at low MOI (Fig. 1A and B and Supplementary Fig. S2). L1210 leukemia cells show considerable permissiveness to MG1 infection and result in efficient, rapid cytolysis yet virus production is modest over 24 to 40 hours incubation (Fig. 1C). Next, a cohort of leukemia-bearing mice was given 1×10^8 pfu of MG1-eGFP daily every 3 days for 3 doses. This was unable to prevent disease progression (Fig. 1D). Organs were recovered from all mice at endpoint. Following homogenization, an aliquot of each organ was cocultured for 15 hours on Vero cells and the monolayer was then scanned under a fluorescence microscope for presence of green fluorescing cells. Homogenates from the brain and liver of a single mouse, which died 3 days following the second virus injection, contained MG1 and resulted in GFP positivity on the Vero monolayer. Despite the ability of MG1 to infect and kill leukemic cells *in vitro*, the oncolytic effect of live MG1 was ineffective at controlling leukemia at doses large enough to cause toxicity in leukemia-bearing hosts.

MG1-infected leukemia cells (iLOV) acts as a vaccine, eliminating otherwise lethal acute leukemia

Barriers to systemic replication-competent virotherapy for leukemia may include inadequate cytolysis at tolerable doses and rapid tumor kinetics that outpace establishment of antitumor immune responses. To address the latter issue, mice were administered 3 weekly doses of γ-IR virus-infected L1210 cells (MG1-iLOV). This was followed, a week later, by injection of viable L1210 cells. Mice that received MG1-iLOV showed more than 90% long-term survival following challenge with viable leukemia cells compared with untreated control mice, which reproducibly reached leukemic endpoints with median survival of 18 days (Fig. 2A), confirming that iLOV was able to establish highly protective antitumor responses. However, when leukemic challenge was administered 1 day before the MG1-iLOV vaccination series, 100% of control mice succumbed to leukemia, whereas 50% of mice that received MG1-iLOV survived (Fig. 2B), illustrating that iLOV is able to induce a protective effect even in the presence of early-disseminated leukemia. This incomplete protection is likely due to rapid growth of L1210 leukemia in this aggressive tumor model, which outstrips the development of antitumor responses.

To test whether the protective effects of iLOV were mediated through development of antitumor immunity, MG1-iLOV was administered to athymic nude or immunocompetent DBA/2 mice once weekly for 3 doses. Treated and untreated nude mice died from leukemia in a median of 18 and 23 days, respectively, following injection of viable L1210 cells. In contrast, immunocompetent mice that received iLOV rejected L1210 cells (Fig. 3A). To further examine the immune requirements of the host, a BMT model was used. After receiving myeloablative TBI, DBA/2 mice were administered 10^6 rescue marrow cells from B6D2F1 donors. Following a 43-day recovery, absolute numbers of lymphocyte populations were compared between unimmunized BMT recipients versus healthy donors. Although NK cells, $CD3^+/4^+$ T cells, and B cells were similar in number between the groups, $CD3^+/8^+$ T cells were significantly reduced in the BMT recipients (Fig. 3B). This depletion of CTLs was associated with a reduction in long-term protective immunity against a leukemic challenge by approximately 40% in a parallel cohort of iLOV-vaccinated BMT recipients (Fig. 3B). The additional control cohorts of unimmunized BMT recipients and

Published OnlineFirst May 28, 2013; DOI: 10.1158/1078-0432.CCR-12-3199

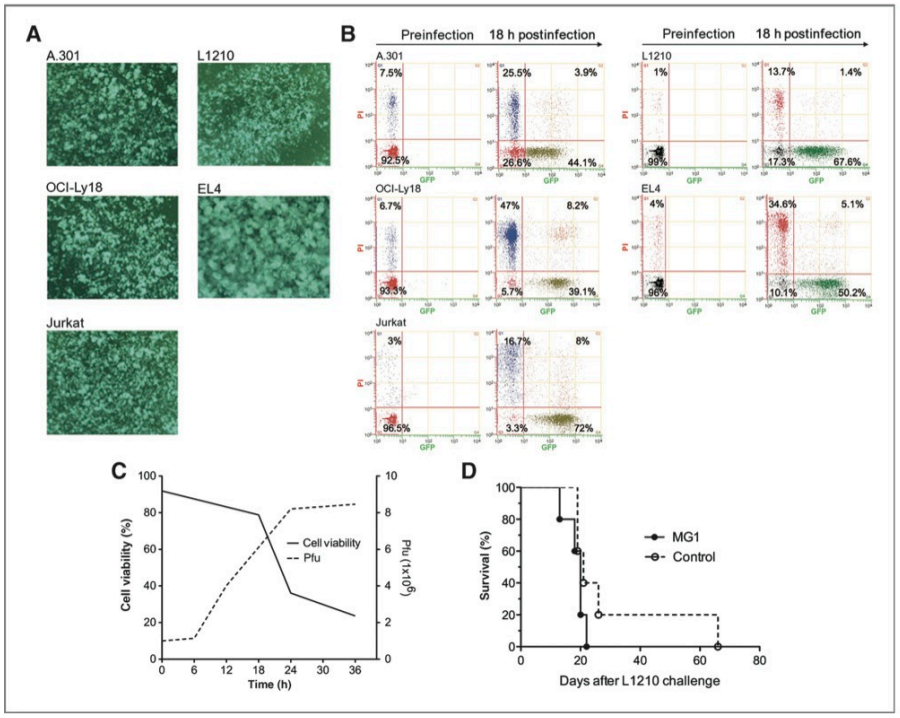

Figure 1. MG1 virus infects human and murine leukemia cells *in vitro*; however, it is ineffective at halting progression of established murine leukemia *in vivo*. A, fluorescence microscopy (×10) showing expression of viral GFP at 18 hours after infection of MG1-GFP (MOI 0.1) in human T-cell leukemia lines A.301 and Jurkat, human B-cell leukemia OCI-Ly18, murine T-cell lymphoblasts EL4, and murine B-cell lymphoblasts L1210. B, flow cytometry dot plots of the same cell lines in A, pre- and 18 hours post-MG1-GFP infection indicating viral gene replication and protein expression by GFP. Cell viability decreases as indicated by increased PI staining. Dot plots are representative of vesiculovirus infections of cell lines conducted on several occasions. C, L1210 cell-viability (PI) versus virus enumeration by viral pfu over time following infection with MG1 at low MOI (0.1). D, survival of DBA/2 mice that received systemic MG1 virotherapy compared with untreated DBA/2 mice for the treatment of established L1210 leukemia ($n = 5$ each group), $P = 0.19$.

unimmunized B6D2F1 mice all reached typical endpoints by day 28. In a separate experiment, we wished to examine the effect of adoptive splenocyte transfer from long-term iLOV-protected mice to naïve recipients. Accordingly, 17 mice that received MG1-iLOV and survived between 211 to 349 days following leukemic challenge were used as splenocyte donors. Pooled donor splenocytes were administered to 8 naïve DBA/2 recipients followed 7 days later by injection of viable L1210 cells. Long-term survival was observed in 63% of recipients, whereas control mice that received the same number of splenocytes from untreated donors were unable to reject leukemic challenge (Fig. 3C). Collectively, these observations indicate an intact thymocyte compartment mediates the antileukemic protection afforded by iLOV and CTLs are critical for optimal effect.

To examine the strength of the immune response that develops following iLOV, cohorts of unimmunized and MG1-iLOV–treated mice were challenged with increasing amounts of viable L1210 cells. The LD_{50} of unimmunized mice was approximately 4.9×10^4 cells, whereas the LD_{50} for MG1-iLOV–vaccinated mice was estimated to be 3.8×10^6 cells. Thus, iLOV was able to protect mice against an almost 100-fold larger inoculum of leukemia than would be spontaneously rejected by unimmunized mice (Fig. 3D). The durability of such a response is particularly critical as the ability to prevent leukemic recurrence may wane over time. iLOV-treated mice that survived a primary leukemic challenge were administered a second L1210 leukemia challenge either 100, 134, or 255 days after initial L1210 challenge. The majority of mice were able to reject this additional leukemic challenge, but there may be a time-

Published OnlineFirst May 28, 2013; DOI: 10.1158/1078-0432.CCR-12-3199

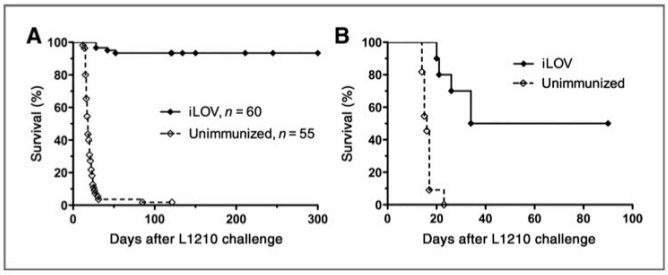

Figure 2. MG1-iLOV eliminates otherwise lethal leukemic challenge. A, DBA/2 mice immunized with iLOV reliably (>90%) achieve long-term protection from L1210 leukemic challenge, as compared with unimmunized mice. Combined survival from 8 independent experiments ($n = 5$–15 per group per experiment), $P < 0.0001$. B, DBA/2 mice immunized with iLOV 24 hours after high-dose L1210 administration maintain survival advantage compared with unimmunized mice ($n = 10$ both groups), $P < 0.0001$.

dependent decline in the ability to reject a late secondary leukemic challenge (Fig. 3E).

The effectiveness of iLOV treatment was not limited to a single rhabdovirus, leukemic cell line, or mouse strain. Survival following leukemic challenge was observed when animals were administered iLOV prepared using a different rhabdovirus—VSVd51, indicating that the protective effects were independent of the specific rhabdovirus (Supplementary Fig. S3). Similarly, mice survived an otherwise lethal challenge with EL4, a T lymphoma cell line, when MG1-iLOV prepared using these cells was used to vaccinate syngeneic C57BL/6 mice (Supplementary Fig. S4). To examine the specificity of the antitumor protection afforded by iLOV, two cohorts of B6D2F1 hybrid mice were administered 3 weekly doses of MG1-L1210 iLOV. One cohort was subsequently challenged with viable 1×10^7 L1210 cells, whereas the other received 1×10^7 EL4 cells. Mice that received the L1210-based iLOV were protected from L1210 challenge, whereas survival of EL4-challenged mice was identical to unimmunized mice challenged with EL4 (Fig. 3F). The specificity of the immune response was further examined using reciprocal immunization combinations of EL4-iLOV or L1210-iLOV in cohorts of both DBA/2 and C57BL/6 mice. To control for immune recognition of leukemia cells based on the MHC disparity alone, additional cohorts of C57BL/6 and DBA/2 mice were immunized with γ-IR L1210 or γ-IR EL4 cells, respectively. All groups were subsequently challenged with viable leukemia cells syngeneic to the breed. Only mice that received iLOV produced using syngeneic leukemia cells were protected (Supplementary Fig. S5). Together, these observations suggest that iLOV induces antitumor immunity functionally restricted to the specific antigenic profile of the leukemic cell used to produce iLOV rather than commonly expressed leukemic antigens.

Virus infection is critical to induction of iLOV-mediated antileukemic immunity

We examined whether the cellular and viral components of iLOV could be individually effective at inducing protective antitumor immunity. Mice administered 3 doses of γ-IR *ex vivo* MG1-infected L1210 cells (iLOV) survived subsequent administration of an otherwise lethal dose of L1210 cells, whereas all mice that received γ-IR–uninfected L1210 cells before leukemic challenge succumbed with median survival that was not significantly different from unimmunized mice that received the same leukemic challenge dose. Furthermore, the virus must infect the cell for iLOV to be effective as 3 weekly separate coinjections of γ-IR L1210 cells and MG1, or the administration of 3 weekly doses of γ-IR L1210 cells mixed with MG1 at room temperature for 1 hour before injection, were unable to prevent the lethality of a subsequent L1210 leukemia challenge (Fig. 4A).

In vitro, leukemic cells exposed to UV-inactivated MG1-eGFP virus did not express GFP nor developed cytopathology. In contrast, L1210 cells exhibit green fluorescence following *in vitro* exposure to live spread-incompetent VSVd51ΔG-eGFP, and delayed cytolysis occurs as long as 72 hours after infection (Fig. 4B). Immunization with iLOV produced by infection of L1210 cells with VSVd51ΔG protected 80% of mice from the lethal effects of subsequent L1210 challenge (Fig. 4C), indicating that iLOV is effective even if the virus is incapable of fully completing its lifecycle. Administration of iLOV produced with UV-inactivated MG1 before challenge with viable L1210 leukemia was unable to prevent death from fulminant leukemia in 80% of mice. iLOV preparations fixed with PFA after virus infection but immediately before γ-IR were capable of protecting immunized mice just as effectively as freshly produced, unfixed iLOV preparations (Fig. 4D). PFA-fixed iLOV preparations did not contain detectable viable MG1 in a standard plaque assay. Thus in this model, live rhabdovirus was used for the manufacturing of iLOV but it was not critical at the time of administration.

MG1-infected leukemia cells exhibit superior immunogenicity

The protective effects induced by injection of *ex vivo* virus-infected leukemia cells cannot be mimicked solely by activation of antiviral defense pathways in leukemia cells used

Published OnlineFirst May 28, 2013; DOI: 10.1158/1078-0432.CCR-12-3199

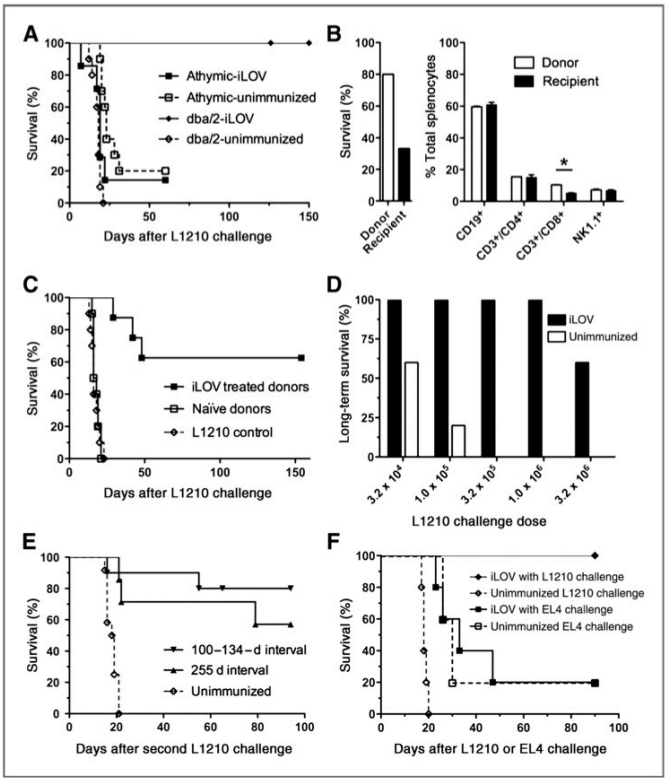

Figure 3. iLOV induces potent and durable immune-mediated leukemia-specific protection. A, survival following leukemic challenge for iLOV-immunized or unimmunized immunocompetent DBA/2 and immunodeficient athymic mice ($n = 10$/group). $P = 0.0002$, iLOV-immunized DBA/2 versus iLOV-immunized athymic mice; $P = 0.12$, iLOV-immunized versus unimmunized athymic mice. B, 100-day survival following L1210 challenge (10^7 cells) for iLOV-immunized DBA/2 BMT recipients ($n = 6$) and immunized B6D2F1 donors ($n = 5$). Lymphocyte enumeration by flow cytometry in unimmunized parallel cohorts ($n = 2$/group), conducted in triplicate. *, $P \leq 0.007$. C, survival following L1210 challenge for naïve DBA/2 recipients ($n = 8$) of pooled splenocytes from iLOV-immunized DBA/2 donors surviving 211 to 349 days post-L1210 challenge versus naïve recipients ($n = 5$) of pooled splenocytes from unimmunized DBA/2 donors ($P = 0.0001$), and unimmunized ($n = 10$) without splenocyte transfer ($P = 0.0001$). D, long-term (125 days) survival for iLOV-immunized and unimmunized DBA/2 mice ($n = 5$ each group) challenged with increasing doses of L1210 cells. E, survival following second L1210 leukemic challenge for iLOV-immunized mice surviving 100 to 134 days ($n = 10$) or 255 days ($n = 7$) after first leukemic challenge versus unimmunized mice ($n = 10$); $P = 0.0002$ (255 day interval) and $P < 0.0001$ (100–134–day interval) versus unimmunized. Trend observed ($P = 0.45$) for time-dependent decrease in survival following late second challenge. F, survival of L1210-iLOV–immunized and -unimmunized B6D2F1 mice ($n = 5$ each group) following L1210 or EL4 challenge (10^7 cells). $P = 0.0133$, iLOV-immunized L1210-challenged versus iLOV-immunized EL4-challenged mice; $P = 0.0018$, iLOV-immunized versus -unimmunized L1210-challenged mice; $P = 0.84$, iLOV-immunized versus -unimmunized EL4-challenged mice.

for immunization. L1210 cells were cultured for 18 hours with either MG1, poly I:C, LPS, or both TLR agonists and inactivated virus, before γ-IR and injection. Activation of L1210 cells by virus or TLR agonists was confirmed by measuring cell-surface expression of the B-cell immunopotentiating activation molecules CD40 and CD252 by flow cytometry (Supplementary Fig. S6). Mice that received 3 weekly injections of these TLR-agonist preparations succumbed to subsequent injection of L1210 cells, in contrast to mice that received MG1-iLOV (Fig. 5A). Similarly, pulsed stimulation of host innate immunity by direct injection of either poly I:C or LPS concurrently with 3 weekly injections of γ-IR L1210 cells was also incapable of protecting animals from subsequent injection of viable L1210 cells (Fig. 5B). The protective effects induced by injection of *ex vivo* virus-infected leukemia cells cannot be mimicked solely by the

Published OnlineFirst May 28, 2013; DOI: 10.1158/1078-0432.CCR-12-3199

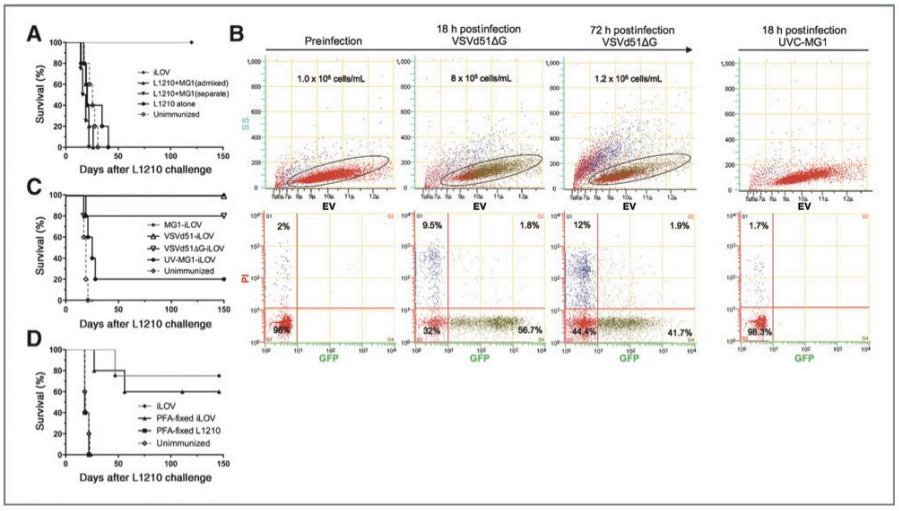

Figure 4. Virus infection is critical to the induction of iLOV-mediated antileukemic immunity. A, survival following leukemic challenge for DBA/2 mice immunized with iLOV versus L1210 cells alone, L1210 cells admixed with live MG1 for 1 hour at room temperature before injection, or unimmunized ($n = 5$ each group), all $P = 0.0018$; or versus L1210 cells coinjected simultaneously with live MG1 using a separate syringe ($n = 5$), $P = 0.0027$. B, flow cytometry dot plots of infected L1210 cells. Cells incubated with UV-inactivated MG1 virus do not express GFP and exhibit negligible PI staining at 18 hours. In contrast, cells infected with attenuated VSVd51ΔG-eGFP virus express GFP at 18 to 72 hours following infection, with viability slowly decreasing over time. Oval region indicates viable L1210 lymphoblasts. C, survival of DBA/2 mice following L1210 leukemic challenge. Four cohorts immunized as follows; iLOV prepared using MG1 (MG1-iLOV), VSVd51 (VSVd51-iLOV), VSVd51ΔG (VSVd51ΔG-iLOV), or UV-inactivated MG1 (UV-MG1-iLOV; $n = 5$ each group). The unimmunized and iLOV-immunized cohorts shown here were conducted simultaneously with experiment shown in Fig. 3F. $P = 0.0133$, MG1-iLOV or VSVd51-iLOV versus UV-inactivated MG1-iLOV; $P = 0.32$, MG1-iLOV or VSVd51-iLOV versus VSVd51ΔG-iLOV; $P = 0.0228$, VSVd51ΔG-iLOV versus unimmunized; $P = 0.0019$, MG1-iLOV or VSVd51-iLOV versus unimmunized. D, survival following leukemic challenge in DBA/2 mice immunized with PFA-fixed iLOV versus freshly prepared unfixed iLOV, PFA-fixed L1210 cells, or unimmunized ($n = 5$ each group). $P = 0.6649$ PFA-fixed iLOV versus iLOV; $P = 0.0023$ PFA-fixed iLOV versus PFA-fixed L1210; $P = 0.0017$ PFA-fixed iLOV versus unimmunized.

presence of apoptotic or necrotic cells that are contained in iLOV preparations (Fig. 5C). Apoptosis was induced in L1210 cells by UV irradiation (Supplementary Fig. S7A), whereas parallel samples of L1210 were pressure disrupted into cellular necrosis (Supplementary Fig. S7B). Cohorts of mice received 3 weekly injections of either MG1-iLOV, UV-irradiated apoptotic L1210, or pressure-disrupted necrotic L1210 followed by challenge of viable L1210 leukemia. Mice that received UV-irradiated or pressure disrupted L1210 expired because of leukemia in contrast to the mice that received MG1-iLOV. Administration of 3 weekly injections of apoptotic or necrotic L1210 cells mixed with MG1 virus just before injection, were similarly ineffective (Fig. 5D and E).

Preexisting antiviral immunity does not impair development of antileukemia immunity

We wondered whether preexisting antiviral immunity to the rhabdovirus component would modulate iLOV efficacy as antiviral responses have impaired the efficacy of other vector-based vaccines (30). Accordingly, mice were injected 10^7 pfu MG1 by tail vein to generate antiviral immunity. Before receiving MG1, mice did not manifest serum virus-neutralizing antibody, whereas the titer of MG1-neutralizing antibody was $\geq$1:800 in serum of mice 10 days following administration of virus. Three doses of MG1-iLOV were administered starting 18 days after MG1 injection. The survival of MG1-immunized mice was no different than a cohort of mice that received MG1-iLOV without preceding MG1 inoculation when challenged with 1×10^6 L1210 cells (Fig. 6A). However, when L1210 challenge was increased 10-fold, mice immunized against MG1 before MG1-iLOV treatment had a significant survival advantage over mice that received MG1-iLOV treatment alone (Fig. 6B). These results suggest iLOV efficacy is not dampened but indeed may be augmented following development of antiviral immunity.

Discussion

We show that live-attenuated rhabdoviruses are able to infect and kill leukemia cells *in vitro* but are incapable of treating mice with established systemic leukemia. An alternative approach, injecting mice with γ-IR virus-infected leukemia cells, or iLOV, controls leukemic progression.

Published OnlineFirst May 28, 2013; DOI: 10.1158/1078-0432.CCR-12-3199

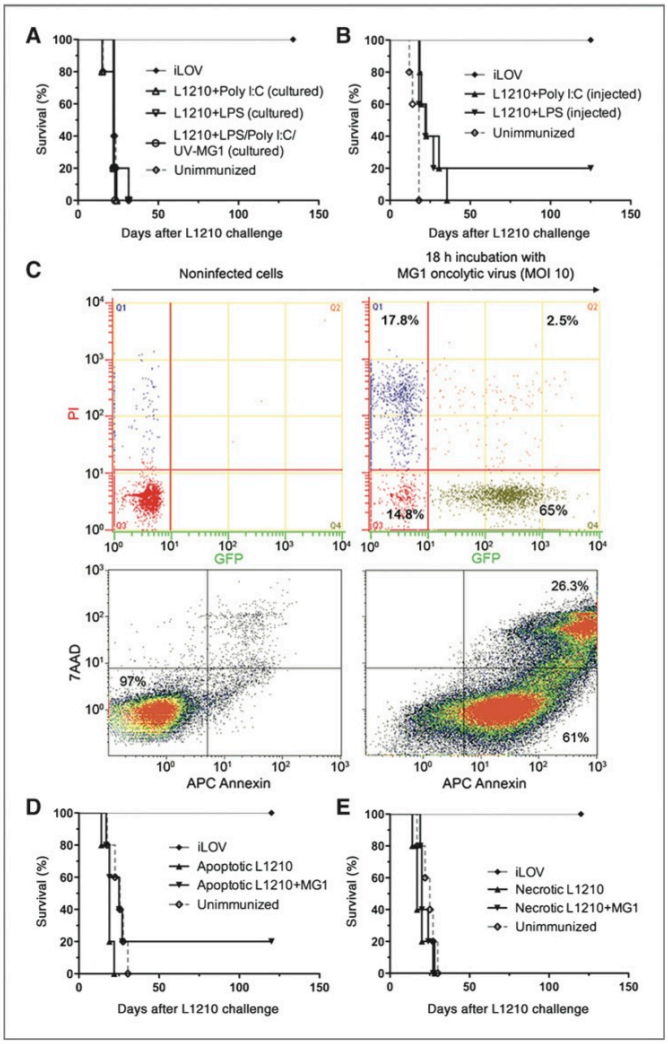

Figure 5. Host or leukemia cell stimulation with TLR agonists, or injection of necrotic or apoptotic leukemia cells are insufficient to produce effective antileukemia immunity. A, survival following leukemic challenge of DBA/2 mice immunized with MG1-iLOV versus immunization with L1210 cells previously cultured for 18 hours in TLR agonists (LPS or poly I:C) or L1210 cells incubated with both TLR agonists and UV-inactivated MG1 (MOI 10; $n = 5$ each group). $P \leq 0.002$, iLOV versus other groups. B, survival following leukemic challenge of DBA/2 mice immunized with MG1-iLOV versus immunization with L1210 cells injected with poly I:C or LPS ($n = 5$ each group). $P = 0.0034$, iLOV versus unimmunized; $P = 0.0018$, iLOV versus poly I:C; $P = 0.0128$, iLOV versus LPS. C, flow cytometry dot plots of Annexin V (apoptotic cells) versus viability dye 7-AAD (necrotic cells). MG1-iLOV preparations include substantial proportions of apoptotic and necrotic cells at 18 hours—shown is a representative analysis. D and E, survival following leukemic challenge of DBA/2 mice immunized with iLOV versus immunization with apoptotic or necrotic L1210 cells, respectively. MG1 was either admixed (apoptotic L1210 + MG1, necrotic L1210 + MG1) or omitted (apoptotic L1210, necrotic L1210) with cells 1 hour before injection ($n = 5$ each group). The unimmunized and iLOV-immunized cohorts shown were conducted simultaneously for this experiment and the experiment shown in Fig. 4A. $P = 0.0133$, iLOV versus apoptotic cells + MG1; $P = 0.002$, iLOV versus apoptotic cells; $P = 0.0018$, iLOV versus necrotic cells ± MG1 and unimmunized.

This effect is mediated by development of a robust adaptive antitumor immunity, wherein CTLs are essential for optimal efficacy. The immune response is specifically directed against the cell used to produce iLOV. It is longstanding, protecting the animal from repeat leukemic challenge more than 8 months following immunization. Both cellular and viral components of the vaccine are necessary. In this model, infection of viable leukemia cells with a transcription-competent oncotropic rhabdovirus leads to the induction of protective immune responses; however, virus spread is not essential. Furthermore, the immune effects are not simply a consequence of administering γ-IR leukemic cells

Published OnlineFirst May 28, 2013; DOI: 10.1158/1078-0432.CCR-12-3199

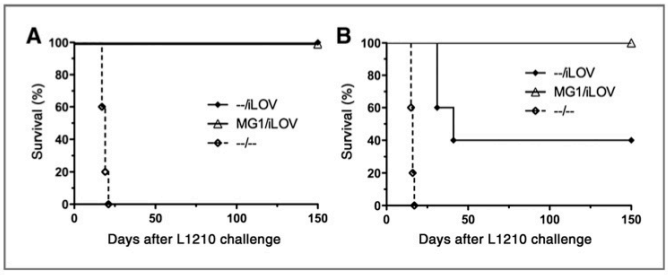

Figure 6. Preexisting antiviral immunity does not impair the development of antileukemia immunity. A, survival of iLOV-immunized DBA/2 mice, challenged with 1×10^6 L1210 cells, previously immunized against MG1 acquiring neutralizing antibodies (MG1/iLOV) versus mice that were not preimmunized against MG1 (–/iLOV) and unimmunized (–/–; $n = 5$ each group), $P = 0.0019$. B, survival of iLOV-immunized DBA/2 mice, challenged with 1×10^7 L1210 cells, previously immunized against MG1 acquiring neutralizing antibodies (MG1/iLOV) versus mice that were not preimmunized against MG1 (–/iLOV) and unimmunized (–/–; $n = 5$ each group). $P = 0.0486$ (MG1/iLOV) versus (–/iLOV); $P = 0.0019$ (MG1/iLOV) versus (–/–).

responding to noxious stimuli or due to simultaneous injection of γ-IR leukemic cells during nonspecific or viral provocation of the host's innate immune system. In preclinical models, iLOV seems to be an effective immunotherapy for ALL.

It has been suggested that at the interface between infected tumor cells and immune system, viral pathogen-associated molecular patterns (PAMP) ligate various TLRs in host dendritic cells, leading to NF-κB or IRF3 activation, dendritic cell maturation and licensing for expansion of tumor specific T cells (31). However, the effectiveness of iLOV is not the result of presenting leukemia cells to an immune system stimulated by systemic administration of TLR agonists or viable oncotropic virus. TLRs have been shown to activate caspases leading to apoptotic cell death (32) and constituents of dead or dying cells are immunomodulatory (33). For example, phosphatidylserine externalized to the outer membrane during apoptosis activates both dendritic cells and T cells (34). Necrotic cell debris provokes inflammation and innate immune system activation through pattern recognition receptor ligation of danger-associated molecular patterns (DAMP; refs. 35, 36). In this model, the use of UV-inactivated MG1 virus with or without concurrent activation through TLR-ligation using poly I:C and LPS is insufficient to increase the cell's recognition by the immune system. iLOV contains apoptotic and necrotic cells, however, these alone or combined with live MG1 virus are insufficient to induce protective antileukemia immunity. These results suggest that additional pathways beyond PAMP or DAMP signaling may be activated and responsible for induction of an effective antileukemia immune response.

Vesiculovirus infections induce marked antiviral immune responses. When used as priming or boosting agent, immunization with recombinant VSV expressing a tumor antigen prolonged survival and reduced tumor burden in cancer-bearing mice (37, 38). Nonetheless, viruses encoding a single or few antigen targets induce an oligoclonal immune response. Furthermore, the paucity of known tumor-associated antigens (TAA) along with their weak immunogenicity and variable expression on individual cancers (39), ultimately limits widespread applicability of this approach. Alternate approaches are being developed to create personalized anticancer vaccines. Recently, the mutanome, the sum total of somatic mutations in a tumor, was shown to encode multiple tumor-specific immunogenic peptides (40). Vesiculovirus-expressed cDNA libraries, optimally derived from xenogeneic tumor cells, have been reported to induce antitumor immunity in animal models, although varying degrees of autoimmunity were observed (41). At the present time, substantial effort would be required to manufacture personalized vaccines based on these methods.

Similar to the above methodology, our cell-based vaccine harnesses the entire library of immunologically recognized epitopes (33) in the leukemic mutatome without the need for involved recombinant DNA or "–omic" technology. The cell-based nature of iLOV may confer additional advantages, as the vaccine would contain the extensive array of aberrant posttranslational modified proteins common in tumors, which could serve to broaden the epitope library iLOV presents to the immune system, resulting in a potentially more robust immune response (42–44).

Although the effectiveness of iLOV requires a virus, the neoplasia-selective replication of the attenuated virus, limited viral replication in leukemia cells, and the development of neutralizing antiviral antibodies following first injection contribute to the inherent safety of this therapeutic. The small risk of uncontrolled viral replication can be mitigated by using viral mutants incapable of spreading, treating the preparation with PFA, or by preimmunizing the patient against the virus, none of which diminish effectiveness of the antitumor response. In contrast to other viral-based anticancer therapies (30, 45), preexisting antiviral immunity increases the potency of iLOV.

This platform represents a feasible technology to produce a safe and effective individualized immunotherapeutic for

Published OnlineFirst May 28, 2013; DOI: 10.1158/1078-0432.CCR-12-3199

controlling disseminated leukemia. We envision generating autologous iLOV from leukemia cells collected and stored at the time of diagnosis or relapse. Future clinical testing will determine its role in the treatment of patients with ALL.

Disclosure of Potential Conflicts of Interest

J.C. Bell is employed as CSO by Jennerex Biotherapeutics and has ownership interest (including patents) in the same. No potential conflicts of interest were disclosed by the other authors.

Authors' Contributions

Conception and design: D.P. Conrad, J.C. Bell, H.L. Atkins
Development of methodology: D.P. Conrad, K.A. Parato, J.C. Bell, H.L. Atkins
Acquisition of data (provided animals, acquired and managed patients, provided facilities, etc.): D.P. Conrad, J. Tsang, M. Maclean, T.J. Falls, J.C. Bell
Analysis and interpretation of data (e.g., statistical analysis, biostatistics, computational analysis): D.P. Conrad, J.-S. Diallo, C.G. Lemay, J.C. Bell, H.L. Atkins
Writing, review, and/or revision of the manuscript: D.P. Conrad, J. Tsang, F. Le Boeuf, K.A. Parato, J.C. Bell, H.L. Atkins
Administrative, technical, or material support (i.e., reporting or organizing data, constructing databases): D.P. Conrad, T.J. Falls
Study supervision: J.C. Bell, H.L. Atkins

Acknowledgments

The authors thank D. Stojdl for providing initial MG1 virus stock.

Grant Support

This study was financially supported by grants from Canadian Institutes for Health Research awarded to H.L. Atkins and J.C. Bell, Ontario Institute for Cancer Research, and Terry Fox Foundation awarded to J.C. Bell.

The costs of publication of this article were defrayed in part by the payment of page charges. This article must therefore be hereby marked *advertisement* in accordance with 18 U.S.C. Section 1734 solely to indicate this fact.

Received October 11, 2012; revised April 25, 2013; accepted May 14, 2013; published OnlineFirst May 28, 2013.

References

1. Swerdlow SH, Swerdlow E, Harris NL, Jaffe ES, Pileri SA, Stein H, et al. WHO classification of tumours of haematopoietic and lymphoid tissues 4th ed. Lyon, France: IARC; 2008. p. 149–78.
2. Pui C, Robison LL, Look AT. Acute lymphoblastic leukaemia. Lancet 2008;371:1030–43.
3. Robison L. Late effects of acute lymphoblastic leukemia therapy in patients diagnosed at 0–20 years of age. Am Soc Hematol Educ Program Book 2011;2011:238–42.
4. Oeffinger KC, Mertens AC, Sklar CA, Kawashima T, Hudson MM, Meadows AT, et al. Chronic health conditions in adult survivors of childhood cancer. N Engl J Med 2006;355:1572–82.
5. Fielding AK, Richards SM, Chopra R, Lazarus HM, Litzow MR, Buck G, et al. Outcome of 609 adults after relapse of acute lymphoblastic leukemia (ALL); an MRC UKALL12/ECOG 2993 study. Blood 2007; 109:944–50.
6. Jansson J, Hsu Y-C, Kuzin II, Campbell A, Mullen CA. Acute lymphoblastic leukemia cells that survive combination chemotherapy *in vivo* remain sensitive to allogeneic immune effects. Leuk Res 2011;35:800–7.
7. Fielding AK. Current therapeutic strategies in adult acute lymphoblastic leukemia. Hematol Oncol Clin North Am 2011;25:1255–79.
8. Goldstone AH, Richards SM, Lazarus HM, Tallman MS, Buck G, Fielding AK, et al. In adults with standard-risk acute lymphoblastic leukemia, the greatest benefit is achieved from a matched sibling allogeneic transplantation in first complete remission, and an autologous transplantation is less effective than conventional consolidation. Blood 2008;111:1827–33.
9. Ram R, Storb R, Sandmaier BM, Maloney DG, Woolfrey A, Flowers MED, et al. Non-myeloablative conditioning with allogeneic hematopoietic cell transplantation for the treatment of high-risk acute lymphoblastic leukemia. Haematologica 2011;96:1113–20.
10. Verneris MR, Eapen M, Duerst R, Carpenter PA, Burke MJ, Afanasyev BV, et al. Reduced-intensity conditioning regimens for allogeneic transplantation in children with acute lymphoblastic leukemia. Biol Blood Marrow Transplant 2010;16:1237–44.
11. Litzow M. Evolving paradigms in the therapy of Philadelphia chromosome–negative acute lymphoblastic leukemia in adults. Am Soc Hematol Educ Program Book 2009:362–70.
12. Boatsman EE, Fu CH, Song SX, Moore TB. Graft-versus-leukemia effect on infant lymphoblastic leukemia relapsed after sibling hematopoietic stem cell transplantation. J Pediatr Hematol Oncol 2010;32: 57–60.
13. Socié G, Blazar BR. Acute graft-versus-host disease: from the bench to the bedside. Blood 2009;114:4327–36.
14. Greiner J, Ono Y, Hofmann S, Schmitt A, Mehring E, Götz M, et al. Mutated regions of nucleophosmin 1 elicit both $CD4^+$ and $CD8^+$ T-cell responses in patients with acute myeloid leukemia. Blood 2012; 120:1282–9.
15. Wang J, Zhang W, He A, Zhao W, Cao X. Screening of novel immunostimulatory CpG ODNs and their anti-leukemic effects as immunoadjuvants of tumor vaccines in murine acute lymphoblastic leukemia. Oncol Rep 2011;25:519–29.
16. Köchling J, Prada J, Bahrami M, Stripecke R, Seeger K, Henze G, et al. Anti-tumor effect of DNA-based vaccination and dSLIM immunomodulatory molecules in mice with Ph+ acute lymphoblastic leukaemia. Vaccine 2008;26:4669–75.
17. Dubensky TW, Reed SG. Adjuvants for cancer vaccines. Semin Immunol 2010;22:155–61.
18. Rousseau RF, Biagi E, Dutour A, Yvon ES, Brown MP, Lin T, et al. Immunotherapy of high-risk acute leukemia with a recipient (autologous) vaccine expressing transgenic human CD40L and IL-2 after chemotherapy and allogeneic stem cell transplantation. Blood 2006; 107:1332–41.
19. Rezvanie K, de Lavallade H. Vaccination strategies in lymphomas and leukaemias. Drugs 2011;71:1659–74.
20. Ma W, Smith T, Bogin V, Zhang Y, Ozkan C, Ozkan M, et al. Enhanced presentation of MHC class Ia, Ib and class II-restricted peptides encapsulated in biodegradable nanoparticles: a promising strategy for tumor immunotherapy. J Transl Med 2011;9:34.
21. Vähä-Koskela MJV, Heikkilä JE, Hinkkanen AE. Oncolytic viruses in cancer therapy. Cancer Lett 2007;254:178–216.
22. Stojdl DF, Lichty B, Knowles S, Marius R, Atkins H, Sonenberg N, et al. Exploiting tumor-specific defects in the interferon pathway with a previously unknown oncolytic virus. Nat Med 2000;6:821–5.
23. Parato KA, Senger D, Forsyth PA, Bell JC. Recent progress in the battle between oncolytic viruses and tumours. Nat Rev Cancer 2005;5:965–76.
24. Lichty BD, Power AT, Stojdl DF, Bell JC. Vesicular stomatitis virus: reinventing the bullet. Trends Mol Med 2004;10:210–6.
25. Brun J, McManus D, Lefebvre C, Hu K, Falls T, Atkins H, et al. Identification of genetically modified Maraba virus as an oncolytic rhabdovirus. Mol Ther 2010;18:1440–9.
26. Lai F, Kazdhan N, Lichty BD. Using G-deleted vesicular stomatitis virus to probe the innate anti-viral response. J Virol Methods 2008; 153:276–9.
27. Melcher A, Parato K, Rooney CM, Bell JC. Thunder and lightning: immunotherapy and oncolytic viruses collide. Mol Ther 2011;19:1008–16.
28. Breitbach CJ, Paterson JM, Lemay CG, Falls TJ, McGuire A, Parato KA, et al. Targeted inflammation during oncolytic virus therapy severely compromises tumor blood flow. Mol Ther 2007;15:1686–93.
29. Lichty BD, Stojdl DF, Taylor RA, Miller L, Frenkel I, Atkins H, et al. Vesicular stomatitis virus: a potential therapeutic virus for the

Published OnlineFirst May 28, 2013; DOI: 10.1158/1078-0432.CCR-12-3199

treatment of hematologic malignancy. Hum Gene Ther 2004;15:821–31.
30. Irvine KR, Chamberlain RS, Shulman EP, Surman DR, Rosenberg SA, Restifo NP. Enhancing efficacy of recombinant anticancer vaccines with prime/boost regimens that use two different vectors. J Natl Cancer Inst 1997;89:1595–601.
31. Lapteva N, Aldrich M, Rollins L, Ren W, Goltsova T, Chen S-Y, et al. Attraction and activation of dendritic cells at the site of tumor elicits potent antitumor immunity. Mol Ther 2009;17:1626–36.
32. Lehner M, Bailo M, Stachel D, Roesler W, Parolini O, Holter W. Caspase-8 dependent apoptosis induction in malignant myeloid cells by TLR stimulation in the presence of IFN-alpha. Leuk Res 2007;31:1729–35.
33. Chiang CL-L, Kandalaft LE, Coukos G. Adjuvants for enhancing the immunogenicity of whole tumor cell vaccines. Int Rev Immunol 2011;30:150–82.
34. Freeman GJ, Casasnovas JM, Umetsu DT, DeKruyff RH. TIM genes: a family of cell surface phosphatidylserine receptors that regulate innate and adaptive immunity. Immunol Rev 2010;235:172–89.
35. Strowig T, Henao-Mejia J, Elinav E, Flavell R. Inflammasomes in health and disease. Nature 2012;481:278–86.
36. Iyer SS, Pulskens WP, Sadler JJ, Butter LM, Teske GJ, Ulland TK, et al. Necrotic cells trigger a sterile inflammatory response through the Nlrp3 inflammasome. Proc Natl Acad Sci U S A 2009;106:20388–93.
37. Bridle BW, Boudreau JE, Lichty BD, Brunellière J, Stephenson K, Koshy S, et al. Vesicular stomatitis virus as a novel cancer vaccine vector to prime antitumor immunity amenable to rapid boosting with adenovirus. Mol Ther 2009;17:1814–21.
38. Bridle BW, Stephenson KB, Boudreau JE, Koshy S, Kazdhan N, Pullenayegum E, et al. Potentiating cancer immunotherapy using an oncolytic virus. Mol Ther 2010;18:1430–9.
39. Mellman I, Coukos G, Dranoff G. Cancer immunotherapy comes of age. Nature 2011;480:480–9.
40. Castle JC, Kreiter S, Diekmann J, Löwer M, van de Roemer N, de Graaf J, et al. Exploiting the mutanome for tumor vaccination. Cancer Res 2012;72:1081–91.
41. Pulido J, Kottke T, Thompson J, Galivo F, Wongthida P, Diaz RM, et al. Using virally expressed melanoma cDNA libraries to identify tumor-associated antigens that cure melanoma. Nat Biotechnol 2012;30:337–43.
42. Petersen J, Purcell AW, Rossjohn J. Post-translationally modified T cell epitopes: immune recognition and immunotherapy. J Mol Med 2009;87:1045–51.
43. Krueger KE, Srivastava S. Posttranslational protein modifications: current implications for cancer detection, prevention, and therapeutics. Mol Cell Proteomics 2006;5:1799–810.
44. Sarkies P, Sale JE. Cellular epigenetic stability and cancer. Trends Genet 2012;28:118–27.
45. Bell JC. Oncolytic viruses: what's next? Curr Cancer Drug Targets 2007;7:127–31.

APPENDIX II

The Ex Vivo Purge of Cancer Cells Using Oncolytic Viruses: Recent Advances and Clinical Implications

Jovian Tsang[1,3] and Harold L. Atkins[1,2,4]

[1] Ottawa Hospital Research Institute, Center for Cancer Therapeutics, Ottawa Ontario, Canada

[2] Departments of Medicine, University of Ottawa, Ottawa, Ontario, Canada

[3] Department of Biochemistry, Immunology and Microbiology, University of Ottawa, Ottawa, Ontario, Canada

[4] Ottawa Hospital Blood and Marrow Transplant Program, Ottawa, Ontario, Canada

Contributions of author: J. Tsang researched, wrote and prepared the review for submission in collaboration with Dr. H. Atkins.

Submitted: *Journal of Oncolytic Virotherapy*, under review (September 2014)

APPENDIX III

Copyright approval for **Figure 1**:

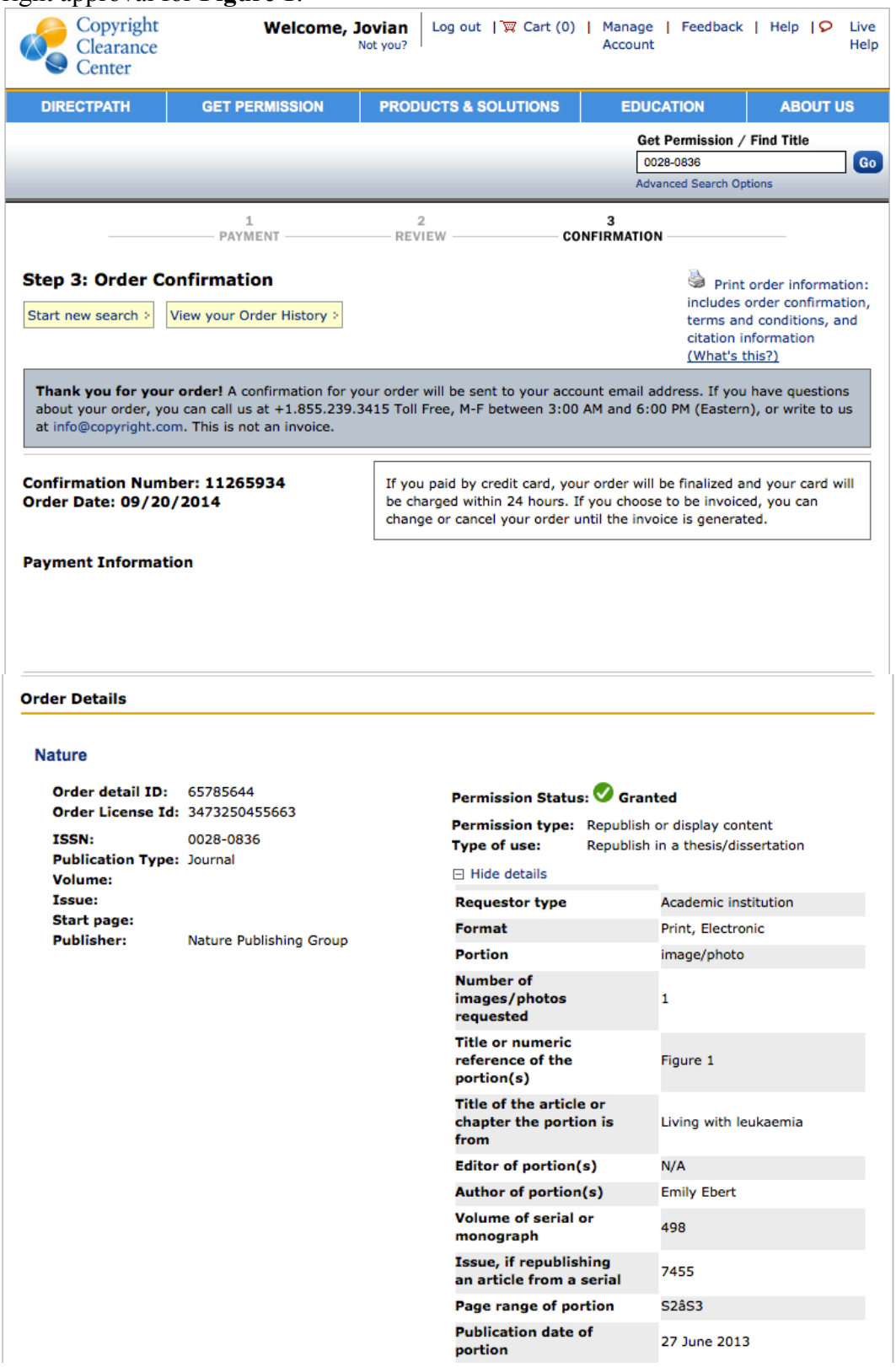

Copyright Clearance Center

Welcome, Jovian
Not you?

Log out | Cart (0) | Manage Account | Feedback | Help | Live Help

DIRECTPATH | GET PERMISSION | PRODUCTS & SOLUTIONS | EDUCATION | ABOUT US

Get Permission / Find Title
0028-0836 Go
Advanced Search Options

1 PAYMENT — 2 REVIEW — 3 CONFIRMATION

Step 3: Order Confirmation

Start new search | View your Order History

Print order information: includes order confirmation, terms and conditions, and citation information (What's this?)

Thank you for your order! A confirmation for your order will be sent to your account email address. If you have questions about your order, you can call us at +1.855.239.3415 Toll Free, M-F between 3:00 AM and 6:00 PM (Eastern), or write to us at info@copyright.com. This is not an invoice.

Confirmation Number: 11265934
Order Date: 09/20/2014

If you paid by credit card, your order will be finalized and your card will be charged within 24 hours. If you choose to be invoiced, you can change or cancel your order until the invoice is generated.

Payment Information

Order Details

Nature

Order detail ID: 65785644
Order License Id: 3473250455663
ISSN: 0028-0836
Publication Type: Journal
Volume:
Issue:
Start page:
Publisher: Nature Publishing Group

Permission Status: Granted
Permission type: Republish or display content
Type of use: Republish in a thesis/dissertation

Hide details

Requestor type	Academic institution
Format	Print, Electronic
Portion	image/photo
Number of images/photos requested	1
Title or numeric reference of the portion(s)	Figure 1
Title of the article or chapter the portion is from	Living with leukaemia
Editor of portion(s)	N/A
Author of portion(s)	Emily Ebert
Volume of serial or monograph	498
Issue, if republishing an article from a serial	7455
Page range of portion	S2âS3
Publication date of portion	27 June 2013

Rights for	Main product
Duration of use	Life of current edition
Creation of copies for the disabled	no
With minor editing privileges	yes
For distribution to	Worldwide
In the following language(s)	Original language of publication
With incidental promotional use	no
Lifetime unit quantity of new product	Up to 499
Made available in the following markets	Education
The requesting person/organization	Jovian Tsang
Order reference number	
Author/Editor	Jovian Tsang
The standard identifier	
Title	The biology and interplay of iLOV immune responses
Publisher	University of Ottawa
Expected publication date	Oct 2014
Estimated size (pages)	80

Note: This item will be invoiced or charged separately through CCC's **RightsLink** service. More info **$ 0.00**

This is not an invoice.

Total order items: 1 **Order Total: 0.00 USD**